

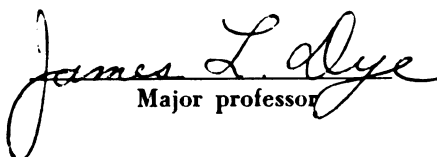
A STOPPED-FLOW STUDY OF
THE PROTONATION OF AROMATIC
RADICAL ANIONS

Thesis for the Degree of Ph. D.
MICHIGAN STATE UNIVERSITY
E. RANDALL MINNICH
1970

THESIS



This is to certify that the
thesis entitled
A STOPPED-FLOW STUDY OF THE PROTONATION
OF AROMATIC RADICAL ANIONS
presented by
E. Randall Minnich
has been accepted towards fulfillment
of the requirements for
Ph.D. degree in Chemistry


Major professor

Date August 5, 1970



ABSTRACT

A STOPPED-FLOW STUDY OF THE PROTONATION OF AROMATIC RADICAL ANIONS

By

E. Randall Minnich

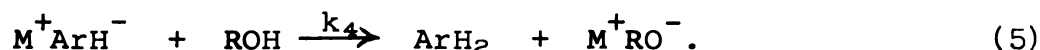
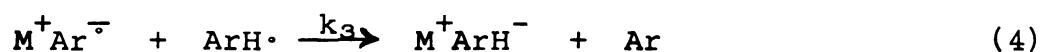
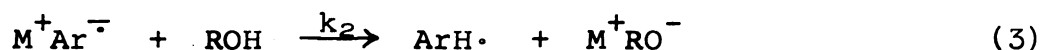
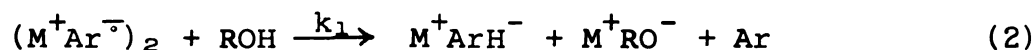
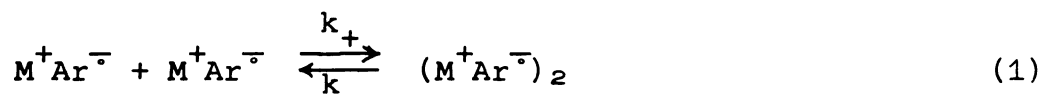
A study of the reactions of the radical anions of anthracene and terphenyl with a series of proton donors is reported. Previous investigations (1-3) employed polar solvents and concentrations of the proton donors which were high enough to affect the solvent composition significantly. In the present investigation, lower concentrations of proton donors and less polar solvents were employed. The reactions were followed spectrophotometrically by using the stopped-flow method.

In tetrahydrofuran (THF), the reactions of potassium anthracenide with a series of alcohols and with water were second-order in the anion and about half-order in ROH. The reaction rates were independent of the concentration of RO^- . Similar results were observed for the reactions in dimethoxyethane (DME), but the pseudo-second-order rate constants were lower ($k_{THF} \simeq 1 \times 10^4 M^{-1} sec^{-1}$; $k_{DME} \simeq 1 \times 10^3 M^{-1} sec^{-1}$).

The reactions of sodium anthracenide in THF appear to be similar to those of the potassium salt in the same solvent. However, in DME they are a factor of ten slower than those of potassium anthracenide. Moreover, the decay of sodium anthracenide is first-order in DME.

The reaction of potassium terphenylide with ethanol in THF appears to be first-order in each reactant and exhibits a rate constant of about $1 \times 10^5 \text{M}^{-1} \text{sec}^{-1}$.

These results are consistent with a mechanism in which both first- and second-order paths are available for the reaction between a radical anion and a proton donor:



In the case of potassium anthracenide, the second-order process (Equations 1, 2, and 5) is thought to predominate in situations which favor the formation of contact ion-pairs. When such ion-pairing is not favored, the first-order process (Equations 3-5) is observed.

REFERENCES

1. S. Arai and L. M. Dorfman, J. Chem. Phys., 41, 2190 (1964).
2. A. P. Krapcho and A. A. Bothner-By, J. Am. Chem. Soc., 82, 751 (1960).
3. K. Umemoto, Bull. Chem. Soc. Japan, 40, 1058 (1967).

A STOPPED-FLOW STUDY OF THE PROTONATION
OF AROMATIC RADICAL ANIONS

By
E. Randall Minnich

A THESIS

Submitted to
Michigan State University
in partial fulfillment of the requirements
for the degree of

DOCTOR OF PHILOSOPHY

Department of Chemistry

1970

G-65454

1-20-71

To Claudia

ACKNOWLEDGEMENTS

The author wishes to express his appreciation for the assistance he has received during the course of this work. Professor James L. Dye suggested the problem and provided valuable guidance during the study of it. Dr. Vincent A. Nicely contributed creative ideas, constructive criticism, and invaluable assistance in the data analysis. Dr. Earl M. Hansen and Marc G. DeBacker helped with both the acquisition and the analysis of the data.

Financial assistance from the United States Atomic Energy Commission is gratefully acknowledged.

TABLE OF CONTENTS

	Page
I. INTRODUCTION	1
II. HISTORICAL	4
A. Introduction.	4
B. General Properties of Aromatic Anions	4
1. Early Studies.	4
2. Electrochemical Studies.	5
3. Studies of the Optical Spectra	8
4. E.S.R. Studies	8
5. Studies of Ion-pairing	10
a. Evidence for a dissociative equilibrium	12
b. Evidence for a non-dissociative equilibrium	14
c. Conclusions regarding ion-pairing . . .	17
C. Kinetic Studies	19
1. An Early Mechanism	19
2. Kinetic Studies in Ammonia	20
3. Kinetic Studies by Pulse Radiolysis. . . .	23
4. A Kinetic Study Using ESR and Polarography	25
5. Summary.	26
III. EXPERIMENTAL	28
A. General Laboratory Techniques	28
B. Purification Techniques	30
1. Alkali Metals.	30
2. Anthracene and Terphenyl	32
3. Alcohols and Water	32
4. Tetrahydrofuran and Dimethoxyethane. . . .	33
5. Helium	35
C. Preparations.	36
1. Potassium Hydroxide and Potassium Ethoxide	36
2. ROH Solutions.	38
3. Anion Solutions.	40
D. The Stopped-Flow Experiment	43
1. Introduction	43
2. The Mixing System.	45
3. Data Acquisition	48

TABLE OF CONTENTS--continued

Page

4. Data Analysis	57
a. Program PUNDAT	57
b. Program KINET	58
IV. RESULTS AND CONCLUSIONS	62
A. A Survey of the Data	62
1. Preliminary Experiments	62
2. Principal Experiments	63
3. Discussion of the Data	66
4. Summary	69
B. Results	70
1. Dependence on the Anion Concentration	70
2. Dependence on ROH	74
3. Dependence on RO ⁻	80
4. Search for Intermediates	84
5. Dependence on Solvent	84
6. Dependence on the Cation	88
a. The reactions of Na ⁺ An ⁻ in THF	89
b. The reactions of Na ⁺ An ⁻ in DME	93
c. Conclusions	98
7. Dependence on the Anion	98
C. A Discussion of Mechanisms	101
1. Inapplicable Mechanisms	101
2. A Suggested Mechanism	106
a. Formulation	106
b. Experimental basis	108
c. Implications	112
D. Conclusions	114
REFERENCES	116
APPENDIX--Representative Sets of Kinetic Data	120

LIST OF TABLES

TABLE	Page
1. List of Experiments.	64
2. Pseudo-second-order Rate Constants for the Reaction $2K^+An^- + 2ROH \xrightarrow{THF} AnH_2 + An + 2K^+OR^-$. . .	75
3. Values of the Order, n , of ROH in the Reactions of K^+An^- with ROH in THF	76
4. Rate Constants Calculated from Equation 46 for the Reactions of Potassium Anthracenide with Various Proton Donors in THF	79
5. Pseudo-second-order Rate Constants for the Reactions of Potassium Anthracenide with (a) Ethanol and (b) Water in DME	87
6. Pseudo-second-order Rate Constants for the Reaction $Na^+An^- + EtOH$ in THF.	89
7. Rate Constants Which Result From Application of a Parallel First- and Second-order Rate Law (Equation 58) to the Reaction of Na^+An^- with Water in THF	92
8. Bimolecular Second-order Rate Constants for the Reaction of Sodium Anthracenide with Ethanol in DME.	96
9. Pseudo-first-order Rate Constants for the Reaction of Sodium Anthracenide with Water in DME. .	96
10. Bimolecular Second-order Rate Constants for the Reaction of Potassium Terphenylide with Ethanol in THF	101
11A. Rate Constants Which Result from Application of Equation 71 to the Protonations of K^+An^- and Na^+An^- in THF and in DME	110
11B. Estimates of Uncertainty for the Rate Constants in Table 11A	110a

LIST OF FIGURES

FIGURE	Page
1. A syringe used in the stopped-flow system. . .	31
2. Two vessels used in the preparation of RO^- . Weighed samples of potassium were prepared in vessel (a). The bulblets of potassium were broken in the presence of ROH in vessel (b). . .	37
3. Vessels used for the preparation and storage of (a) ROH and (b) anion solutions	39
4. Optical spectra of (a) a yellow-green solution of potassium terphenylide in THF at 25°C and (b and c) similar solutions after partial de- composition to a red color. Spectra b and c were obtained by using RCA 6199 and 7102 multiplier phototubes, respectively, with the scanning monochromator	42
5. E.S.R. spectrum of a red (partially decomposed) solution of potassium p-terphenylide in THF at 25°C	44
6. Stopped-flow system.	46
7. Block diagram of the data-acquisition system .	49
8. Decay of the 714 nm. peak of potassium anthra- cenide after mixing with 0.00175 M ethanol in THF.	53
9. Block diagram of the apparatus used to trans- form analog data to digital form	54
10. The decay of sodium anthracenide upon mixing with 0.000498M ethanol in THF. The problems of mechanical vibration and poor stopping are illustrated. The spectrum was monitored at 714 nm	67

LIST OF FIGURES--continued

FIGURE	Page
11. The decay of sodium anthracenide upon mixing with 0.00282M ethanol in THF. This push is representative of the majority of the data. A segment of the 714 nm. peak was scanned. . . .	68
12. Pseudo-first-order (a) and pseudo-second-order (b) kinetics applied to the reaction of potassium anthracenide with 0.223 M water in THF. . .	72
13. Pseudo-second-order plots of the reactions of potassium anthracenide with (a) 3.08×10^{-3} M ethanol and with (b) 5.40×10^{-3} M t-butanol in THF	73
14. Determination of the [ROH] dependence. Log \bar{k}' is plotted <u>vs.</u> log [ROH] for the reactions of K^+An^- with (a) water, (b) t-butanol, and (c) isopropanol in THF.	77
15. Determination of the [ROH] dependence. Log \bar{k}' is plotted <u>vs.</u> log [ROH] for the reactions of K^+An^- with (a) ethanol in THF and (b) water in DME.	78
16. A pseudo-second-order curve and the observed decay of K^+An^- after mixing with 0.00605M ethanol and 0.00214M potassium ethoxide in THF .	82
17. Determination of the effect of RO^- . The pseudo-second-order rate constants are plotted <u>vs.</u> the concentrations of RO^- for the reactions of K^+An^- with (a) 6.4×10^{-3} M ethanol and (b) 0.07 M water in THF	83
18a. Pseudo-second-order kinetics applied to the reaction $K^+An^- + .0118$ M H_2O in DME.	86
18b. Pseudo-second-order plot of the reaction of potassium anthracenide with .00263 M ethanol in DME.	86
19. Pseudo-second-order kinetics applied to the reaction: $Na^+An^- + 0.00282$ M EtOH in THF	90

LIST OF FIGURES--continued

FIGURE	Page
20. Parallel first- and second-order equation applied to the reaction: $\text{Na}^+\text{An}^- + 0.00236\text{M H}_2\text{O}$ in THF.	90
21. Reaction of $\text{Na}^+\text{An}^- + \text{EtOH}$ in DME, $[\text{EtOH}] = 1.34 \times 10^{-3}\text{M}$. Bimolecular second-order fit of the decay	95
22. Reaction of $\text{Na}^+\text{An}^- + 0.0085\text{M H}_2\text{O}$ in DME. A pseudo-first-order fit of the decay	97
23. Bimolecular second-order kinetics applied to the reaction: $\text{K}^+\text{Ter}^- + 5.75 \times 10^{-4}\text{ M ethanol}$ in THF.	100
24. Simultaneous fitting of Equation 71 to three data sets. The reactions of K^+An^- with (a) 0.008 M, (b) 0.02 M, and (c) 0.0054 M t-BuOH in THF are treated	109

I. INTRODUCTION

The study to be presented is an examination of certain reactions of ionic species known generically as the aromatic radical anions. The properties of these anions and the contributions of several investigators toward the understanding of these properties are discussed in some detail in the Historical section of this thesis. For purposes of orientation, however, a very general discussion of the aromatic anions and our study of them is presented at this point. The reader is referred to the Historical section for more details and for references.

Aromatic radical anions are highly conjugated organic molecules to which one or more extra electrons have been added. Three very common methods for forming these anions are: reduction via reaction with alkali metals, whereby the outer "s" electron of the metal is transferred to the organic molecule, electrolytic reduction, and reduction by solvated electrons produced by ionizing radiation. Once formed, they are, themselves, strong reducing species which react with air and various proton-donating compounds. If kept in aprotic solvents under either vacuum or an inert atmosphere, their strongly colored solutions can be kept for months.

In addition to the property of deep coloration, solutions of the mononegative anions, with which we are chiefly concerned, are paramagnetic and conducting.

In recent years, pulse radiolysis studies of solutions of various aromatic compounds in several different alcohols have shown that the anions thus formed react rapidly (pseudo-first-order rate constants of the order of 10^5 sec^{-1}) with the alcoholic medium. The disappearance of the anionic species was shown to be first-order in the concentration of anions, but, of course, the order with respect to the alcohol could not be determined in the pure alcohol.

The present study was initiated on the basis of these pulse radiolysis results. It was reasoned that, by using low alcohol concentrations (approximately 10^{-2} M) in an inert solvent, the reactions could be slowed sufficiently to be studied by the stopped-flow method. The anion was to be formed by reaction with an alkali metal; its reaction with alcohol was then to be studied spectrophotometrically. There were two main objectives. The first was to obtain a comparison between the results of two different methods applied to the same reaction. The second was to extend the kinetic data to lower and varied alcohol concentrations in order to aid in the establishment of a mechanism for the reaction.

Initially, our studies were limited to the reaction of the mononegative anion of anthracene (formed by reaction

with potassium) with ethanol or water in tetrahydrofuran (THF). This system was chosen because the physical properties of potassium anthracenide in THF had been studied rather extensively by other workers previous to our study.

It very quickly became apparent that the results could not be compared directly with those from pulse radiolysis experiments. The anion decay was not first order. The main objective then became the discovery of a mechanism which would explain this difference. The scope of the research was expanded to include the effects of changing the cation, anion, and solvent, as well as the alcohol.

An internally consistent mechanism for the protonation reaction of potassium anthracenide has resulted from these studies. In the following pages, we will present the background of ideas and the experimental results which led us to propose the mechanism. Finally, the implications of the mechanism will be discussed, and experiments which might be done to test its validity will be suggested.

II. HISTORICAL

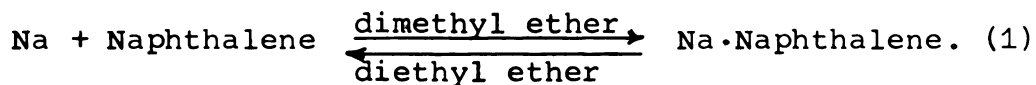
A. Introduction

The background information which forms the basis for an understanding of our experiments is divided into two sections. The first part concerns the production and properties of stable solutions of aromatic radical anions. Among these properties, of course, are the types of reactions which they undergo. These are discussed briefly, but the emphasis is placed on the basic nature of the anions under non-reactive conditions. In the second section, direct kinetic studies of the protonation reactions of the species are examined.

B. General Properties of Aromatic Anions

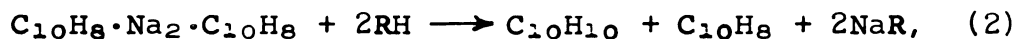
1. Early Studies

In 1914, Schlenk and co-workers (1) first produced aromatic radical anions when they mixed sodium and anthracene in diethyl ether. Later, Scott et al. (2) were able to extend the reaction to other metals and aromatic molecules by using other ethereal solvents. The latter investigators studied the reaction:



Dark green conducting solutions were produced in dimethyl ether. The reversibility and the importance of solvation effects were shown by the observation that the addition of diethyl ether restored the starting materials. The stoichiometry of the reaction is given by Equation 1.

Two classes of reactions were reported (2). A reversible addition was observed when mercury, oxygen, benzyl chloride, or sodium was added to a solution of naphthalene. The irreversible reaction of naphthalene in the presence of an alkali metal with water, alcohols, and a range of other proton donors was described by



where R is the conjugate base. The formula for the naphthalene-sodium complex given by Equation 2 was chosen to explain the stoichiometry of the overall reaction

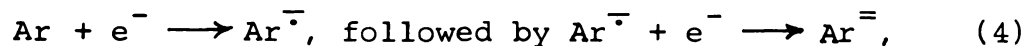


even though the solution exhibited high conductivity, which would indicate the presence of ionic species.

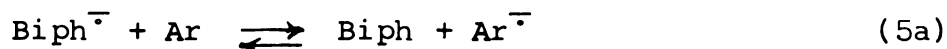
2. Electrochemical Studies

Another method of production of the aromatic anions is via electrochemical reduction of the parent molecules.

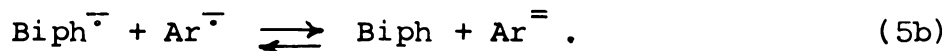
Polarographic reductions indicated that two distinct one-electron additions occurred (3,4,5), i.e.,



where Ar indicates an aromatic molecule. Later, potentiometric titrations of various aromatic compounds were carried out by using the anion produced from biphenyl and sodium ($\text{Biph}^{\cdot-}$) as a reducing agent (6). The results of these titrations were interpreted to show that both the mono- and the di-negative anions could be produced, but that the dianion was formed in two one-electron additions,



and



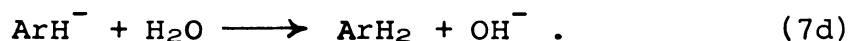
The difference in the reduction potentials of the hydrocarbons and the univalent anions agreed well with the polarographic data.

Since the polarographic studies were done in dioxane-water mixtures, the final products were the dihydro adducts of the parent molecules. In order to test the proposed mechanism of the reduction (4)



Maccoll (3) plotted the observed reduction potentials of

some aromatic hydrocarbons against the energies of the lowest unoccupied π -electron levels which had been obtained from zero-order molecular orbital calculations. A linear relationship was both predicted and observed. His results were verified by Hoiijtink and Van Schooten (5), who noted, however, that the data were also consistent with the mechanism



Polarographic experiments with varying dioxane-water mixtures and with varying concentrations of HI showed that the applicability of Equations 6a-c or 7a-d was dependent upon a competition between steps 6b and 7b (7). High concentrations of water or the addition of HI resulted in a fast protonation step, while for solutions in 96% dioxane-4% water mixtures, the addition of a second electron was faster than the protonation. In the former case, one two-electron wave resulted; in the latter, two one-electron waves were seen. These data also indicate that the protonated radical ($\text{ArH}\cdot$) has a higher electron affinity than does the parent molecule (Ar).

Regardless of the reduction mechanism, however, the success of the molecular orbital calculations provided a good model for the electronic structure of the anions.

3. Studies of the Optical Spectra

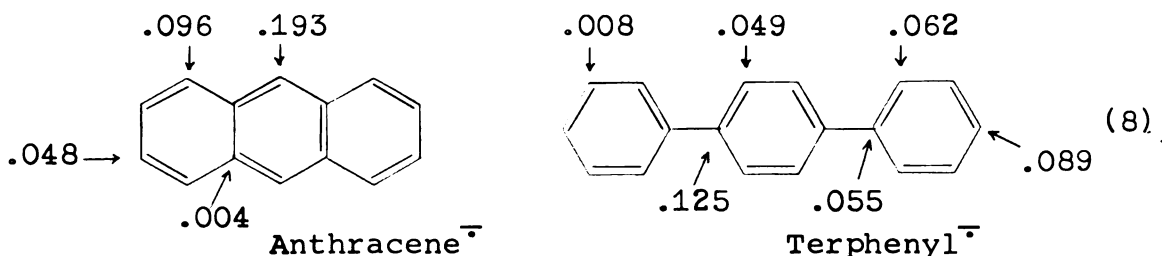
In a comprehensive study of the properties of the anions, Paul, Lipkin and Weissman (8) verified the previously published (2) stoichiometry of formation of the anions with metals and measured the conductivity of the solutions thus formed. They studied the optical spectra of a few compounds which had been reduced with sodium in 1,2-dimethoxyethane (DME) and in tetrahydrofuran (THF), noting strong absorptions in the ultraviolet, as well as in the visible region. The Beer-Lambert law was shown to apply to sodium anthracenide (4.6×10^{-4} to 3.4×10^{-3} M) and sodium naphthalenide (1.3×10^{-4} to 8.67×10^{-3} M) in THF.

Later studies involved both the mono- and di-anions of a large number of compounds which were formed with Li, Na, and K in both DME and THF (9,10). Extinction coefficients of the order of $10^4 \text{ M}^{-1} \text{ cm}^{-1}$ were generally found. The polarizations of the electronic transitions were studied by Hoijtink et al. (11,12).

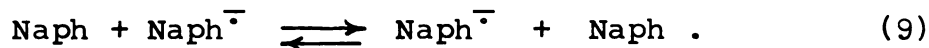
4. E.S.R. Studies

Since the aromatic mono-anions are odd-electron systems, they are, of course, paramagnetic. The dianions, on the other hand, have been found to be diamagnetic (13). Early electron spin resonance studies of the mono-anions of naphthalene (14), anthracene, and biphenyl (15) showed both paramagnetism and hyperfine splitting of the electron signal due to magnetic interactions between the electron and the

protons on the aromatic molecule. The spectra correlate surprisingly well with the predictions of simple Hückel molecular orbital calculations. Comparisons between the calculated and the observed spectra, as well as the calculated spin densities, have been reported by DeBoer and Weissman (16). Calculated spin densities at the various carbon atoms of the anthracene and terphenyl anions are reproduced below:



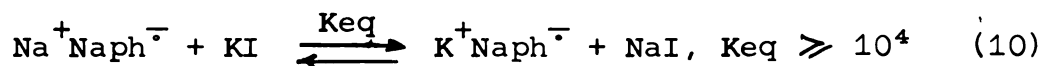
As would be expected, the electron density is distributed over the whole aromatic system. The species thus formed can be extremely stable and non-reactive towards the solvent. Some radical anion solutions last for months. Still, the electron is readily transferred to other acceptors, as was shown by Ward and Weissman (17). They added excess naphthalene (Naph) to solutions containing naphthalenide anion (Naph⁻). A broadening of the e.s.r. spectrum was found to accompany addition of naphthalene. This behaviour was attributed to the reaction



Depending on the cation and solvent used, second-order rate

constants ranging from 1×10^7 to $1 \times 10^9 \text{ M}^{-1} \text{ sec}^{-1}$ were measured.

The cation dependence indicated some sort of cation participation in the structure of the free radical species or in the electron-transfer process. Although Li, K, Rb, and Cs plus naphthalene in either DME or THF gave the same spectra, the sodium salt in DME produced much wider lines (17). In THF, it displayed a completely different spectrum. Addition of KI to sodium naphthalenide in DME caused a narrowing of the spectrum to that typical of the potassium salt. This suggested an equilibrium condition



in which the species Na^+Naph^- and K^+Naph^- were considered to be different enough to be spectroscopically distinguishable. Interest in such species became intense, as witnessed by the large number of investigators who are still trying to determine the structures of the ion-pairs (18).

5. Studies of Ion-pairing

Early data indicated that, even in solutions containing only one cationic and one anionic species, at least two spectroscopically distinguishable species might exist. Atherton and Weissman (19) found that, in THF, sodium naphthalenide (Na^+Naph^-) exhibited the same 25 line e.s.r. spectrum as was seen in DME, but with each of the lines further split into a quadruplet. This suggested the

influence of the 3/2 spin of the sodium nucleus. Cooling of the solution from 25°C to -70°C caused a diminishing of the sodium splitting and a simultaneous growth of the unsplit 25 line spectrum which was superimposed on the split spectrum. An ion-pairing equilibrium was postulated

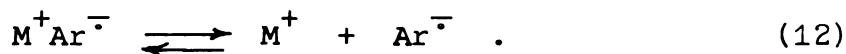


At low concentrations (less than 10^{-3} M), the superposition of the two distinct spectra could be observed even at room temperature. This further supported the idea of a dissociative equilibrium.

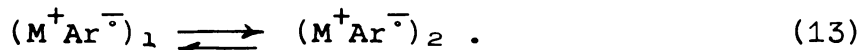
Atherton and Weissman (19) also considered the structure of the ion-paired complex. The observation of splitting due to sodium implied a certain amount of spin density at the sodium nucleus. This requirement could be met if the sodium were directly above the center of either of the benzene rings at a distance of 2.5 Å. Sufficient overlap of the sodium 3s orbital and the singly occupied π orbital of naphthalene would then result. If, however, the equilibrium position of the sodium ion were to shift with temperature toward a spot above the intersection of the naphthalene rings, the splitting would decrease.

This initial description of ion-pairing was shown to be inadequate by later experiments. These studies also indicated that aromatic anions could exist in two or more forms in solution and that these forms were in equilibrium (24-28).

However, the nature of these forms was in question. The results of the various studies generally fell into one of two distinct categories. One class of results could be explained by a dissociative equilibrium



The second class was characterized by its explanation via a non-dissociative equilibrium between two kinds of ion pairs,



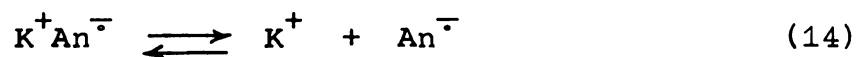
Further data which indicate the presence of a dissociative equilibrium will be discussed before consideration of the nature of the ion pairs.

a. Evidence for a dissociative equilibrium: A superposition of two distinct e.s.r. spectra was observed in solutions of sodium anthracenide in methyl-tetrahydrofuran (MTHF) at -95°C (20). A change in the relative intensities of the two spectra with concentration of the anion was interpreted to indicate the occurrence of a dissociative process.

Dodson and Reddoch (21) extended the study of the e.s.r. spectra of the naphthalene radical anions to include those formed with all of the alkali metals in both THF and DME. Sodium and rubidium naphthalenide in DME and both the lithium and the sodium salts in THF exhibited concentration dependent

superpositions of spectra at room temperature. Again, a dissociative equilibrium was suggested by the concentration dependence. The authors noted that, in order to see superimposed spectra such as these, the species must have lifetimes of at least 10^{-6} seconds. The e.s.r. spectrum of lithium naphthalenide in DME exhibited neither a metal splitting nor a concentration dependent proton shift. This was interpreted as evidence for completely dissociated lithium naphthalenide.

Some conductance data also indicate dissociative equilibria. Buschow, Dieleman, and Hoijsink (22) measured the temperature dependence of the conductance for solutions of several aromatic anions which had been reduced with a variety of alkali metals in THF. For potassium anthracenide (K^+An^-), for example, the conductance was measured from $-75^{\circ}C$ to $+20^{\circ}C$. An initial increase from about $10 \text{ mho. cm}^2 \text{ mole}^{-1}$ at $-75^{\circ}C$ to a maximum of approximately $25 \text{ mho. cm}^2 \text{ mole}^{-1}$ at $0^{\circ}C$ was observed. Increasing the temperature from $0^{\circ}C$ to $25^{\circ}C$ resulted in a slight decrease in conductivity. The behavior from $-75^{\circ}C$ to $0^{\circ}C$ was considered to be caused by the normal increase in conductivity of the ionic species with a decrease in the viscosity of the solvent. The decrease of the conductance above $0^{\circ}C$ was postulated to be due to a shift to the left of the equilibrium



which was pronounced enough to overcome the effect of viscosity on conductance. The conductance of sodium and lithium anthracenide solutions increased continuously from -75°C to $+25^{\circ}\text{C}$, indicating that these solutions have appreciable concentrations of free ions, even at room temperature.

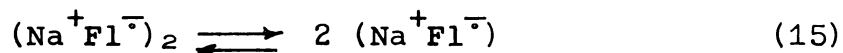
Optical spectra of these same solutions (22) showed that, for the smaller cations, the absorption peaks occurred at higher energies. The spectral shifts were usually of the order of 200 to 500 cm^{-1} for peaks in the ultraviolet or visible region. The conductance data indicated that the free ions were responsible for the absorptions at higher energies.

Examination of the results for a series of compounds led to the following suggestion (22): dissociation of ion-pairs into free ions is enhanced by small cations, large anions, and low temperatures.

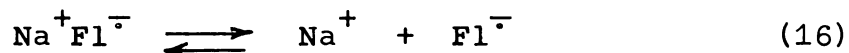
By using a combination of potentiometric, polarographic, conductometric, and spectroscopic techniques, Slates and Szwarc (23) were able to measure the dissociation constants for a number of anions. These constants increased with the size of the anion. The mobilities of the ions were also measured; radical anions were shown to have much larger mobilities than the cations. Thus, coordination of the negative ions by solvent (THF) does not appear to be favored.

b. Evidence for a non-dissociative equilibrium: While some anion solutions probably do contain free ions, as shown

in the previous section, other data suggest that Equation 13 may also apply in many instances. For example, the optical spectrum of sodium fluorenyl (Na^+Fl^-) in THF was shown to contain a number of peaks whose relative intensities could be varied, reversibly, by changing the temperature (24). For instance, a peak at 356 nm. gradually diminished in size as the temperature was changed from $+25^\circ\text{C}$ to -50°C . At the same time, a peak at 373 nm. grew in size. This interconversion was not concentration dependent and was not affected by the addition of a common ion. Therefore, the authors eliminated the dissociative equilibria



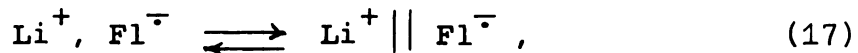
and



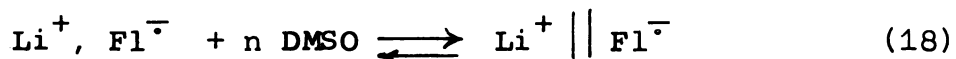
as possible explanations of the temperature dependence.

A study of the effects of various solvents on the spectrum of lithium fluorenyl (24) suggested an explanation for the temperature dependence. In dioxane at 25°C , only a single peak at 346 nm. was observed. In THF, of course, two peaks were seen, whereas in DME, only the absorption at 373 nm was observed. Lower temperatures and more strongly solvating solvents seemed to favor the species which was responsible for the lower energy peak.

These observations indicated an equilibrium between two differently solvated ion-pairs:



where $(\text{Li}^+ || \text{Fl}^-)$ represents a more strongly solvated, or "solvent-separated", ion-pair. The "contact ion-pair" $(\text{Li}^+, \text{Fl}^-)$ was considered to be a pair of ions held together by coulombic attraction. Insertion of one or more solvent molecules between the ions would produce a solvent-separated ion-pair. The driving force for such an insertion might be a lowering of the energy through solvation of the cation. In order to test for both the existence and the structure of such species, Hogen-Esch and Smid (24) added small (2×10^{-3} M) quantities of dimethyl sulfoxide (DMSO) to a solution of lithium fluorenyl in dioxane. The addition of such a strong solvating agent would be expected to shift the equilibrium

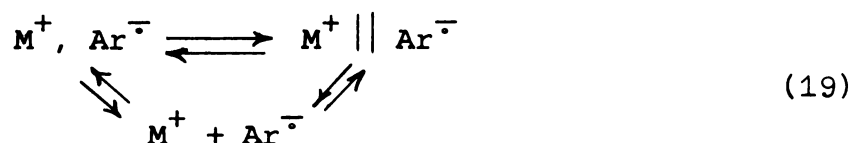


to the right. The 346 nm.band was converted to the peak at 373 nm,by this addition and a plot of $\log (346 \text{ nm.band}/373 \text{ nm.band})$ vs. $\log [\text{DMSO}]$ produced a straight line with a slope of 1.15. Therefore, the authors suggested that the insertion of one DMSO molecule would form a solvent-separated ion-pair.

Other evidence for the existence of two types of ion-pairs included the studies of Biloen, Fransen, Tulp, and Hoijsink (25). These authors reported a lack of concentration dependence in the temperature dependent conversion of ultraviolet absorption bands of sodium terphenylide in THF.

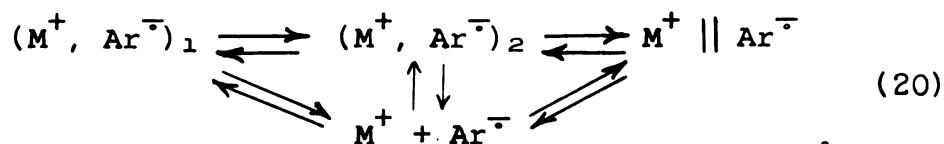
Also, Hirota and co-workers (26) were able to explain the temperature dependence of the sodium splitting of the e.s.r. spectrum of sodium naphthalenide in various solvents by using the concept of solvent-separated ion-pairs.

c. Conclusions regarding ion-pairing: Neither a model based entirely on a dissociative nor on a non-dissociative equilibrium could fit all of the data. Hogen-Esch and Smid (27) found that both their spectroscopic and conductance data could be described by the set of equilibria



in which two kinds of ion-pairs were in equilibrium with the dissociated ions. The species M^+ is an alkali metal cation; M^+, Ar^- is a contact ion-pair.

Another model was presented by Hirota (28). On the basis of measurements of the temperature dependence of the alkali metal splitting and the line width dependence on the magnetic quantum numbers of the alkali metals, the following set of equilibria was proposed:



The species $(M^+, Ar^-)_1$ and $(M^+, Ar^-)_2$ were both designated "contact ion-pairs", but were considered to be solvated differently.

Chang, Slates, and Szwarc (29) suggested a model which did not require two or more distinct kinds of ion-pairs in equilibrium with each other. Rather, the ion-pairing was considered to be described by a potential well whose shape was temperature and solvent dependent.

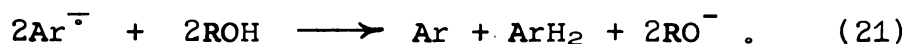
However, none of the above models is totally satisfactory. At this time, it is probably safe to acknowledge the existence of both contact and solvent-separated ion-pairs in ethereal solutions of aromatic anions. Their detailed structure is not yet known.

Of course, in this study, the detailed structure of ion pairs and, indeed, even the existence of ion-pairs is of major concern only insofar as it affects kinetics. Certain studies do indicate such an effect. Hirota et al. (26) and Ward and Weissman (17) have shown that, in the electron exchange reaction between sodium naphthalenide and naphthalene (Equation 9), the rate of exchange is strongly dependent upon the solvent used. The latter authors report rate constants of $1 \times 10^7 \text{ M}^{-1} \text{ sec}^{-1}$ in THF and $1 \times 10^9 \text{ M}^{-1} \text{ sec}^{-1}$ in DME. Since there appears to be a large difference in the ion-pairing in these solvents, these results provide evidence of a kinetic effect of ion-pairing. Hogen-Esch and Smid (24) presented evidence that the anionic homopolymerization reaction of styrene in THF proceeds 10^3 times faster through the free ion form than through the ion-paired form. Thus, ion-pairing can be kinetically significant.

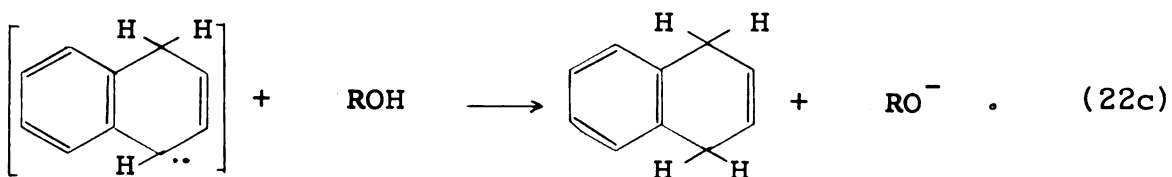
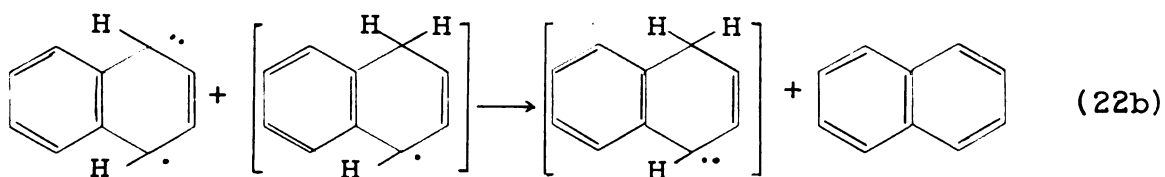
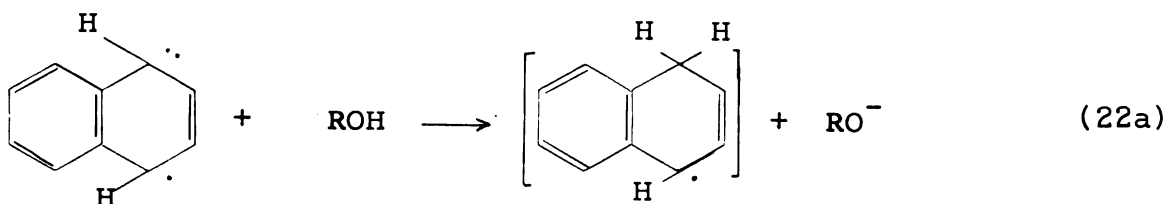
C. Kinetic Studies

1. An Early Mechanism

The reactions of interest are the protonations of aromatic radical anions in ethereal solvents. The stoichiometry and products of such reactions have been shown to be (2,30,31)



Paul, Lipkin, and Weissman (8), basing their suggestions on the stoichiometry only, came forward with a mechanism for the reaction of either CO_2 or various proton donors with the naphthalene radical anion. Written for the reaction with an alcohol, the mechanism was:

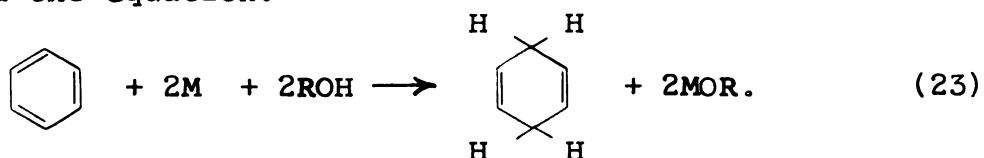


The electron transfer (22b) was assumed to be very rapid compared with the proton transfers. The first proton transfer (22a) was assumed to be the rate-determining step. On the basis of this suggestion, one would expect the decay of the anion to proceed according to a first-order rate law. Of course, confirmation of this hypothesis awaited actual kinetic studies.

2. Kinetic Studies in Ammonia

The early studies of aromatic anion protonation were carried out under conditions which were very different from ours. In the studies to be discussed (32,33) benzene and its alkyl derivatives were reduced with an alkali metal in liquid ammonia. The differences between the anions, the temperature, and especially the solvent properties tend to make direct comparisons of mechanisms and rates in this system with those in ethereal solutions hazardous. Nevertheless, there are enough similarities to make the comparisons interesting.

In these early studies, a hydrocarbon, then an alkali metal, and finally an alcohol were added to liquid ammonia. Aliquots were periodically extracted, quenched, and analyzed. Such a method was possible because half-times were of the order of hundreds of seconds. The observed stoichiometry followed the equation:

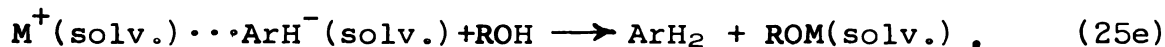
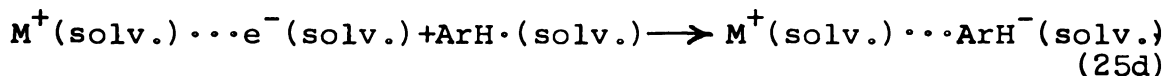
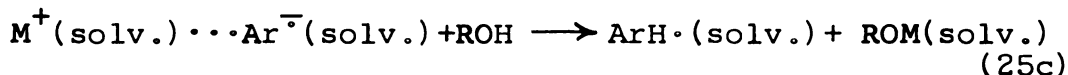
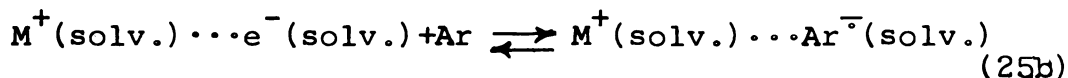
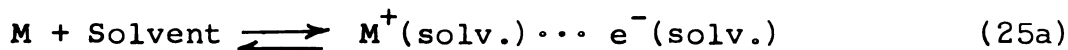


Analysis showed that unreacted benzene was also present at the end of the reaction, but this was considered to be unreacted starting material. Therefore, it is possible that the stoichiometries of the reactions in ammonia and in ethers are the same.

The authors found that their results were consistent with a third-order rate law,

$$\frac{-d[\text{Ar}]}{dt} = k[\text{Ar}][\text{M}][\text{ROH}] \quad (24)$$

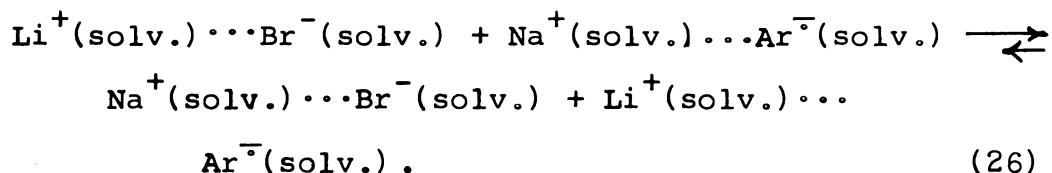
This led them to propose the following mechanism:



Except for the implied participation of the cation and the use of solvated electrons as an electron source, the mechanism is very similar to that given by Equation 22. Equation 25c was considered to be the rate-determining step.

The inclusion of the cation in the mechanism was based on the following observations. The sodium adduct reacted more slowly than did the hydrocarbon which had been reduced with lithium. Addition of sodium bromide to the solution of Na^+Ar^- did not affect the rate of the reaction, whereas the

addition of lithium bromide to such a solution caused the reaction rate to increase. Equilibrium 26 was proposed to account for the observation:

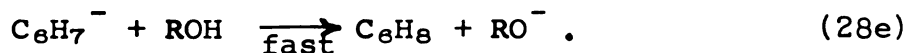
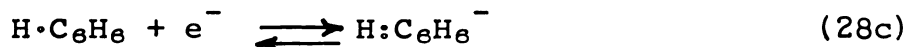
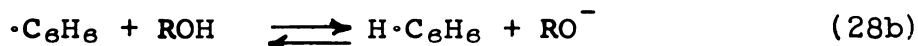
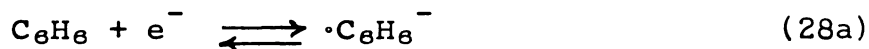


Another interesting observation was that bulky substituents slowed the reaction significantly. Hindrance of both the solvation of the anion and the accessibility of the anion to ROH were suggested causes of this effect.

Other investigators (34), however, found different kinetics for the same system. They used the expression

$$\frac{-d[\text{Ar}]}{dt} = k [\text{Ar}] [\text{M}]^2 [\text{ROH}] \quad (27)$$

to describe their results. This fourth-order rate law led them to mechanism (28):



Addition of ethoxide ion inhibited the reaction. Consequently, a reversible proton addition (28b) was postulated. Step 28d was considered to be rate determining. The authors suggested

that the intermediate ($\text{H:C}_6\text{H}_6^-$) could be a π -complex which would slowly rearrange to form another, more readily protonated intermediate (C_6H_7^-).

3. Kinetic Studies by Pulse Radiolysis

Later investigations of these protonation reactions were accomplished by utilizing the method of pulse radiolysis. In this method, electrons in solution are produced by high energy electrons from a linear accelerator. In the most relevant experiments, aromatic hydrocarbons were dissolved in cyclohexane (35) and in ethanol (36), bombarded with electrons, and observed spectroscopically. Absorbing species with lifetimes in the microsecond time range formed and then decayed. Mapping of the spectral region (400-800 nm.) gave spectra which were very similar to those obtained when the same hydrocarbons are reduced with alkali metals. Therefore, the transient species were identified as the familiar radical anions, formed this time by the reaction



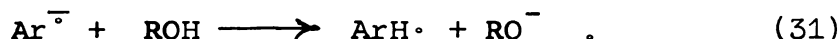
Arai and Dorfman (36) found the rate constant of this reaction to be approximately $10^9 \text{ M}^{-1} \text{ sec.}^{-1}$, depending upon the particular hydrocarbon used. The formation of the radical anions was accompanied by, but was not itself, the formation of a species in the triplet state (36,37).

Anthracene, biphenyl, and terphenyl radical anions were produced in a series of four alcohols (36,38). In each case,

the decay of the anion followed the rate law,

$$\frac{-d[\text{Ar}^-]}{dt} = k' [\text{Ar}^-] \quad , \quad (30)$$

with k' designating a pseudo-first-order rate constant. For a given anion, the rates of reaction with the various alcohols increased in the same order as did the acidity of the alcohols. This was strong evidence that the reaction being investigated was a protonation of the anion. A likely mechanism was proposed to be:



Second-order rate constants ranged from $2 \times 10^2 \text{ M}^{-1} \text{ sec}^{-1}$ to $8 \times 10^4 \text{ M}^{-1} \text{ sec}^{-1}$. Activation energies were calculated to vary from 2 to 7 kcal. mole⁻¹, depending on the alcohol and anion studied (39).

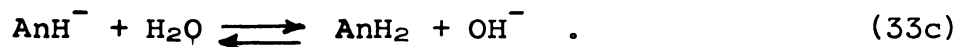
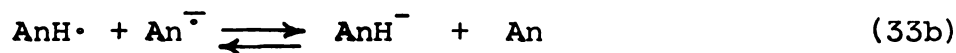
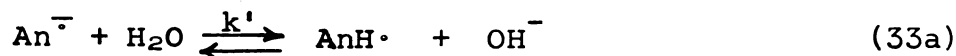
No complete mechanism for the reactions in these systems has been published. However, an interesting possibility has been suggested (40). When a biphenyl solution was pulsed, a relatively long-lived transient species with a peak at 360 nm. was observed (36). The decay of this species was a second-order process. It was tentatively identified as $\text{C}_{12}\text{H}_{11}^\cdot$, the intermediate product of the protonation. Hoijtink and Velthorst (41,42) have shown that the protonated anion (ArH^-) is often very stable. Therefore, the intermediate ArH^\cdot might be stable enough to be observed. Thus, a possibility for the mechanism is the sequence:



4. A Kinetic Study Using ESR and Polarography

Umemoto (43) studied the protonation reactions by yet another means in still another solvent. The anthracene radical anion ($\text{An}^{\cdot -}$), among others, was produced electrochemically in *N,N'*-dimethylformamide (DMF). As in the studies mentioned earlier (3-5), d.c. polarograms indicated that two reversible one-electron additions to the aromatic hydrocarbon took place in the dry solvent. Addition of water resulted in an increase of the height of the first wave at the expense of the second. Alternating current polarography also indicated that two reversible reductions occurred. In dry DMF, the peak currents were 0.35 and 0.04 mV for the first and second waves, respectively. As the concentration of water in DMF was increased from 0 to 40%, the height of both of these peaks decreased. The results of both the a.c. and the d.c. polarography experiments were interpreted as evidence for a protonation reaction between water and anthracenide.

The mechanism which was proposed to explain these results was similar to equation 7:



The steady-state assumption was made for the concentration of AnH^\bullet and the proton addition step (33a) was considered to be irreversible. The rate law which was derived on the basis of these assumptions predicted a decay which would be first-order in anthracenide:

$$\frac{-d[\text{An}^-]}{dt} = 2 k' [\text{An}^-] [\text{H}_2\text{O}] . \quad (34)$$

The experimental arrangement in this study allowed the author to pass electrochemically produced anions into an e.s.r. cavity. Since the protonation reaction was relatively slow (of the order of minutes), it was possible to observe the decay of the e.s.r. signal of anthracenide in this way. A first-order curve was observed in H_2O -DMF mixtures which contained from 1 to 6% water. However, the pseudo-first-order rate constant did not vary linearly with the water concentration as equation 34 would predict. This was attributed to changes in the solvation because of the changing solvent composition. An alternative explanation might be that the role of water in the proposed mechanism is incorrect. The data given for the anthracenide-water reaction indicate that, between 1 and 3% of water, a rate law which is second-order in water would be more nearly correct.

5. Summary

The kinetic experiments to date have been conducted under very different conditions. Certainly, many of the differences

in the experimental results can be attributed to this fact. Nevertheless, there are many points of agreement in spite of the differences in the experimental conditions. In each case, the anion was observed to decay according to a first-order rate law. There seems to be general agreement that the first step is the addition of a proton to the radical anion, although the reversibility of this step is questionable. In both the studies with liquid ammonia and the pulse radiolysis studies, the rate of reaction with a series of alcohols increases as the acidic character of the alcohols increases. The ion-pairing data indicate that different cations and solvents should affect the kinetics. The kinetic data do show such effects. Beyond this point, physical and chemical effects such as differences in temperature, solvent polarity, cationic species, hydrogen bonding, etc. probably mask other chemical similarities which may exist.

III. EXPERIMENTAL

A. General Laboratory Techniques

Because of the extreme reactivity of the aromatic radical anions, special care must be taken if stable solutions are to be prepared. Since the solutions decompose when exposed to air, high vacuum techniques are necessary. Rigorous cleaning of all glassware is also important.

The following cleaning procedure was used for all storage vessels and related glassware. The item to be washed was soaked in a cleaning solution which consisted of the following reagents, measured by volume:

60% distilled water
33% Fisher reagent grade HNO_3
5% Baker reagent grade 48% HF
2% acid-soluble detergent (Tide)

After a few minutes of soaking in the HF cleaner, the vessel was rinsed with distilled water and soaked in aqua regia for several hours. Finally, it was rinsed ten times with distilled water, followed by five rinses with conductance water. All vessels were pumped to pressures of the order of 1×10^{-5} torr for several days before they were used.

The cleaning procedure for the stopped-flow system was less rigorous because of the difficulty involved in

dismantling and reassembling it. Aqua regia was poured into the system and left for half a day. The system was then rinsed out with distilled water, followed by conductance water as before. The entire stopped-flow system was pumped to at least 4×10^{-5} torr for several days before a run.

The anions' sensitivity to air requires that all liquid transfers be done in a closed system. Vacuum distillation was the most common method of transferring pure liquids from one place to another, while solutions were transferred under a helium atmosphere. In either case, a vacuum system was necessary. Pumping was done with a Cenco Hyvac 7 mechanical pump and a Veeco air-cooled diffusion pump. Dow Corning 704 diffusion pump oil was used in the latter. The pumps were separated from the vacuum system by a liquid nitrogen trap. Pressures of 7×10^{-6} torr could be regularly attained in the vacuum manifold.

Tetrahydrofuran, the main solvent used, dissolves most stopcock greases and attacks Viton-A "o-rings" which are used in many greaseless stopcocks. Therefore, a system in which liquids and vapors could contact only Teflon and glass was desirable. Two commercially available needle-valve type stopcocks were found to be acceptable after some modification. The Fischer-Porter Lab-Crest 4 mm. Quick Opening Valve uses a glass-to-Teflon seat and isolates the "o-ring" from the vacuum system with a Teflon ridge. It can be made leak-tight by wrapping the threaded part of the Teflon insert with

Teflon tape. The Delmar-Urry valve employs four "o-rings", two of which are susceptible to attack by the solvent. New Teflon inserts, in which these two "o-rings" were replaced by Teflon ridges, were made and used very successfully.

Design of a syringe for the stopped-flow system which would be both greaseless and air-tight posed a special problem which was solved by using a design which was first suggested by Dr. V. A. Nicely. Hamilton No. 1010 Gastight syringe barrels were modified by attaching a 5 mm. Fischer-Porter Solv-Seal joint and a sidearm. Teflon plungers having two sets of double Teflon ridges were made (see Figure 1). Teflon ridges form an adequate seal for liquids, but not always for gases. By pumping between the pairs of ridges, the gas leakage problem was eliminated.

B. Purification Techniques

1. Alkali Metals

Sodium and potassium were both handled in the same way. In a helium-filled dry-bag, lumps of metal were cut into small cubes and put into a tall vessel along with several two-foot-long tubes that had been sealed at the top end. The vessel was then connected to a vacuum line and evacuated. The vessel was heated until the metal melted and formed a pool which covered the open ends of the tubes. At this time, helium was admitted, which forced the molten metal up into the tubes, where it was allowed to cool and solidify.

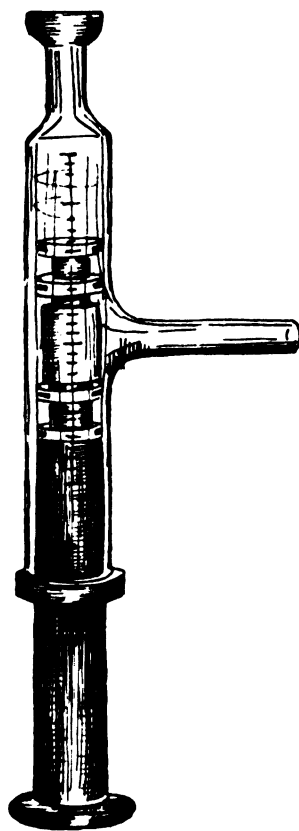


Figure 1. A syringe used in the stopped-flow system.

These tubes then served as convenient containers which could be cut to the desired length when a small amount of metal was needed.

Metal was introduced into a vessel by inserting the appropriate length of metal-filled tube into a sidearm, pumping the vessel to $< 5 \times 10^{-5}$ torr, and distilling the metal into the vessel. The sidearms were constricted in four or five places so that, after the metal had been distilled through a particular constriction, that constriction could be sealed off. In this way, solid residue was eliminated and several independent distillations were effected.

2. Anthracene and Terphenyl

Zone-refined anthracene and p-terphenyl were obtained from James Hinton Co., Valparaiso, Florida. No further purification was attempted. Samples were weighed and transferred to tubes that were constricted at one end and had a break-seal at the other. The air was then pumped out, the constriction sealed off, and the sample stored in the dark. The sample was put into a vessel for use by sealing the tube to a sidearm on the vessel, pumping out the vessel, and breaking the break-seal with a glass- or Teflon-enclosed magnet (Figure 3).

3. Alcohols and Water

Distilled water was passed through a Deminizer ion exchange column made by Cristolab, then redistilled through

a three-foot column filled with glass tubing. Degassing was accomplished by freezing with liquid nitrogen, pumping to approximately 1×10^{-5} torr, thawing, and repeating this cycle until the pressure did not jump to more than 5×10^{-5} torr when the frozen sample was opened to the pump. About 200 ml. were vacuum distilled into a storage vessel. Whenever new samples were to be prepared, milliliter amounts were vacuum distilled into very small, weighed vessels in which the degassing procedure was repeated. These small vessels were equipped with a constriction and a break-seal so that the water sample could be admitted into a vessel for mixing with solvent.

All of the alcohols were purified by distillation on a Nester-Faust annular Teflon spinning band distillation column. The alcohols so treated and the fractions retained were: anhydrous, A.C.S. analyzed reagent grade methanol from Matheson, Coleman, and Bell (b.p. = $64.2-64.3^{\circ}\text{C}$), spectral grade absolute ethanol (purified by E.M. Hansen), Fisher certified reagent grade 2-propanol (b.p. = 82.0°C), and Fisher certified reagent grade t-butanol (b.p. = 82.0°C). After distillation, the same degassing and handling procedures were used for the alcohols as described previously for water.

4. Tetrahydrofuran and Dimethoxyethane

Burdick and Jackson "Distilled in Glass" tetrahydrofuran (THF) was siphoned from the bottle into an evacuated vessel

which contained CaH_2 ("purified" grade from Fisher Scientific Company). Since the THF was bottled under nitrogen, it had only a very brief contact with air. After several days of refluxing over CaH_2 , the THF was forced through evacuated tubes into a one-liter distillation pot. From there, it was distilled through a four foot Vigreux column under about 0.75 atmosphere of helium into a vessel which contained NaK (a 1:3 sodium-potassium alloy) and benzophenone from Eastman-Kodak Company. The purple color of the benzophenone ketyl formed immediately when the THF contacted the NaK and benzophenone. The benzophenone ketyl is not stable in the presence of water. It served as both a drying agent and an indicator of dryness. This purple solution could be stored for months at room temperature without decomposing.

The THF used for runs KR1 through KR3 was vacuum distilled from the purple benzophenone ketyl solution onto a potassium mirror in another vessel. After about two days, the clear liquid would turn pale blue. This is thought to be due to the solution of the metal in THF and was the ultimate criterion for dryness. This blue color was more stable at low temperatures than at room temperature. The THF-potassium solutions stayed blue for two days, at most. In the runs noted, the THF was distilled from clear solutions which had been blue with potassium.

For all runs after KR3, solutions were prepared from THF which had been distilled directly from the purple solution

of the benzophenone ketyl. The treatment with potassium was found to be time-consuming and was not required for the preparation of stable solutions.

When a thermal conductivity detector was used, gas chromatography of THF both before and after distillation on the Vigreux column indicated the presence of only one component. A more sensitive flame-ionization detector showed one other component in the undistilled THF. An electron-capture detector indicated that this minor component had a large electron-capture cross-section. We therefore suspected it to be the stabilizer, butylated hydroxytoluene (BHT), which had been put into the solvent by Burdick and Jackson.

New methods of purification were sought in order to make larger scale purifications possible. A zone purification method was tried, unsuccessfully. Although passing THF directly from the CaH_2 vessel into a vessel containing NaK-benzophenone did not produce the stable ketyl, two or three successive vacuum distillations onto NaK-benzophenone did eventually lead to the stable, purple solution. This method of purification was used for runs KR9 through KR14. It eliminated the distillation through the Vigreux column.

5. Helium

Helium used for any purpose was first passed over hot (530°C) copper shavings and then over hot copper oxide. It was then passed through a tube containing Ascarite and finally through a liquid nitrogen trap. All helium was grade A helium from Liquid Carbonics Company.

C. Preparations

1. Potassium Hydroxide and Potassium Ethoxide

These compounds were prepared by vacuum distilling water (or ethanol) onto metallic potassium in order to assure the absence of contaminants. All starting materials were purified in the manner described previously.

In order to produce known amounts of product, weighed amounts of potassium were required. The method of Watt and Sowards (44) was used for this purpose. First, small bulblets of approximately 1.5 cm. diameter were made from 5 mm. Pyrex tubing. The tubing was cleaned by the method described earlier, drawn into thin capillaries, and blown into fragile bulblets. All blowing was done through a plastic diaphragm to avoid contamination by the breath. The bulblets were weighed and then placed in the vessel shown in Figure 2. Potassium was distilled into the vessel through the sidearm until a pool of metal formed around the open ends of the bulblets. When a small pressure of helium was admitted, the potassium was forced up into the bulblets. The vessel was opened in a helium-filled dry-bag where the bulblets were removed. The bulblets, now filled with helium, were quickly sealed off in the open room. This last step afforded a chance for contamination by air. However, only three of the six bulblets showed any sign of contamination, that indication being a very slight bluish tinge on the metallic surface. Finally, the filled bulblets were reweighed.

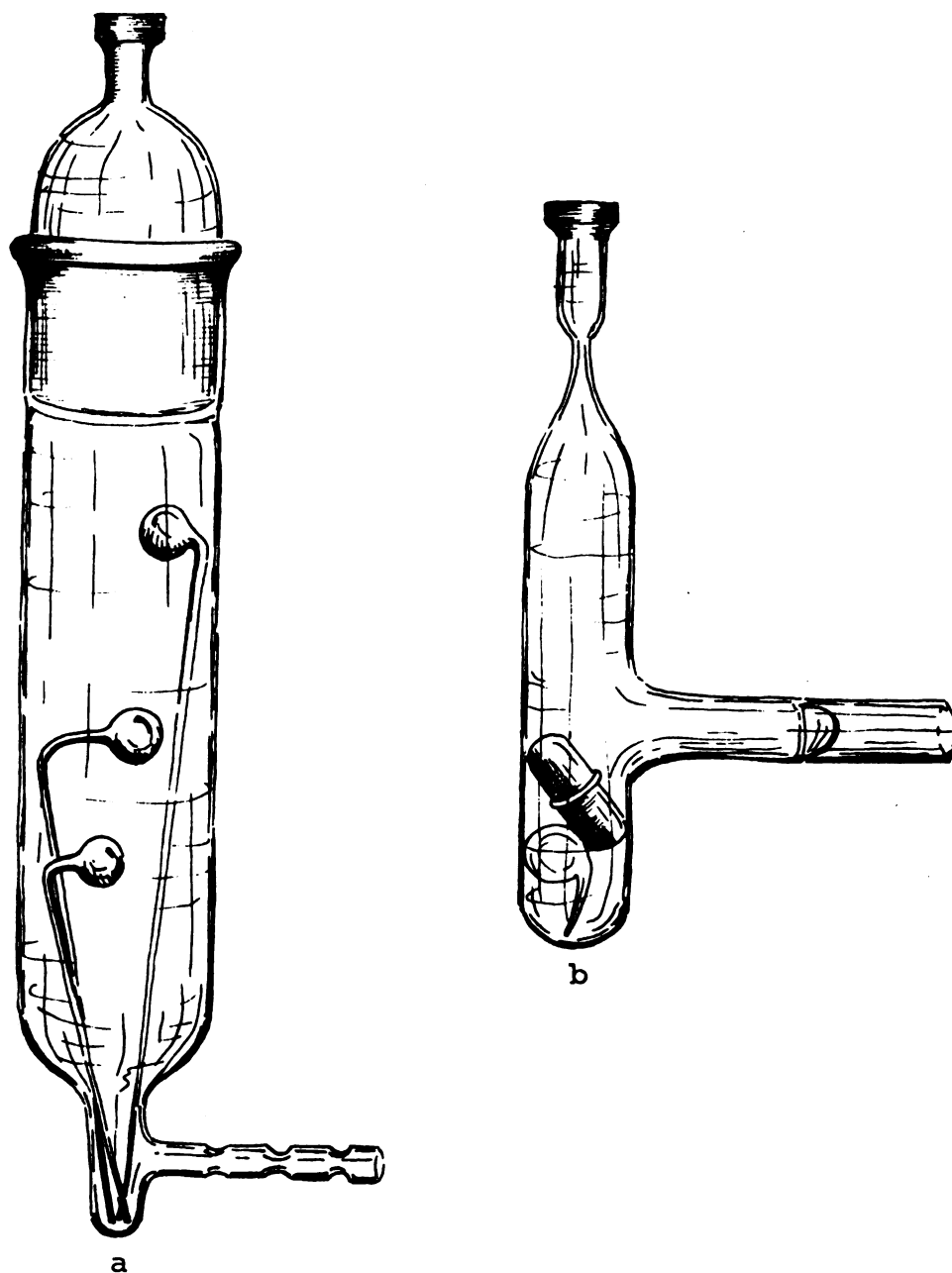


Figure 2. Two vessels used in the preparation of RO^- . Weighed samples of potassium were prepared in vessel (a). The bulblets of potassium were broken in the presence of ROH in vessel (b).

The actual reaction took place in the second vessel shown in Figure 2. The bulblet was cleaned, rinsed, and placed in the tube along with a Teflon-coated magnet. When the system had been pumped to 1×10^{-5} torr, the bulblet was broken and water (or ethanol) was distilled onto the exposed potassium. On completion of the reaction, the excess water (or ethanol) was pumped out and the vessel was sealed off. The break-seal vessel could then be attached to a solvent vessel as shown in Figure 3.

2. ROH Solutions

After an ROH (or K^+RO^-) sample had been sealed to the main vessel, as shown in Figure 3, the vessel was pumped to 1×10^{-5} torr or less for several days. Solvent (THF or DME) was vacuum distilled, usually from the purple solution of benzophenone ketyl, into the vessel. Degassing was accomplished by the freeze-pump-thaw method described earlier. After the vessel had been weighed, helium was added and the solvent was frozen and stored under liquid nitrogen and in the dark until shortly before a run. Storage for one or two weeks was not uncommon. Storage at liquid nitrogen or dry ice temperatures was initiated when the addition of pure THF, which had been stored for two days in the dark at room temperature, caused potassium anthracenide solutions to decompose.

When a solution was to be used, it was thawed, the break-seal was broken, and the solvent was mixed with the ROH.

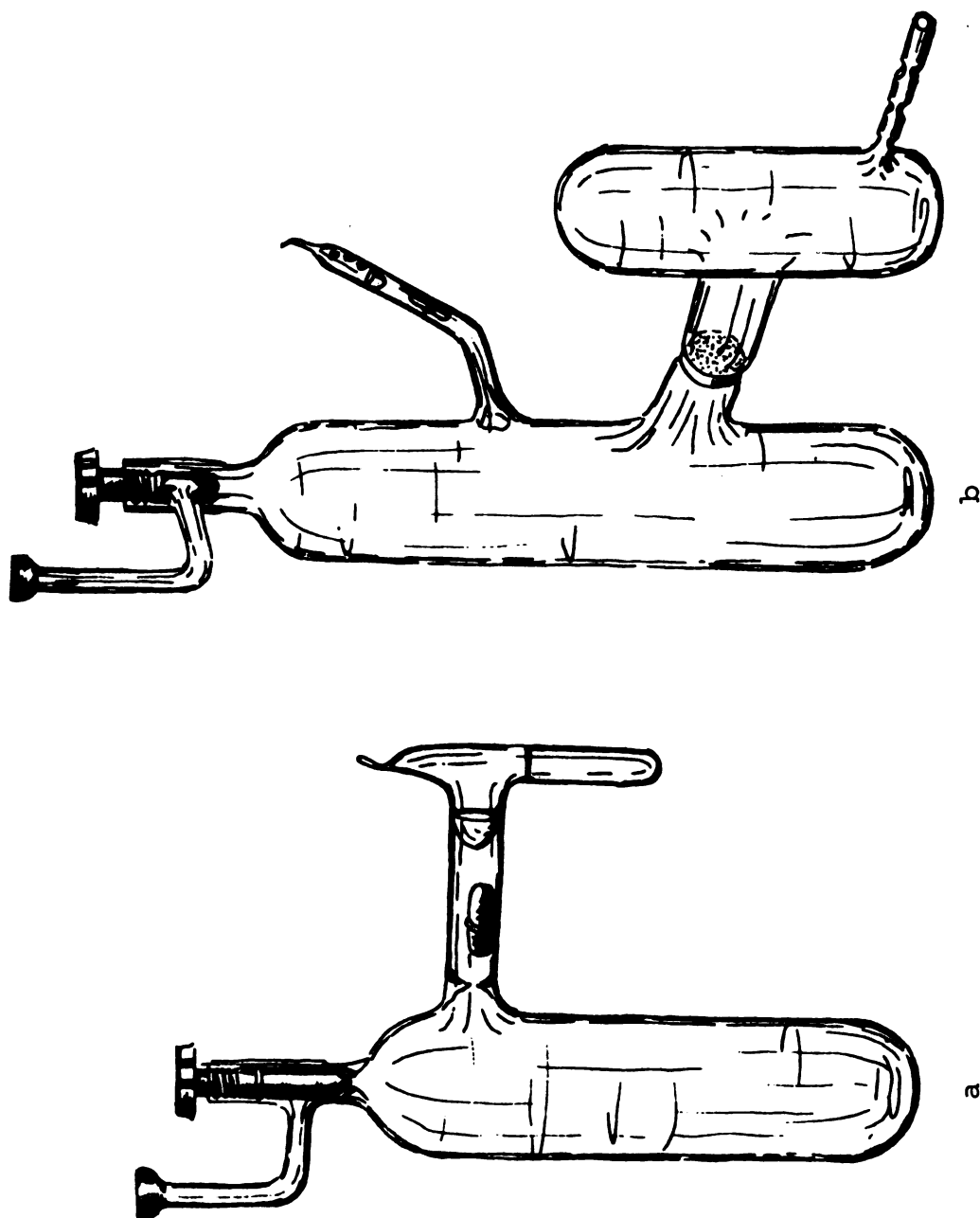


Figure 3. Vessels used for the preparation and storage of (a) ROH and (b) anion solutions.

3. Anion Solutions

Solutions of the aromatic radical anions were prepared in vessels similar to that shown in Figure 3. The procedure was much the same as that described for ROH solutions. After metal had been distilled into one side of the vessel, solvent was distilled into the other side. The break-seal was broken, the aromatic compound dissolved (slowly), and the resulting solution poured through the coarse frit onto the metal. A colored solution formed immediately and slowly increased in depth of color. When the color indicated that the absorbance would be approximately unity in the flow system, the solution was poured from the metal surface, helium was admitted into the vessel, and kinetic experiments were begun. Although the solutions were usually used immediately after their formation, instant use was not necessary. Anthracenide solutions were stable for months, even at room temperature.

Anthracene is only slowly soluble in THF in the quantities we used (approximately 4×10^{-3} M). The concentration of anions was usually around 5×10^{-4} M, so that up to a ten-fold excess of unreacted anthracene was present. This excess prevented the formation of appreciable concentrations of dianions. The spectra of the blue anthracenide solutions were identical to the published spectra of the mono-anions (9). The anion concentration for each run was calculated from the absorbance by using the Beer-Lambert law and extinction coefficients given in the previous reference.

Solutions of potassium p-terphenylide anions were produced in the same way and at about the same concentrations. The yellow-green terphenylide anion seemed to form more rapidly than did the anthracenide anion, but this probably only resulted from the more rapid rate of dissolution of p-terphenyl in THF. This anion was also characterized by its optical spectrum (9) and solution concentrations were determined from the absorbance.

The p-terphenylide anion was found to be a rather unstable species in our system. When solutions of potassium p-terphenylide were stored at room temperature for a few days, red crystals were found growing on the vessel walls. However, the color of the solution was still yellow-green. In the flow system, contamination by the red compound was even more obvious on most occasions. Immediately upon entering the system, the solution turned red. Although rinsing the flow system several times with anion solution finally gave green solution in the burettes, the green color turned to a rusty color and, finally, red, after only minutes of stability. The change in color seemed to occur uniformly throughout the solution. A spectrum of such an orange-red solution, taken on the Cary model 14 spectrophotometer from 340 to 1140 nm., showed the expected spectrum of the terphenylide anion. The only indication of the existence of an impurity was an extraneous peak at 530 nm. This appeared as a small shoulder on the 480 nm. peak of the p-terphenylide anion (see Figure 4).

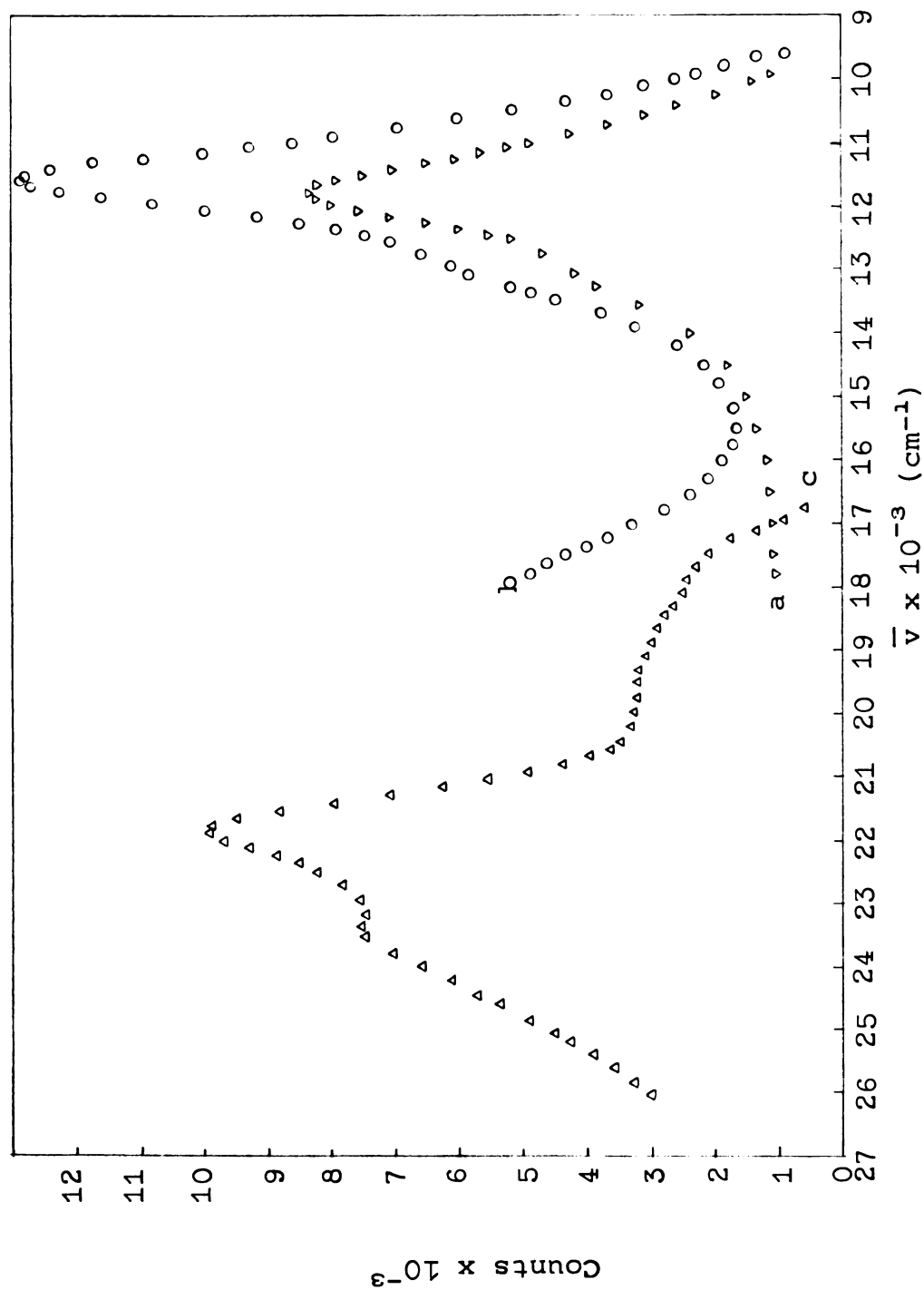


Figure 4. Optical spectra of (a) a yellow-green solution of potassium terphenylide in THF at 25°C and (b and c) similar solutions after partial decomposition to a red color. Spectra b and c were obtained by using RCA 6199 and 7102 multiplier phototubes, respectively, with the scanning monochromator.

Such red-orange solutions were paramagnetic, as would be expected. An e.s.r. spectrum of such a solution is given in Figure 5. The symmetry of the spectrum is striking and probably indicates the existence of only one paramagnetic species. The published splitting values for Na^+Ter^- in DME (45) correspond well with splittings between major peaks in the spectrum of red-orange solution. There is a good, but not exact, correspondence between the spectrum of Na^+Ter^- and that shown in Figure 5. When a non-correspondence occurs, it can be related to the observation that the published spectrum contains more lines. The spectrum of the unknown solution was measured at room temperature in THF with a Varian E4 EPR spectrometer, while the known spectrum was measured at -40°C in DME. The differences in temperature, cation, and solvent would all lead to lower resolution in our spectrum. Thus, we conclude that e.s.r. spectrum of the orange-red solution is that of potassium p-terphenylide.

D. The Stopped-Flow Experiment

1. Introduction

Although the stopped-flow apparatus shown in Figures 6 and 7 may be complex in appearance, its purpose is to solve a very simple problem. For a reaction which occurs in the time range from a few seconds down to a few milliseconds, the reaction is over before more conventional methods of mixing and analysis can be applied. A stopped-flow apparatus

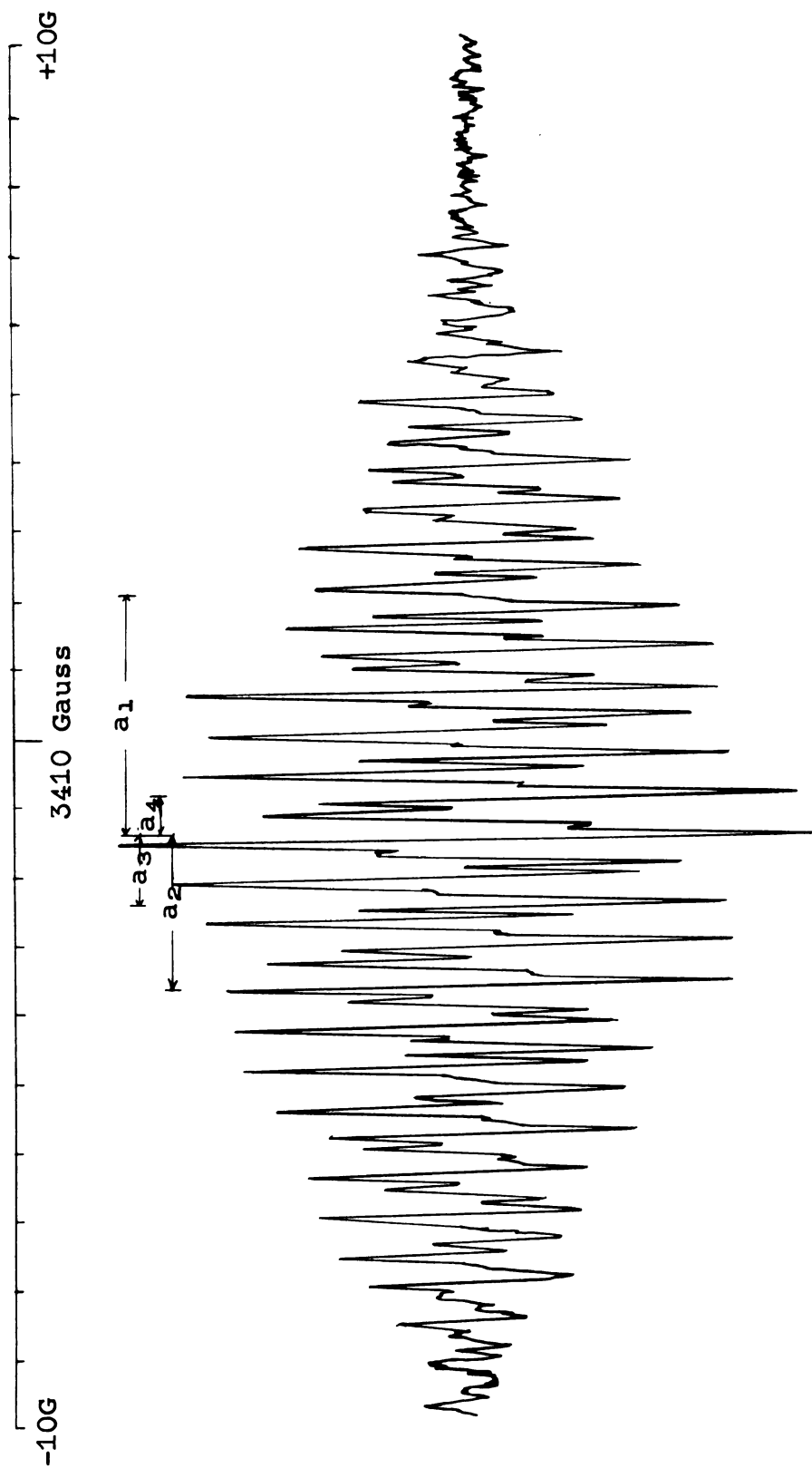


Figure 5. E.S.R. spectrum of a red (partially decomposed) solution of potassium p-terphenylide in THF at 25°C.

is designed to both mix and permit analysis of chemicals in only a few milliseconds and, therefore, allows one to study very fast reactions. Since this apparatus is designed to solve the twofold problem of fast mixing and analysis, a discussion of it is conveniently divided into two parts dealing respectively with the mixing and the analysis.

2. The Mixing System

The mixing system, shown in Figure 6, consisted of four parts: burettes and mixing vessels used to dilute solutions of the reactants, a pair of syringes and a pushing block for initiating the flow, a cell for mixing the two reactant solutions, and a third syringe designed to abruptly stop the flow of liquid. The glassware was held rigidly in place by a set of aluminum plates which were connected by threaded $3/8$ inch brass rods. This whole system was bolted to a table made of $1/4$ inch angle iron.

Solutions were introduced into the system via ports above the burettes. The burettes were standard 50 ml. Pyrex burettes calibrated to 0.1 ml. We estimated the readings to 0.01 ml. The burettes and mixing vessels were always thermostatted at room temperature since the lack of thermostating elsewhere in the system required that all reactions be studied near room temperature. Vessels containing solutions of radical anion and of ROH were connected to the system via 5 mm. Fischer-Porter Solv-Seal joints above the left and right burettes, respectively. A vessel of pure solvent was also attached to each side.

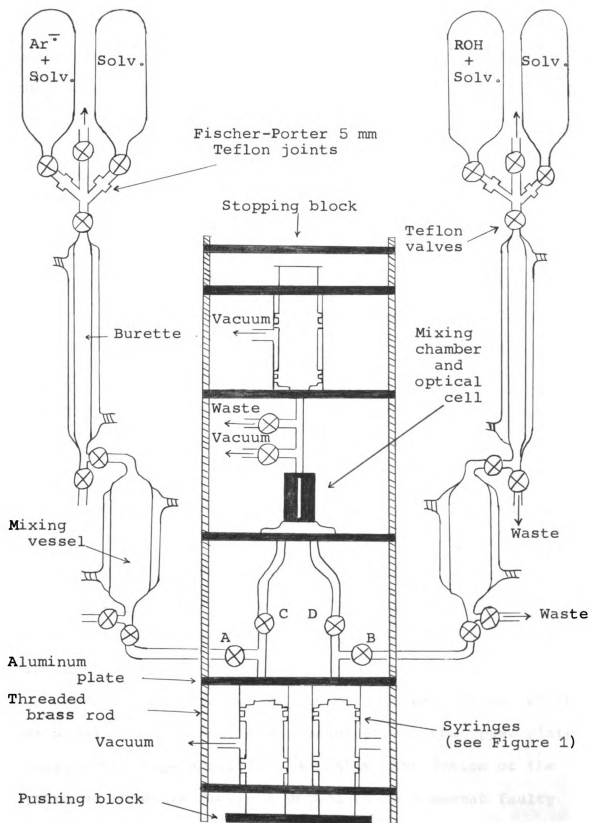


Figure 6. Stopped-flow system.

The entire flow system was pumped to 4×10^{-5} torr before solutions were admitted. Dilutions were made by admitting a measured volume of a solution into the mixing vessel, rinsing the burette with pure solvent, and finally admitting a measured amount of pure solvent into the mixing vessel. Mixing was accomplished by boiling the solution. At these reduced pressures, the heat from one's hand sufficed to cause boiling. The plungers for the bottom syringes were set into an aluminum pushing block which was attached to a lever. By opening stopcocks A and B and pulling the plungers down, the solutions could be drawn into the syringes. Closing A and B, opening C and D, and pushing the syringes up caused the solutions to flow through the mixing cell. Mixing times for similar cells had been previously estimated (46) to be less than 2 msec.

A description of the construction and design of the mixing cells is given by Hansen (47). The particular cell used in this study was made of 1.0 mm. quartz capillary tubing with two optically flat faces. The four tangential jets in its base were drilled by Dr. E. M. Hansen as described by him in the previous reference.

When the top syringe filled to a preset volume, which was usually 3 to 4 ml., the plunger struck the upper plate, stopping the flow abruptly. Actually, the design of the system as shown in Figure 6 proved to be somewhat faulty because of the violence of this collision between the plunger

and the stopping plate. In some of the early kinetic studies, especially for fast decays, an oscillation of the signal amounting to about 0.05 absorbance units was noticed. The oscillation was traced to vibrations set up in the system by the stopping mechanism. Changing the physical arrangement of the top three plates so that they were no longer attached to the rest of the flow system via the brass rods greatly diminished this oscillation. However, the older version is shown in Figure 6 because of its simplicity.

3. Data Acquisition

The reactions between aromatic radical anions and various proton donors were studied by monitoring the disappearance of the anions spectrophotometrically. The analysis system consisted of a light source, monochromator, beam-splitter, sample cell (which in this case was the mixing cell), reference cell, multiplier phototubes, and the data storage system. A block diagram of this network is given in Figure 7.

Two different light sources were used, depending on the wavelength range to be studied. Over the range from 250 to 400 nm., a Bausch and Lomb xenon lamp was employed. A Bausch and Lomb tungsten-iodine lamp was used for work between 400 and 850 nm.

The monochromator, a Perkin-Elmer Model 108 Rapid Scan Monochromator, has been described in detail by Feldman (46). This monochromator is capable of scanning over any desired spectral width compatible with the source and detector at

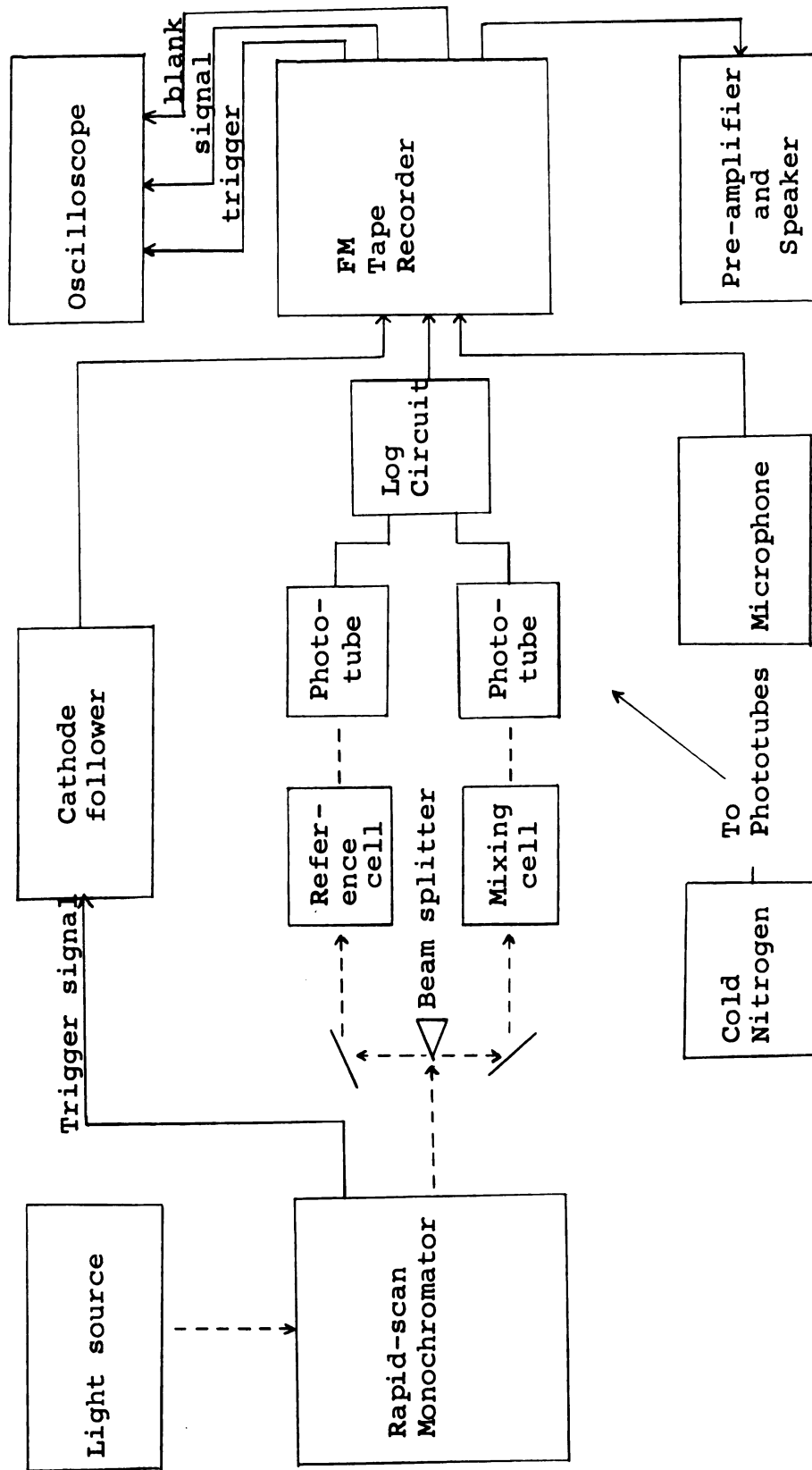


Figure 7. Block diagram of the data-acquisition system.

rates up to 150 scans per second. We usually observed a complete absorption peak of an anion (~ 150 nm.) at a scanning rate of 60 scans per second (16.7 msec. per spectrum). By observing successive spectra, the decay of an entire peak could be followed. Alternatively, a single wavelength could be continuously monitored simply by turning off the motor and choosing the desired wavelength. This method was used for very fast reactions.

When the scanning capability was used, a sharp spike, used for triggering an oscilloscope or other observational device, was produced at the beginning of each spectrum. The method used to produce this signal was changed from that described earlier (46). A slotted wheel was attached to the drive mechanism such that it turned once per revolution of the mirror. A small neon bulb, the slot, and a CdS photocell were positioned so that a spike which rose to approximately 1 volt in 1 millisecond was produced each time a new scan began. This signal was passed through a cathode follower in order to match the impedance of the trigger system to that of the tape recorder. A stacked-mirror beam-splitter of the type used in the Bausch and Lomb Spectronic 505 Spectrophotometer split the single beam of light coming from the monochromator into two beams. These were focused on the mixing cell and on a solvent-filled reference cell, respectively, by spherical focusing mirrors of 98 mm. focal length. These mirrors were obtained from the Karl Lambrecht

Company. Finally, the light fell onto a pair of multiplier phototubes. The type of phototube used depended on the wavelength region which was being studied at the time. The RCA multiplier phototubes 6903, 6199, and 7102 were employed in the wavelength regions between 250 to 400, 400 to 600, and 600-900 nm., respectively. In order to minimize the effect of thermal noise, the RCA 7102 phototubes were cooled with a stream of nitrogen which had been passed through copper tubing immersed in liquid nitrogen.

The anode currents from the phototubes were matched by controlling the amount of light which fell onto each phototube when both reference and mixing cell were filled with solvent. The multiplier output currents were then passed into a log circuit which converted the intensity measurements to an absorbance reading. The components of the circuit include a high impedance input amplifier (P25A), a dual logarithmic transconductor (P11-P), an operational output amplifier (P65AU), and a power supply (PR-30C), all available from Philbrick Researches, Inc. The output voltage could be adjusted to 1, 2, 5 or 10 volts per absorbance unit. Prior to each run, the linearity of the absorbance measurement was checked with neutral density filters purchased from the Oriel Corp.

Data storage during a run was accomplished with an Ampex SP-300 FM Direct Recorder/Reproducer which had four channels available. The absorbance data, trigger signal, and a verbal

explanation were recorded on three channels. The fourth channel was left blank for later common-mode noise rejection. As the absorbance data were recorded, they were simultaneously read from the tape and displayed on a Tektronix 564 Storage Oscilloscope which employed a Type 2A63 Differential Amplifier Unit and a 3B4 Time Base Unit. This display was strictly for monitoring purposes; no attempt was made to analyze the data from the oscilloscope.

After a run had been completed, the kinetic data were read from the tape recorder onto computer cards in digital form and onto graph paper in analog form. A sample graph is given in Figure 8. Such pictures were used for purposes of visualization only; the data which had been punched on cards were analyzed. The apparatus used to effect this data conversion is shown in Figure 9.

Basically, the arrangement shown allowed us to solve the following problem. The kinetic data were in the form of discrete spectra stored on magnetic tape as recorded voltage fluctuations. After the time of flow stop, each spectrum was a slightly decayed version of the spectrum preceding it. In order to study the kinetics of the decay, identical spectral regions had to be abstracted from successive spectra and stored in digital form.

This desired result was obtained by using a Varian C-1024 Computer of Average Transients (CAT). The CAT sampled voltages from the tape at prescribed time intervals, transforming

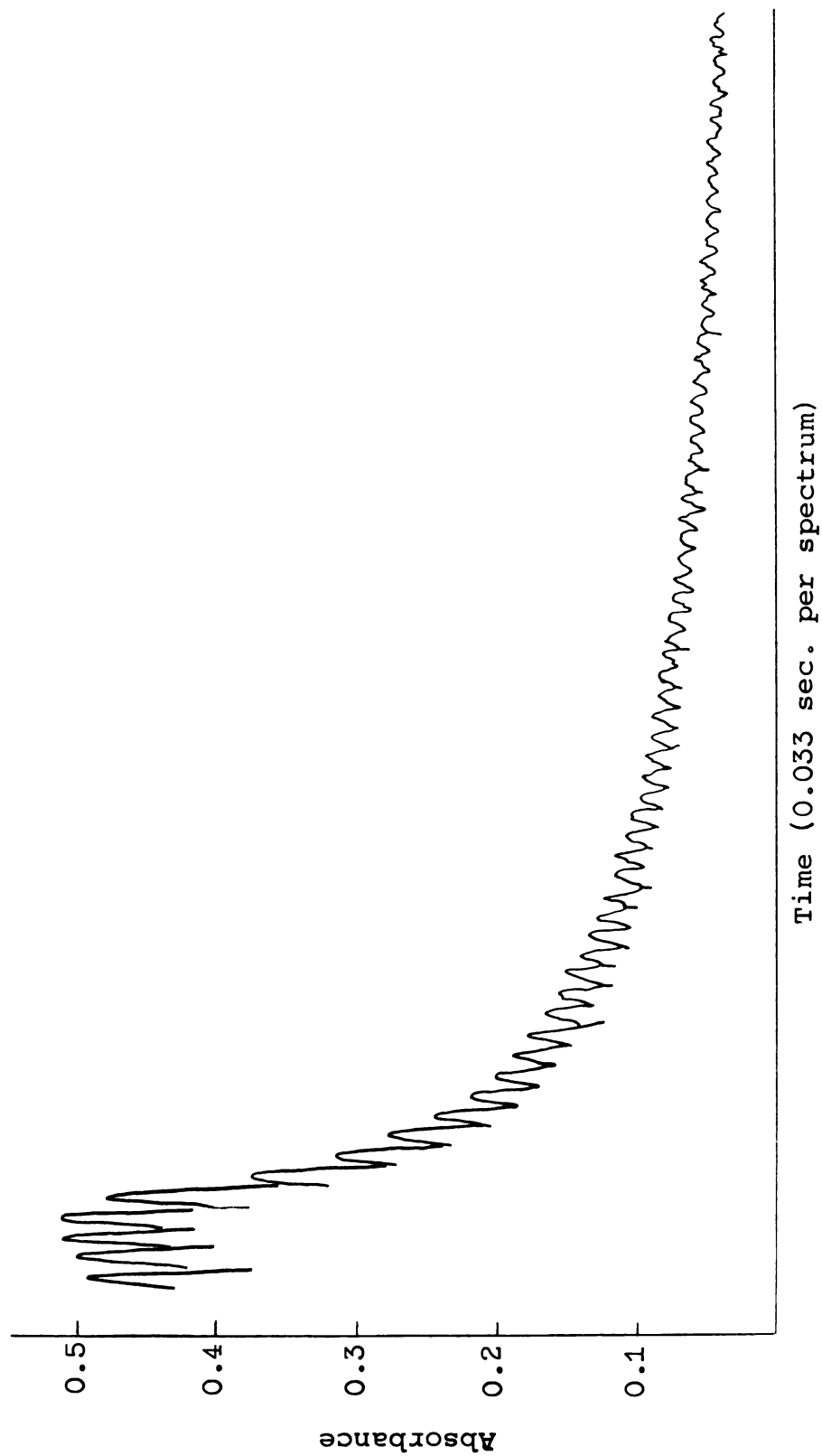


Figure 8. Decay of the 714 nm. peak of potassium anthracenide after mixing with 0.00175 M ethanol in THF.

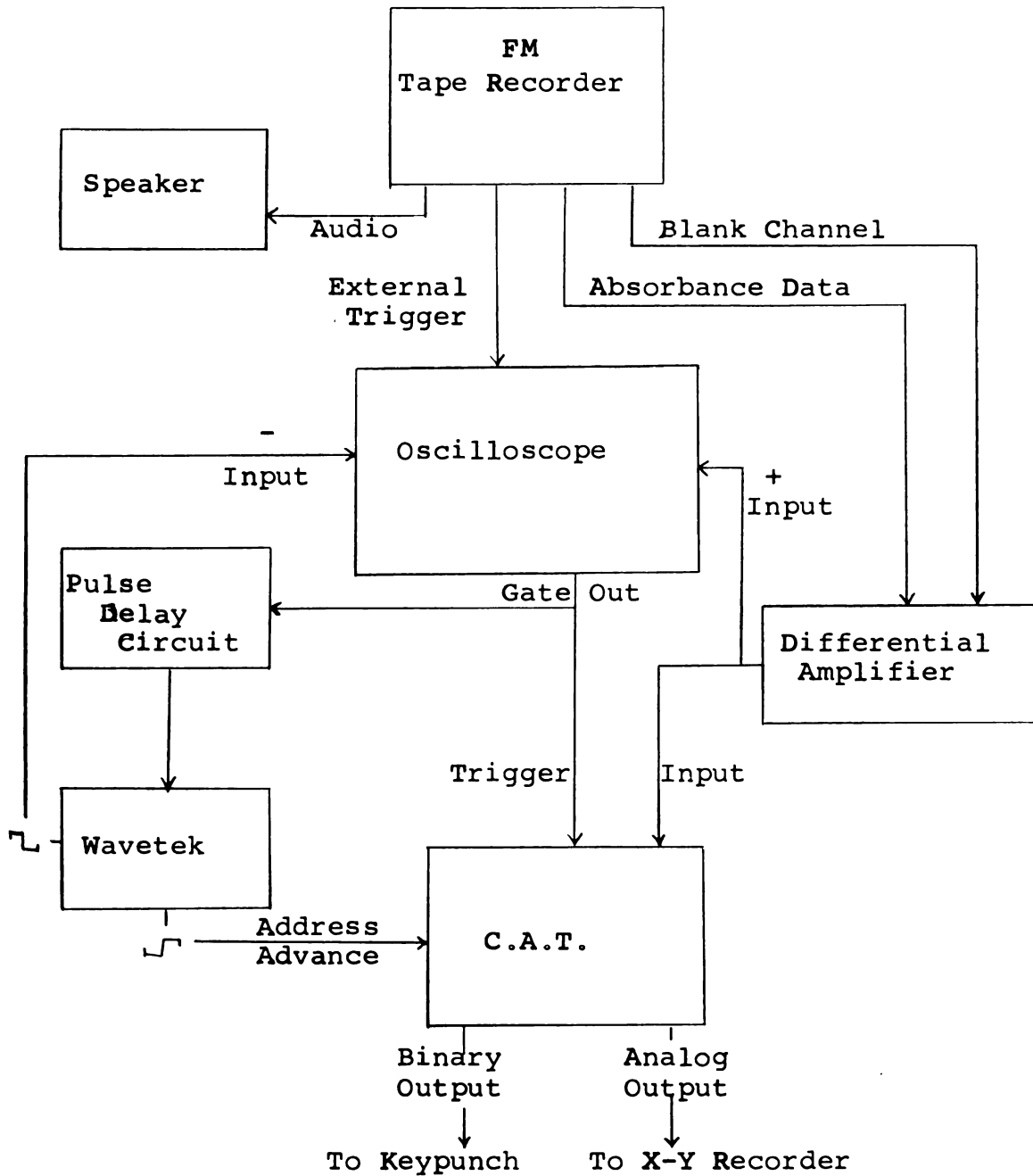


Figure 9. Block diagram of the apparatus used to transform analog data to digital form.

each voltage measurement into a number of counts and storing the result in a channel. The 1024 channels were triggered successively, but independently. By triggering the channels in the way to be discussed next, the spectra could be sampled as desired.

Suppose, for example, that we wish to study eight points near the middle of each of 128 successive peaks. As noted earlier, a trigger signal is produced at the beginning of each spectrum. If this signal is fed into a pulse delay circuit, that circuit can be made to produce yet another trigger signal after a desired time interval has elapsed. In this case, the interval chosen will be the time necessary for the recorder to have played back half of the spectrum. The second trigger commands a waveform generator to produce eight square-wave pulses which cause eight channels to be opened successively for analysis. The time between successive channel-advance pulses relates directly to the spacing, in wavelength between the measured points on the peak and is determined by the frequency of the square-wave generator. The whole system then waits for the next trigger signal from the recorder. Thus, eight measurements of the absorbance at eight different wavelengths in the same spectrum have been made and stored. Of course, the number and separation of the points may be changed by changing the number and frequency of the square waves produced by the waveform generator. When the main trigger again signals the beginning of another

spectrum, the sampling process is repeated. In this example, the sampling procedure will be repeated until eight points from each of 128 successive spectra have been measured. At this point, all 1024 channels in CAT will have been filled.

With this background information, it is possible to describe the system as a whole. The output from two of the recorder's tracks, one containing the absorbance data and the other containing only tape recorder noise, were played into a calibrated differential amplifier. Common mode recorder noise was diminished in this way. The resultant signal was sent into the CAT for conversion and into the Tektronix Storage Oscilloscope for visual observation. Simultaneously, the trigger signal entered the oscilloscope. A gated pulse could be sent out from the oscilloscope either after each spectrum or after two or more spectra had passed. Thus, not every spectrum had to be studied. This gated pulse was fed into the time base of a Tektronix Type 545 A Oscilloscope, which was used as a pulse-delay circuit. The square-waves were produced by a Model 116 Wavetek Signal Generator and were fed into both the CAT and the storage oscilloscope to be superimposed on the spectrum displayed there. In this way, it was possible to see which portion of the spectrum was being analyzed. Verbal identification of the displayed data was played through a speaker through the fourth channel. The data in the CAT were automatically punched on cards by an IBM type 526 Key punch equipped with a Varian C-1001 coupler.

The data on cards were then analyzed with a CDC-6500 computer by using programs which will now be described.

4. Data Analysis

The basic goal in the analysis was, of course, to analyze the ability of a given equation (in this case, a rate law) to describe the data. A computer program which can decide which of two or more rate laws most closely applies to a set of data has not been written. However, Dr. V. A. Nicely has written a program (KINET) which provides criteria upon which the analyst can make such a judgment.

A secondary problem was to transform the data punched by the CAT into a form acceptable to KINET. A program (PUNDAT) which was originally written by Dr. Nicely and modified by the author was used for this purpose.

a. Program PUNDAT: The input to this program consisted of a set of organizational constants, the set of spectra of the reacting aromatic anion, and a set of calibrated neutral density filter data. This latter set was included to allow corrections to be made in case the voltage measurements were not linearly dependent upon the actual absorbances over the wavelength range studied. Actually, in the present study, linearity was observed for absorbances less than 1.5 absorbance units. Therefore, since the measured absorbances were never greater than 0.7 absorbance units, such corrections were not necessary.

After this first (optional) correction for non-linearity, the program analyzed each individual spectrum for spurious electronic noise which was sometimes generated by the CAT. A polynomial was fit to each spectrum and points which deviated from this curve by more than four standard deviations were discarded.

From each calculated spectrum, the absorbance at one or more wavelengths and the time from flow-stop to the time of measurement of that spectrum were calculated. Thus, absorbance versus time curves were obtained for one or more wavelengths from the set of spectra.

In order to speed the convergence process in KINET, each absorbance-time curve was smoothed with two passes of a five-point smoothing formula. The absorbances were converted to concentrations. Finally, the program punched the resulting concentration-time curves, along with a ratio of the estimated variances of the concentration and time measurements, in a format acceptable to KINET. The variances were estimated to be $1 \times 10^{-8} \text{ sec.}^2$ and $25 \times 10^{-6}/E \text{ moles}^2 \text{ liter}^{-2}$, where E is the product of the extinction coefficient times the path length.

b. Program KINET: As stated earlier, this program cannot make decisions regarding the applicability of a particular rate law. Rather, it estimates the set of parameters (rate constants, initial concentrations, etc.) which will give the "best" correlation between a given rate law and a set of data.

The significance of the results must be decided by the user. Since the author of the program discusses both the philosophy and the methods applied in KINET (48), the emphasis in this discussion will be placed on the type of results which are obtained from KINET and the criteria that we used to interpret them.

In this program, the "best" estimates of the parameters are defined to be those obtained from a least-squares treatment of the data, i.e.,

$$S = \sum_{\text{points}} W_i F_i^2 = \text{minimum} . \quad (35)$$

The necessity for including the weights, W_i , and the method for obtaining them are discussed by Wentworth (49). In our case, the weights are given by

$$W_i = \frac{1}{\sigma_{F_i}^2} \quad (36)$$

where

$$\sigma_{F_i}^2 = \left(\frac{\partial F}{\partial t} \right)_i^2 \sigma_{t_i}^2 + \left(\frac{\partial F}{\partial c} \right)_i^2 \sigma_{c_i}^2 . \quad (37)$$

The quantities t_i and c_i are the values of the time and concentration for the i^{th} point. The quantity F_i is defined by

$$F_i = (X_i)_{\text{calc}} - (X_i)_{\text{exp}} \quad (38)$$

where

$$(X_i)_{\text{calc}} = f (Y_i)_{\text{exp}} . \quad (39)$$

Generally, in our study, the experimental values for the concentration and time at the i^{th} point were used for $(X_i)_{\text{exp}}$ and $(Y_i)_{\text{exp}}$, respectively. The dependent variable, $(X_i)_{\text{calc}}$, then became a calculated value of the concentration and was obtained from a rate law in which the independent variable was the experimental value of the time. The result of the minimization procedure was a set of values for the parameters within the rate law which allowed the best fit of the data to a given rate law as defined by Equation 35.

The results which are obtained from these calculations are values for S , F_i (the residual at point i) for all values of i , a_j (the j^{th} parameter) and σ_j (the estimated standard deviation for that parameter) for all j , and an estimate of the correlation between parameters. In addition, the computer prints comparisons of the calculated and experimental concentrations as functions of time.

Several criteria can be used to evaluate such data (50). As a first indication, the magnitude of the sum of the squares of the residuals (S) could be used to compare the "goodness of fit" of two or more rate laws applied to the same data. Since the size of S is strongly dependent upon the weighting, however, such a comparison can be misleading. A better indication is the magnitude of the individual residuals, F_i , and the randomness of the signs of the residuals.

Another potentially useful criterion is the size of the values of the parameters (a_j) relative to their estimated

standard deviations (σ_j). However, for all non-linear equations, these values of the standard deviations are only estimates and should be treated as such. The minimization method is based on a Taylor's Series expansion of the equation with truncation after the linear term. The values of σ_j are therefore dependent upon the accuracy of this linearization. Nevertheless, in general, as the value of σ_j approaches that of a_j , the applicability of the equation under investigation becomes more doubtful.

The multiple correlation coefficients give an indication of the linear dependence among the adjusted parameters. As the values of these coefficients approach unity, the ability of the program to obtain unique solutions diminishes. Often, this problem can be solved by a change in the form of the equation which is being used.

Finally, the values of the parameters must make sense in terms of the chemistry which is involved. This final criterion is simply an affirmation of the fact that a background of chemical knowledge must be applied in the interpretation of any calculation.

While the application of these criteria has not been given explicitly for each of the mechanisms studied, they have been considered in the treatment of the data. The results of the analysis are discussed in the following section.

IV. RESULTS AND CONCLUSIONS

A. A Survey of the Data

1. Preliminary Experiments

As the historical section indicates, the protonation of aromatic anions by alcohols and water has been studied by several investigators. However, the experiments were carried out in media which varied in composition from one to one hundred per cent of the proton source. Even for the case in which the concentration of ROH was lowest (43), the author suggested that its concentration was large enough to alter the properties of the medium. One of our objectives was to study the reactions at very low ROH concentrations and, consequently, in an "inert" medium. In this respect, we were entering an unexplored area.

Our first problem, then, was to decide upon a system for study. For reasons previously cited (p. 3), THF was selected as the primary solvent. The reaction between potassium biphenylide (K^+Biph^-) and methanol (Run KR1) proved to be too fast for us to study quantitatively. The pulse radiolysis studies mentioned previously (p. 23) suggested that the terphenylide anion might react more slowly, especially if less acidic proton sources were used.

Our studies of the reactions of potassium terphenylide (K^+Ter^-) with ethanol and with water (Runs KR2, 3, and 6) showed that this was indeed a slower reaction. However, solutions of the terphenylide anion were rather unstable and reacted, in the absence of ROH, to form a product with an absorption peak at 530 nm. Since the effect of such a species on the protonation of terphenylide was unknown, the results of our studies of that reaction were of questionable reliability. We were unable, at that time, to prevent the appearance of this unknown species, so we sought a more stable system for study. In experiment KR7, the reactions of potassium anthracenide (K^+An^-) with water and with ethanol were studied. Solutions of this anion in THF were stable and the reaction rates were well within our range of study. Therefore, this system (K^+An^- in THF) was chosen for further investigation.

2. Principal Experiments

The course of this investigation may be seen by inspection of Table 1, which gives a list of all the experiments we carried out.

Our choice of experiments was governed by the early observation that the reactions of anthracenide did not follow the simple rate law which was expected. In run KR8, we studied two spectral regions in an attempt to find possible intermediates and to test the reproducibility of the results of run KR7. Experiments 9 through 11 were

TABLE 1
List of Experiments

Run	Anion	ROH	Solvent	Range of ROH concentrations (M)	Number of ROH concentrations	Wavelength region (nm)
KR1	$K^+ Biphen^-$	MeOH	THF	1.1-0.025M	3	550-900
KR2,1-7	$K^+ Ter^-$	EtOH	THF	$(1.0-0.25) \times 10^{-3}$	3	550-900
KR2,8-9	$K^+ Ter^-$	EtOH	THF	2.5×10^{-3}	1	400-600
KR2,10-12	$K^+ Ter^-$	H ₂ O	THF	1.0	1	400-600
KR3-4	$K^+ Ter^-$	anion solutions were unstable; no data obtained				
KR5-6	$K^+ An^-$	anion solutions were unstable; no data obtained				
KR7,1-4	$K^+ An^-$	H ₂ O	THF	0.36-0.038	4	550-900
KR7,5-6	$K^+ An^-$	EtOH	THF	$(4.32-2.20) \times 10^{-3}$	2	550-900
KR7,7	$Na^+ \cdot An^-$	EtOH	THF	2.20×10^{-3}	1	550-900
KR8,1-3	$K^+ An^-$	H ₂ O	THF	0.5-0.08	3	400-600
KR8,4-5	$K^+ An^-$	H ₂ O	THF	0.22-0.08	2	550-900
KR9,1-2	$Na^+ \cdot An^-$	H ₂ O	THF	0.047-0.0046	2	550-900
KR9,3-6	$Na^+ \cdot An^-$	EtOH	THF	$(5.0-0.27) \times 10^{-3}$	4	550-900
KR9,7-8	$Na^+ \cdot An^-$	H ₂ O	THF	$(2.3-1.1) \times 10^{-3}$	2	550-900
KR9,9-10	$K^+ An^-$	H ₂ O	THF	0.047-0.0041	2	550-900
KR9,11-14	$K^+ An^-$	EtOH	THF	$(5.0-0.48) \times 10^{-3}$	4	550-900
KR10,1-3	$K^+ An^-$	iso-PrOH	THF	0.114-0.011	3	550-900
KR10,4-6	$K^+ An^-$	t-BuOH	THF	0.020-0.0054	3	550-900

KR10, 7-9	K ⁺ An ⁻	MeOH	THF	(3.7-0.5)x10 ⁻³	3	550-900
KR10, 11-18	K ⁺ An ⁻	EtOH	THF	(6.45-1.35)x10 ⁻³	8	550-900
		+EtO ⁻		(3.87-0.85)x10 ⁻³		
KR11, 1-5	K ⁺ An ⁻	H ₂ O	THF	0.07	4	550-900
		+OH ⁻		(5.75-1.92)x10 ⁻³		
KR11, 7-9	Na ⁺ An ⁻	EtOH	THF	(2.82-0.84)x10 ⁻³	3	550-900
KR11, 10-13	Na ⁺ An ⁻	H ₂ O	THF	0.0163-0.0399	4	550-900
KR12	K ⁺ Ter ⁻	anion solutions were unstable, no data obtained				
KR13, 2-5	K ⁺ An ⁻	H ₂ O	DME	0.0357-0.00358	3	550-900
KR13, 6-8	K ⁺ An ⁻	EtOH	DME	(2.63-0.68)x10 ⁻³	3	550-900
KR13, 9-11	Na ⁺ An ⁻	EtOH	DME	(2.63-0.91)x10 ⁻³	3	550-900
KR13, 12-15	Na ⁺ An ⁻	H ₂ O	DME	0.0357-0.0085	4	550-900
KR14, 2-5	K ⁺ Ter ⁻	EtOH	THF	(3.00-0.42)x10 ⁻³	4	830

examinations of the effects of the proton donor, the counter-ion, and RO^- . In KR13, the effect of changing to a different solvent (dimethoxyethane) was studied. Finally, in KR14, we were able to obtain a stable solution of potassium terphenylide. Thus, the effect of the proton acceptor was also studied.

3. Discussion of the Data

Table 1 gives a comprehensive list of the experiments which were performed. With the following exceptions, the results of all of these experiments were used in the data analysis. Two sets of experiments contained flaws which precluded a meaningful interpretation. Consequently, they were not considered in the analysis.

The first set consisted of the early attempt to study potassium terphenylide (KR2). As stated earlier, these solutions contained observable (approximately 10^{-4} M) quantities of an unidentified impurity. The presence of this impurity caused us to reject this run.

The second set comprised much of the first part of run KR9. At least two mechanical difficulties combined to cause the decay curves to be unusable. The stopping mechanism was not functioning properly, which caused the initial part of the curve to be poorly defined. At the same time, mechanical vibration in the flow system produced a sinusoidal variation in the observed signal. Figure 10 shows one of these decay curves. It should be contrasted with the kinetic decay shown in Figure 11, which is representative of the majority

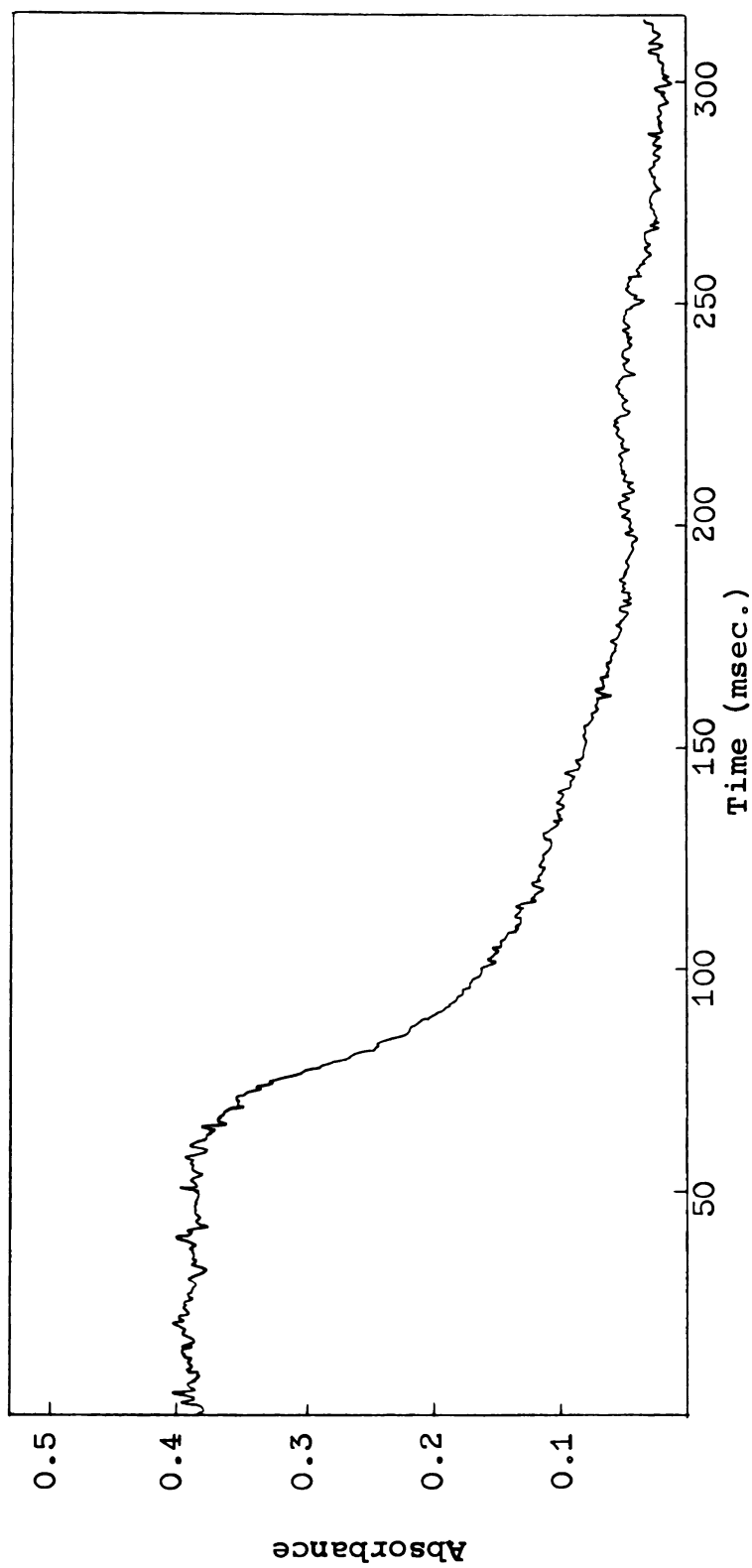


Figure 10. The decay of sodium anthracenide upon mixing with 0.000498M ethanol in THF. The problems of mechanical vibration and poor stopping are illustrated. The spectrum was monitored at 714 nm.

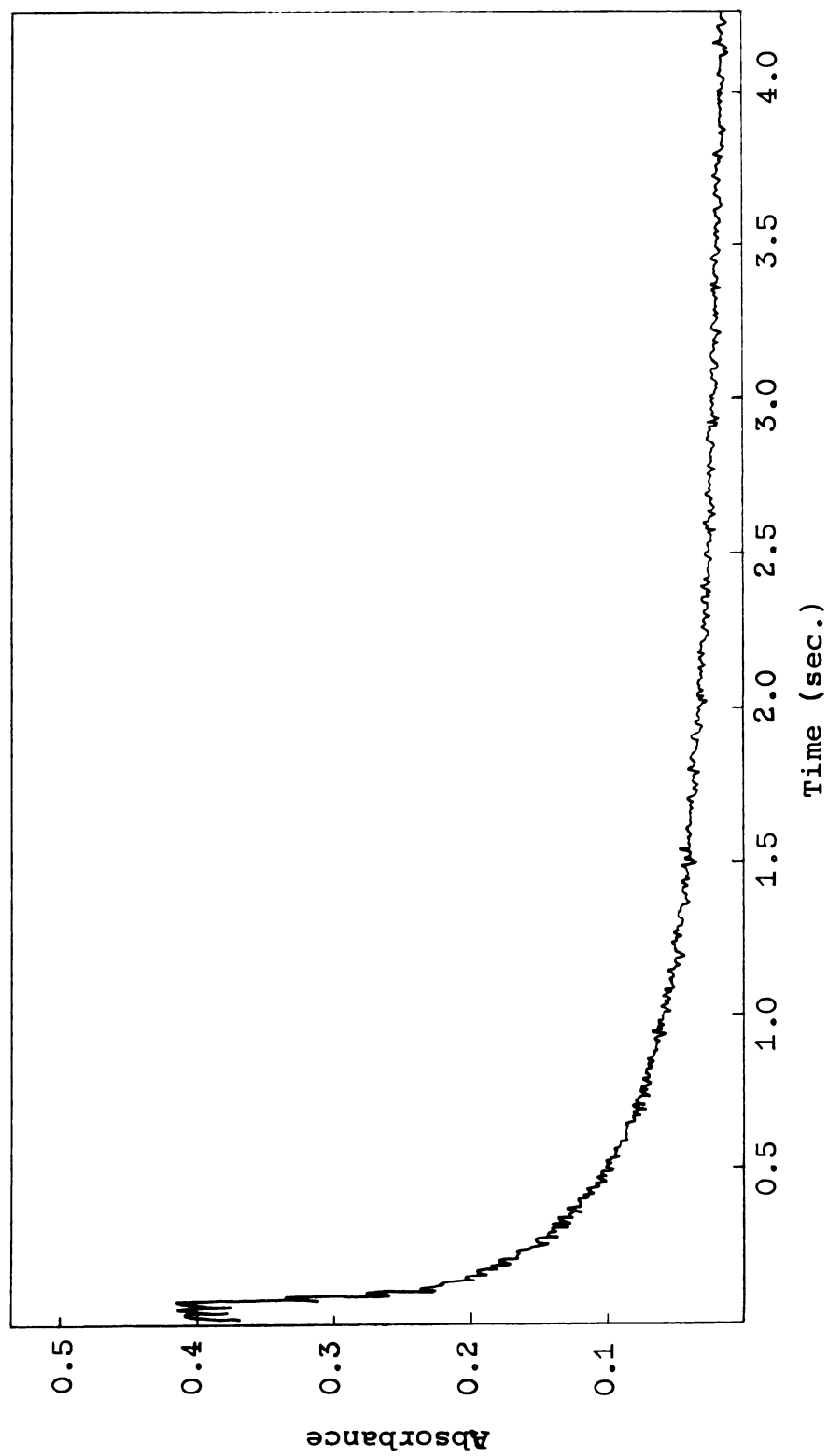


Figure 11. The decay of sodium anthracenide upon mixing with 0.00282M ethanol in THF. This push is representative of the majority of the data. A segment of the 714 nm. peak was scanned.

of our data. These mechanical difficulties were noticed during the analysis of the data after the run and their causes were eliminated as far as possible. While the mechanical vibration was virtually eliminated, the flow-stop continued to be a problem in the study of reactions with half-times of 20 msec. or less. It is possible that an abrupt flow-stop was not attained because of relaxation of the Teflon under pressure.

With the elimination of these data sets, about half of the data which were to be used to examine the effect of changing the cation and the anion were lost. The data which remained will be discussed later. We emphasize this problem, not because of any deficiency in the remaining data, but rather because the checks for reproducibility between runs are absent.

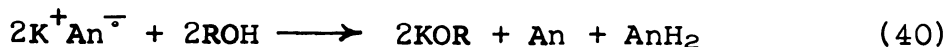
4. Summary

The bulk of our data deals with the reactions of potassium anthracenide with various proton donors. The dependence of this reaction on the particular proton source, the concentration of RO^- , and the solvent were studied. Sufficient data are available to assure us of the internal consistency of the experiments. Several conclusions will be drawn from these results. However, the studies of the dependence on the anion and the counter-ion were not as complete. Their results show some interesting trends, but confirmation of these trends must await further experimentation.

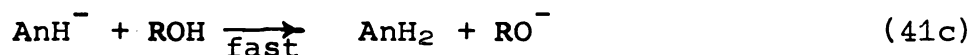
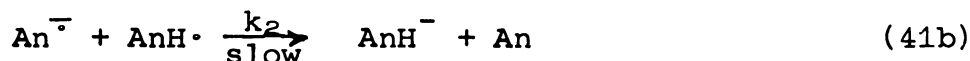
B. Results

1. Dependence on the Anion Concentration

A plausible mechanism for the reaction



might have been derived from Weissman's suggested mechanism simply by assuming all steps to be irreversible, as shown below.



Polarographic studies (7) indicate that the second protonation is faster than the first. Assumption of a steady state concentration for $[AnH^\bullet]$ leads to a first-order decay in $[An^-]$. If Equation 41b is considered to be reversible and the steady state is assumed for both $[AnH^\bullet]$ and $[AnH^-]$, a rate law for the disappearance of An^- may be derived. It is complex, but first-order in $[An^-]$. Of course, replacement of Equation 41b by a fast equilibrium step would cause 41a to be the slow step. A simple rate law which is first-order in $[An^-]$ results (Equation 42):

$$\frac{-d[An^-]}{dt} = k_1 [An^-] [ROH] \quad (42)$$

Certainly, the results of earlier work in other systems make such a mechanism plausible for those systems.

We expected to observe similar behavior. Accordingly, our first efforts were directed toward the confirmation or negation of this supposition. The first graph in Figure 12 contains a plot of the logarithm of the absorbance of $[\text{An}^{\ominus}]$ versus time for the reaction with water. The straight line was drawn by using the pseudo-first-order rate constant which was calculated from a linear least-squares fit of the data. A pseudo-order treatment was certainly justified, since the initial concentration of water was at least one hundred times that of the anion. Such non-adherence to first-order dependence was observed in the reactions of potassium anthracenide with each of the alcohols, as well as with water, in THF. Therefore, the first-order rate law was considered to be invalid for this system.

The deviation from first-order shown in Figure 12 seemed to indicate a decay which was closer to second-order in $[\text{An}^{\ominus}]$. When the rate law

$$\frac{-d[\text{An}^{\ominus}]}{dt} = k_{ps} [\text{An}^{\ominus}]^2 \quad (43)$$

was used to fit the same data set, the results shown in the second graph in Figure 12 were obtained. This ability of a pseudo-second-order rate law to describe individual decay curves over at least three to four half-lives was observed for every reaction of potassium anthracenide, providing, of course, that the ROH concentrations were high enough to permit a pseudo-order treatment. Figure 13 presents two more examples of this behavior.

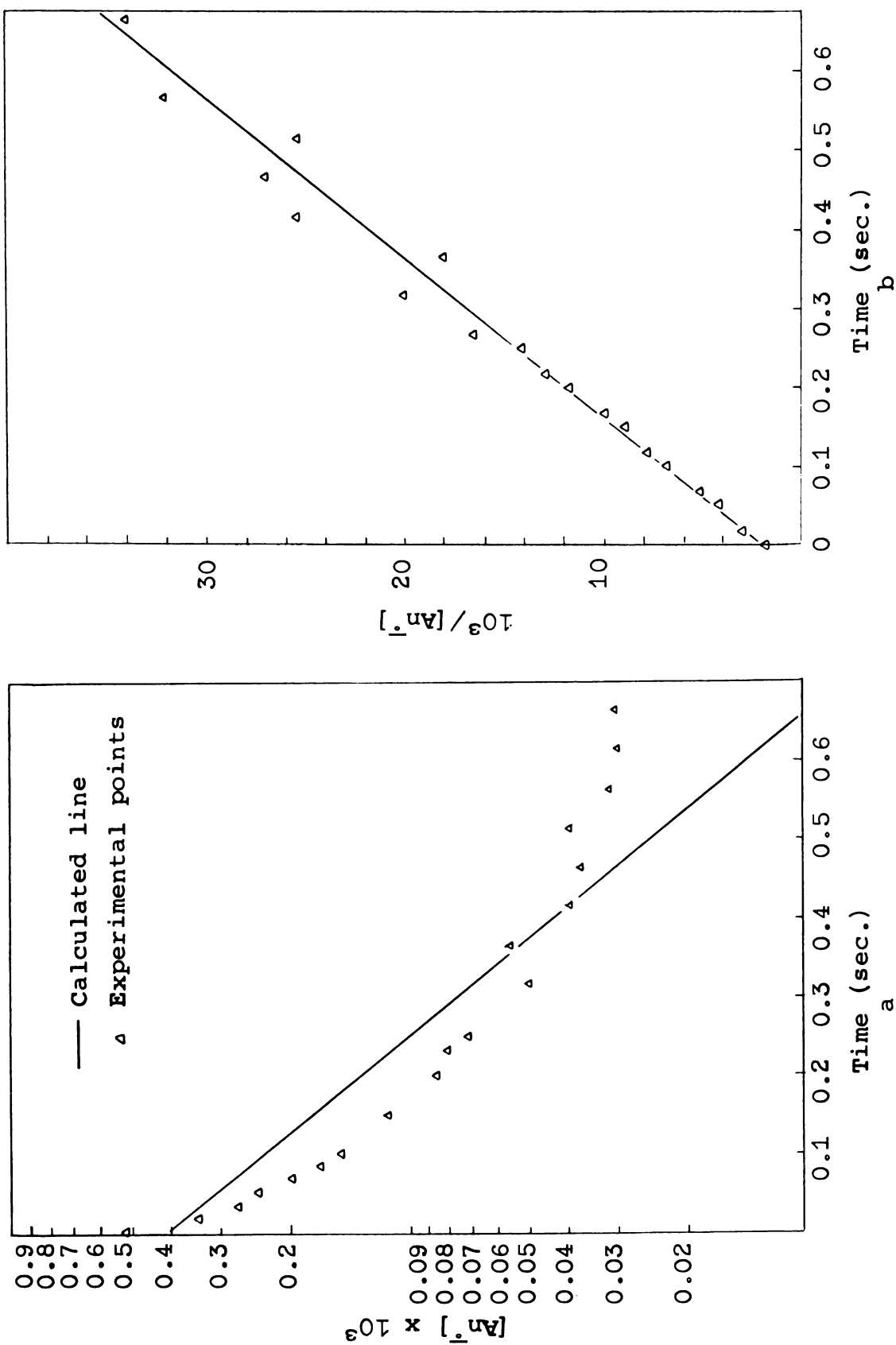


Figure 12. Pseudo-first-order (a) and pseudo-second-order (b) kinetics applied to the reaction of potassium anthracenide with 0.223 M water in THF.

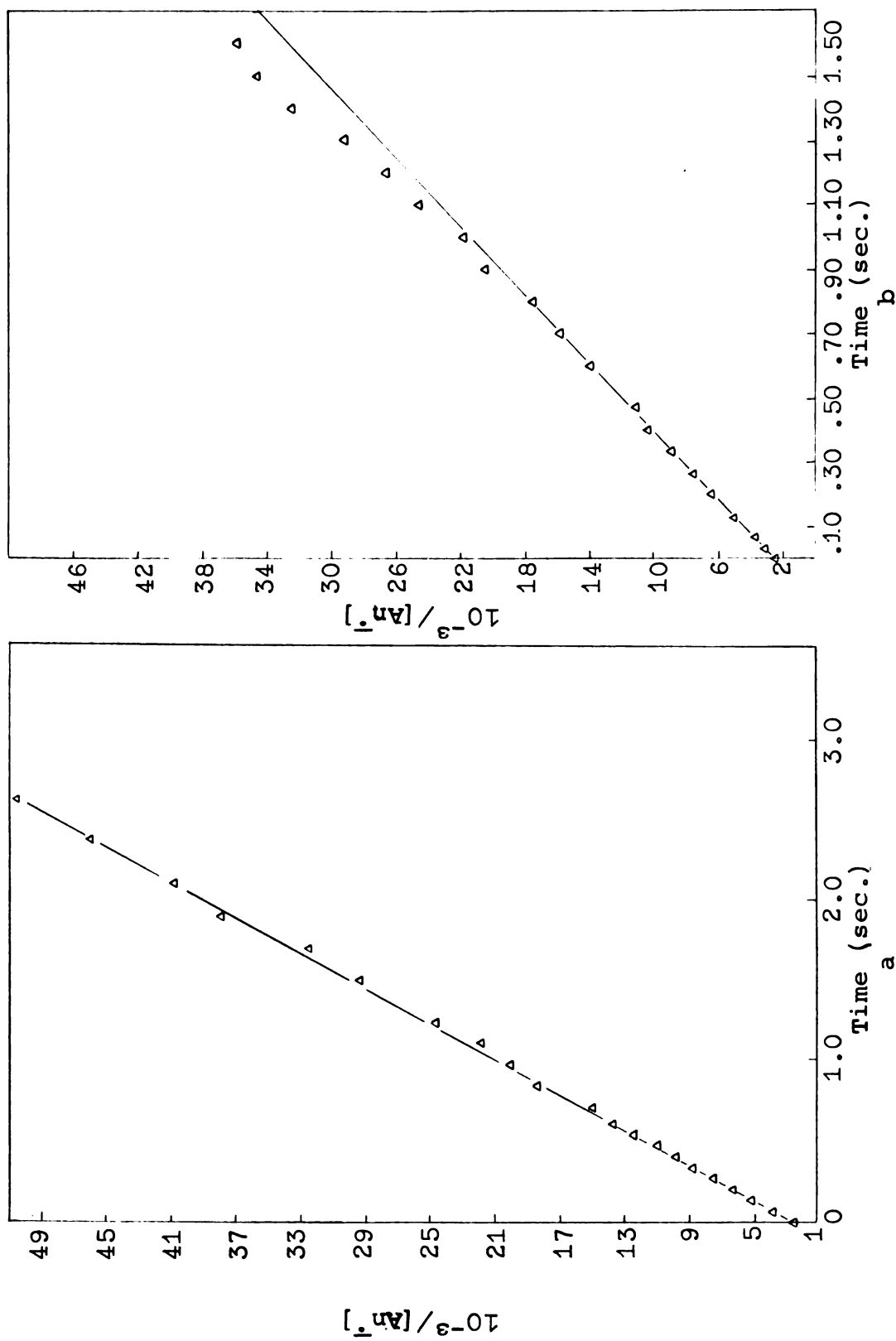


Figure 13. Pseudo-second-order plots of the reactions of potassium anthracenide with (a) 3.08×10^{-3} M ethanol and with (b) 5.40×10^{-3} M t-butanol in THF.

2. Dependence on ROH

The applicability of pseudo-order kinetics allowed us to use the following method to determine the dependence of the reaction on the concentration of the proton donor. While equation 43 described individual decay curves for the reaction with a given proton donor, the pseudo-second-order rate constants, k_{ps} , varied with the initial concentration of the donor. Since the order in ROH may be expressed by

$$k_{ps} = k[ROH]^n, \quad (44)$$

or

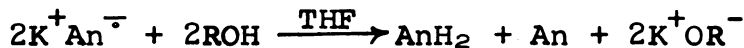
$$\log k_{ps} = \log k + n \log [ROH], \quad (45)$$

the variation of $\log k_{ps}$ with the logarithm of $[ROH]_{initial}$ was treated by the method of least-squares. The values of the order, n , and plots of $\log k_{ps}$ vs. $\log [ROH]_{initial}$ which resulted from this analysis are given in Tables 2 and 3 and in Figures 14 and 15. No value for the reaction with methanol is reported, since pseudo-second-order kinetics does not apply to this case because of the low initial concentrations of methanol. The notation $\bar{k} \pm a$ represents the averaged values of the rate constant and standard deviation obtained from two or more individual experiments.

Two important conclusions can be made on the basis of the results given in Table 3. First, the order with respect to $[ROH]$ is certainly less than unity in all cases and probably is less than 0.5 in most cases. Second, the order is not necessarily the same for all of the alcohols. Both of these observations imply a complex mechanism for the reaction.

TABLE 2

Pseudo-second-order Rate Constants for the Reaction



Run	[MeOH] ₀ × 10 ⁴ M	[An ⁻] ₀ × 10 ⁴ M _{av.}	$\bar{k} \times 10^{-3} \text{ M}^{-1} \text{ sec}^{-1}$	
KR10,7	4.48	5.4	---	*
KR10,8	12.0	5.7	---	*
KR10,9	20.1	5.2	2.01 ± .02	
	[EtOH] ₀ × 10 ³ M		$\bar{k} \times 10^{-4} \text{ M}^{-1} \text{ sec}^{-1}$	
KR7,6	2.20	3.4	2.20 ± .06	
KR9,11	0.485	5.2	---	*
KR9,12	1.00	6.0	---	*
KR9,13	2.42	6.3	1.14 ± .01	
KR9,14	5.00	6.1	1.60 ± .02	
KR10,11	1.75	4.6	1.23 ± .01	
KR10,12	1.35	5.8	0.93 ± .02	*
KR10,13	3.08	3.8	1.82 ± .01	
KR10,14	4.78	4.0	2.54 ± .01	
KR10,15	6.45	4.2	3.02 ± .02	
	[iso-PrOH] ₀ × 10 ⁺¹ M			
KR10,1	1.14	3.7	5.94 ± .1	
KR10,2	0.55	5.2	4.20 ± .05	
KR10,3	0.12	5.2	2.86 ± .03	
	[t-BuOH] ₀ × 10 ² M			
KR10,4	0.80	4.3	2.20 ± .02	
KR10,5	0.54	4.2	1.75 ± .02	
KR10,6	2.03	5.3	3.05 ± .02	
	[H ₂ O] ₀ × 10 ¹ M			
KR7,1	3.60	1.5	8.91 ± .44	
KR7,2	1.85	1.9	6.03 ± .13	
KR7,3	1.11	2.2	4.40 ± .19	
KR7,4	0.378	2.4	3.22 ± .06	
KR8,4	0.860	6.0	3.69 ± .11	
KR8,5	2.23	5.5	5.12 ± .10	
KR9,9	0.0414	5.6	1.07 ± .01	
KR9,10	0.471	5.8	3.62 ± .07	

* Pseudo-second-order treatment probably not valid because of low initial donor concentration.

TABLE 3

Values of the Order, n , of ROH in the Reactions of
 K^+An^- with ROH in THF

	EtOH	iso-PrOH	t-BuOH	H ₂ O
n	$0.53 \pm .15$	$0.33 \pm .03$	$0.41 \pm .04$	$0.44 \pm .04$

If a value for the order in [ROH] could be established such that one value of n applied to all of the alcohols, it would be possible to determine the dependence of the rate constant (k) on the acidity of the alcohol. Tabulation and ordering of the values of k would then indicate the importance of the protonation step (or steps) in determining the rate of reaction. This was done for the rates of decay of the anions produced by pulse radiolysis of solutions of biphenyl and of anthracene in various alcohols (36). The calculated bimolecular rate constants were shown to increase with the acidity of the alcohol. Such results were interpreted to mean that the reaction being studied was, indeed, a proton transfer from the alcohol.

Since this is such an important point, let us assume for the moment that the reaction follows the rate law

$$\frac{-d[An^-]}{dt} = k [An^-]^2 [ROH]^{\frac{1}{2}} \quad (46)$$

This is probably incorrect, but it will enable us to calculate

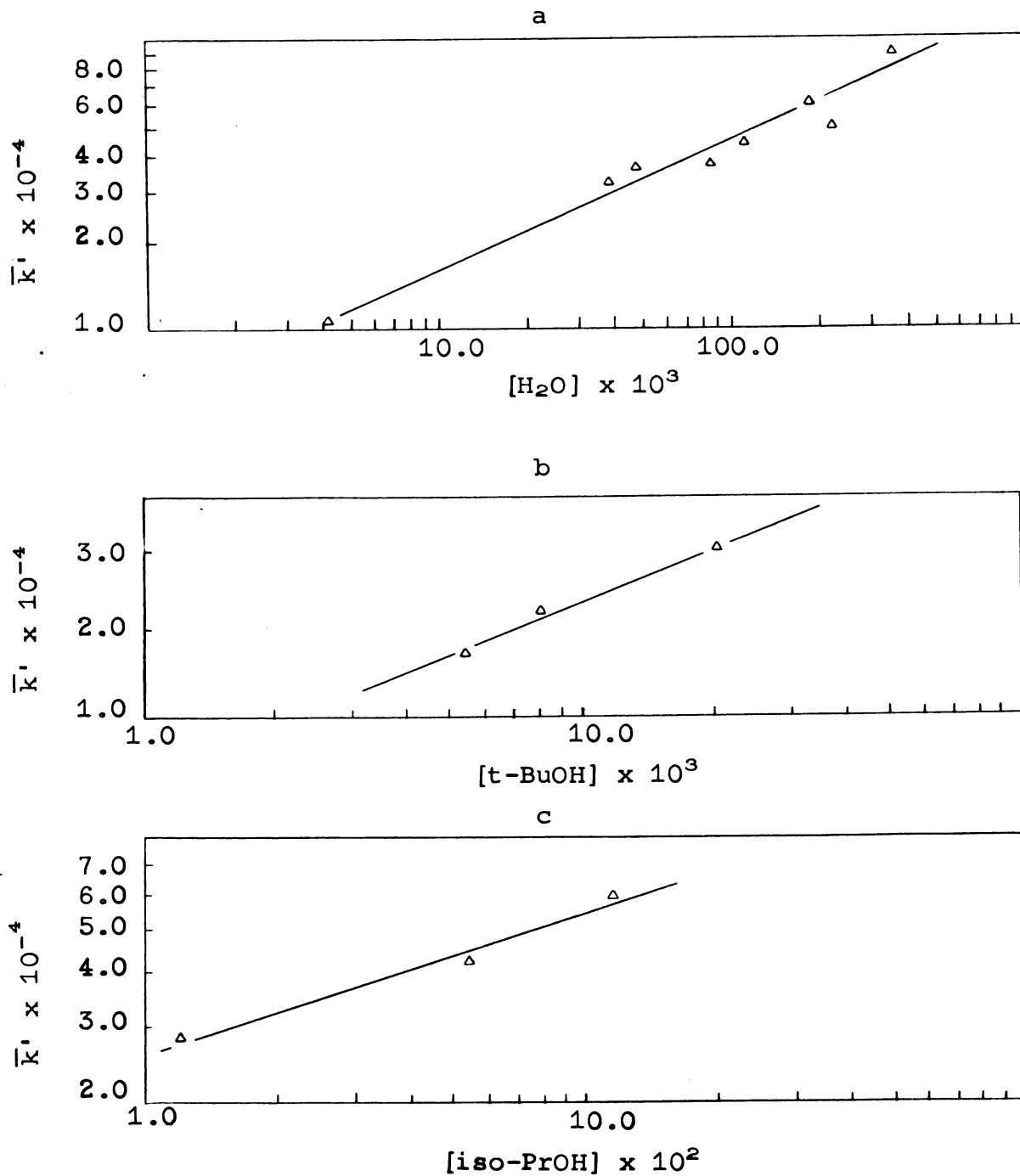


Figure 14. Determination of the $[\text{ROH}]$ dependence. $\log \bar{k}'$ is plotted vs. $\log [\text{ROH}]$ for the reactions of K^+An^- with (a) water, (b) t-butanol, and (c) iso-propanol in THF.

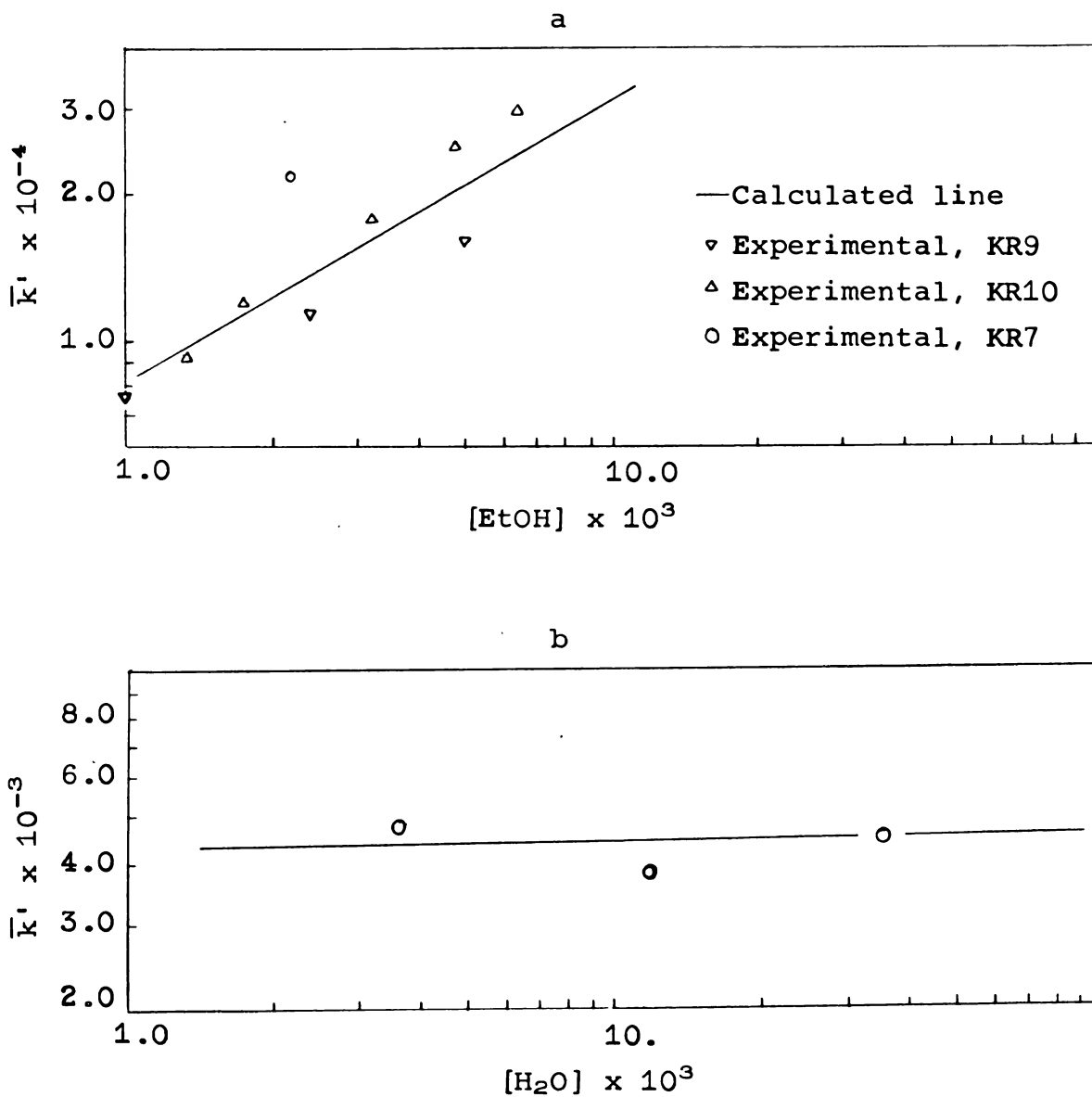


Figure 15. Determination of the $[\text{ROH}]$ dependence. $\log \bar{k}'$ is plotted vs. $\log [\text{ROH}]$ for the reactions of K^+An^- with (a) ethanol in THF and (b) water in DME.

and compare estimates of the rate constants for the various alcohols used. The results are shown in Table 4.

TABLE 4

Rate Constants Calculated from Equation 46 for the
Reactions of Potassium Anthracenide with Various
Proton Donors in THF

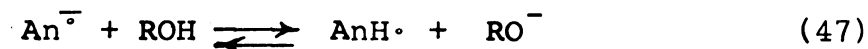
	MeOH	EtOH	iso-PrOH	t-BuOH	H ₂ O
$k(M^{-3} \text{ } ^2\text{sec}^{-1})$	3.28×10^5	3.76×10^5	1.79×10^5	2.14×10^5	1.48×10^5

Realizing that these results are likely to be only qualitatively meaningful, we can only say that the smaller, more acidic alcohols do react more rapidly than do the larger alcohols. Thus, it becomes necessary to retain a protonation step in any mechanism we might propose. Furthermore, protonation must either compete with, or come before, the major rate-determining step. The protonation reaction cannot be the only rate-limiting step, since this would give first-order behavior.

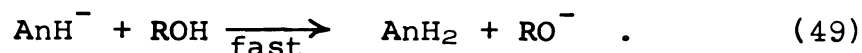
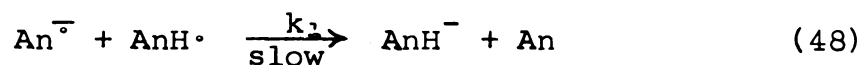
Later, a mechanism which accounts for the variation in dependence on alcohol concentration will be proposed. At that time a more quantitative treatment of the data will be given.

3. Dependence on RO⁻

Since acid-base reactions are often very rapid, we might expect the protonation step



to be fast and reversible. This might be followed by consecutive electron and proton transfers as shown in Equations 48 and 49:



Regardless of the nature of the steps which follow Equation 47, however, the first reversible protonation of An^{•-} requires that the overall rate be suppressed by the addition of RO⁻. Indeed, such an effect could have caused the observed deviation from first-order dependence on the alcohol. For instance, if the concentration of AnH[•] is assumed to be in a steady state, Equations 47 through 49 predict the following rate law:

$$\frac{-d[\text{An}^{\cdot-}]}{dt} = k_1 K [\text{An}^{\cdot-}]^2 \frac{[\text{ROH}]}{[\text{RO}^-]} \quad (50)$$

In order to test for such a reversible protonation, the initial concentration of alkoxide was varied while that of the proton source was kept constant. This experiment was carried out for the reactions of potassium anthracenide with both water and ethanol. A pseudo-second-order equation (51)

was used to fit the data

$$\frac{-d[\text{An}^-]}{dt} = k_{ps} [\text{An}^-]^2 . \quad (51)$$

Figure 16 gives a typical example of the calculated and experimental decay curves. The existence of a reversible proton transfer (Equation 47) requires that k_{ps} decrease with added RO^- . Equations 47 through 49, for example, predict that this decrease should be described by Equations 52 and 53:

$$k_{ps} = k_1 K \frac{[\text{ROH}]}{[\text{RO}^-]} \quad (52)$$

$$\log k_{ps} = \log(k_1 K [\text{ROH}]) - \log [\text{RO}^-] . \quad (53)$$

Figure 17 shows that changing the alkoxide concentration does not affect the reaction rate. Therefore, the reaction mechanism may not include, before the rate-determining step, an equilibrium of the type given by Equation 47. As a result, it is necessary to discard the mechanism described by Equations 47 through 49. One possibility which cannot be tested by these experiments is the reversible attachment of ROH to An^- without formation of RO^- (Equation 54):



This possibility will be commented upon later.

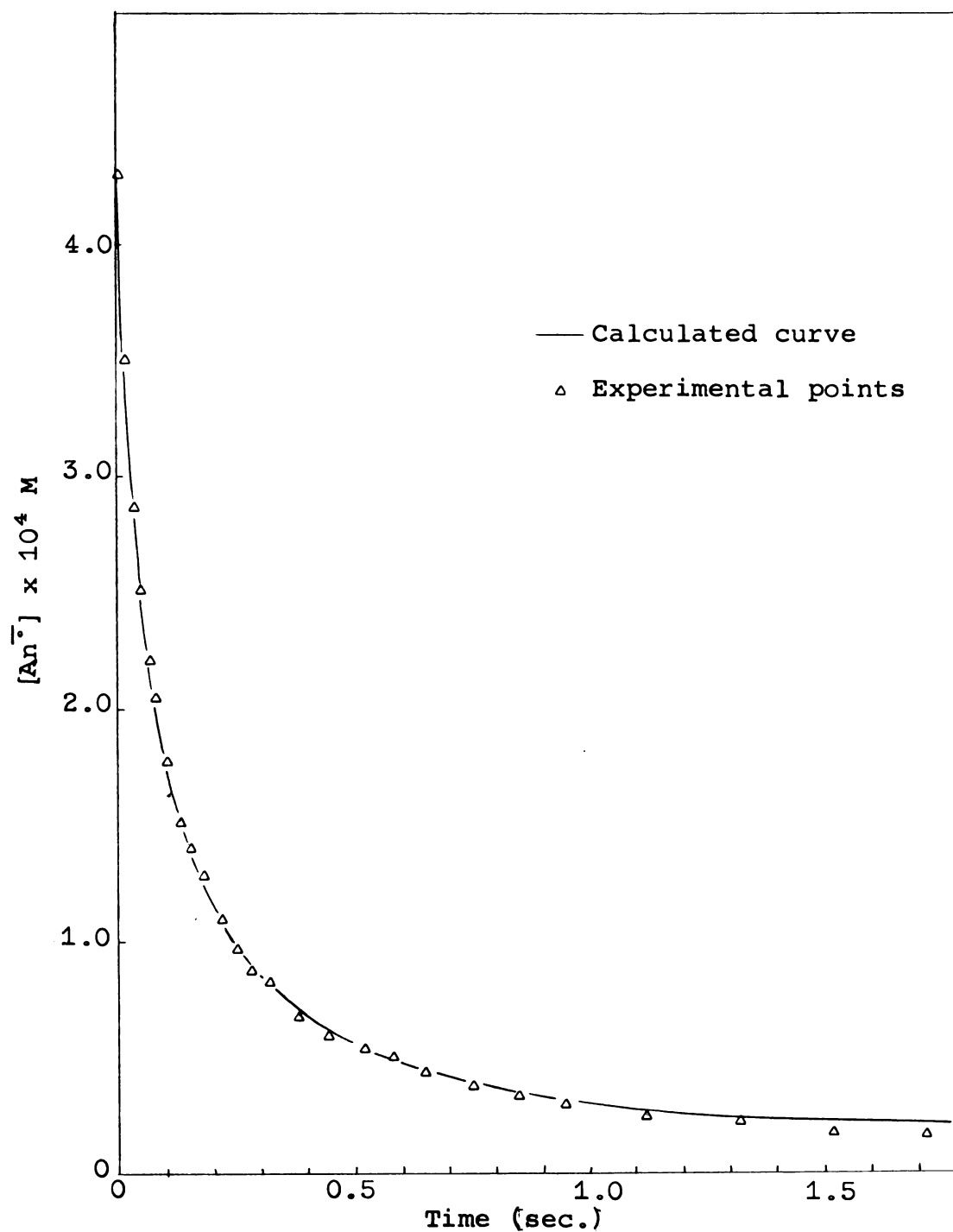


Figure 16. A pseudo-second-order curve and the observed decay of K^+An^- after mixing with 0.00605M ethanol and 0.00214M potassium ethoxide in THF.

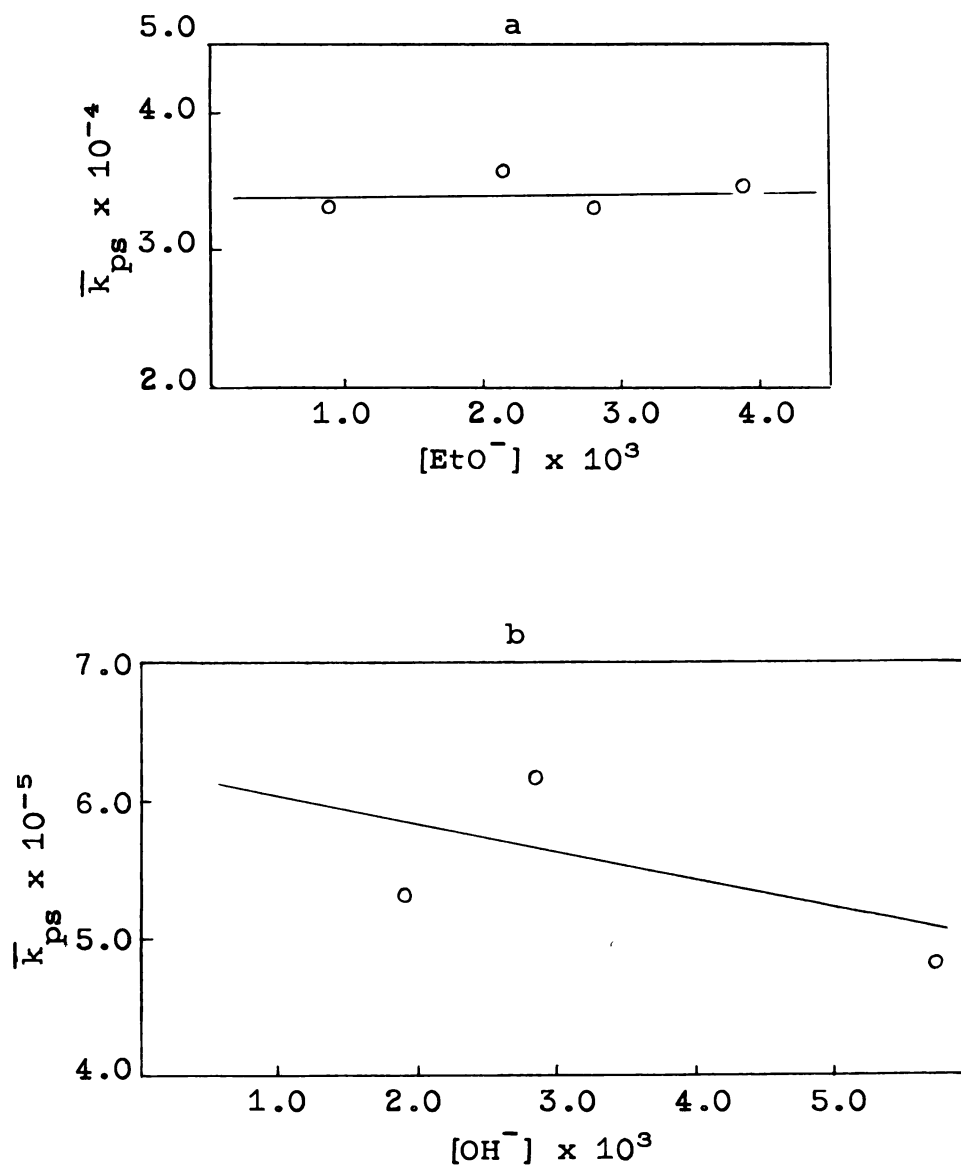


Figure 17. Determination of the effect of RO^- . The pseudo-second-order rate constants are plotted vs. the concentrations of RO^- for the reactions of K^+An^- with (a) $6.4 \times 10^{-3} M$ ethanol and (b) $0.07 M$ water in THF.

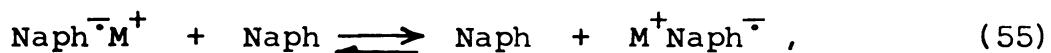
4. Search for Intermediates

It would be an important aid to the development of a mechanism if intermediate species could be observed during the reaction. Since our only means of observation is spectroscopic, direct evidence for intermediate species can be obtained in only one of two ways. If the intermediate has an absorption peak in a region which is free of absorptions due to other species and if this intermediate exists in quantities great enough to be observed, then we should be able to observe the appearance and decay of that peak. No new peaks were observed in the range from 300 to 750 nm. The second possibility is that the absorption peak of an intermediate might occur beneath one of the peaks of either anthracene or anthracenide. In this case, the rate of decay of the major peak should be wavelength dependent. No wavelength dependence was observed for the potassium anthracenide bands at 369 and 714 nm. While some changes were seen in the series of anthracene peaks which occur from 292 to 374 nm., analysis indicated that these variations were due to residual absorbances of anthracenide bands.

Of course, this does not disprove the existence of intermediates at concentrations which are too low to permit direct observation. This suggests that the steady-state treatment may be applied to postulated intermediates.

5. Dependence on Solvent

Hirota et al. (26) obtained evidence that, in the reaction



where "Naph" represents naphthalene, the electron transfer proceeded more slowly for contact ion-pairs than for the solvent-separated form. Both cation and solvent effects were noted. Since ion-pairing has been shown to occur in the system under investigation and to be very dependent upon the solvent, it seemed important to observe the effect of a more polar and/or more strongly solvating medium on the reaction in order to determine whether or not ion-pairing affects proton-transfer rates.

Dimethoxyethane (DME) was chosen to be the solvent for this experiment. Although the dielectric constants of DME and THF are approximately the same (7.15 and 7.39 at 25°C for DME and THF, respectively), the ability of DME to solvate cations is greater (24). Consequently, the formation of solvent-separated ion-pairs is favored in DME. The expectation was that the protonation reactions would proceed more rapidly in DME.

As test cases, we mixed potassium anthracenide with water and with ethanol in DME. As usual, the resulting reactions were second-order in $[\text{An}^-]$ (Figure 18). The rate, however, was much slower in DME. While in THF the pseudo-second-order rate constants were of the order of 3 to $6 \times 10^4 \text{ M}^{-1} \text{ sec}^{-1}$, in DME they were around $1 \times 10^3 \text{ M}^{-1} \text{ sec}^{-1}$. The reaction appeared to be zero-order in the concentration of water, as shown in Table 5 and Figure 15. Because of the

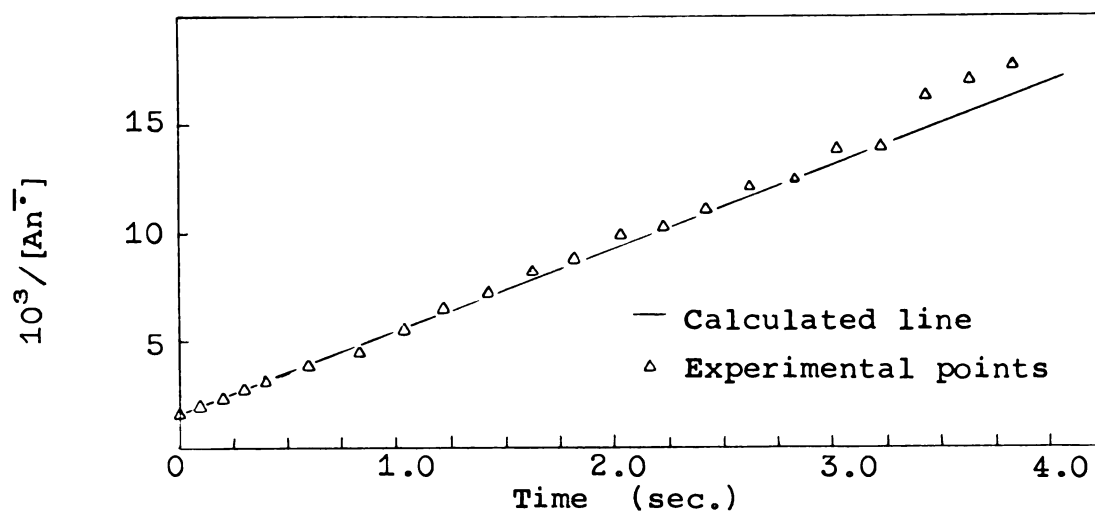


Figure 18a. Pseudo-second-order kinetics applied to the reaction $K^+An^- + .0118\text{ M H}_2\text{O}$ in DME.

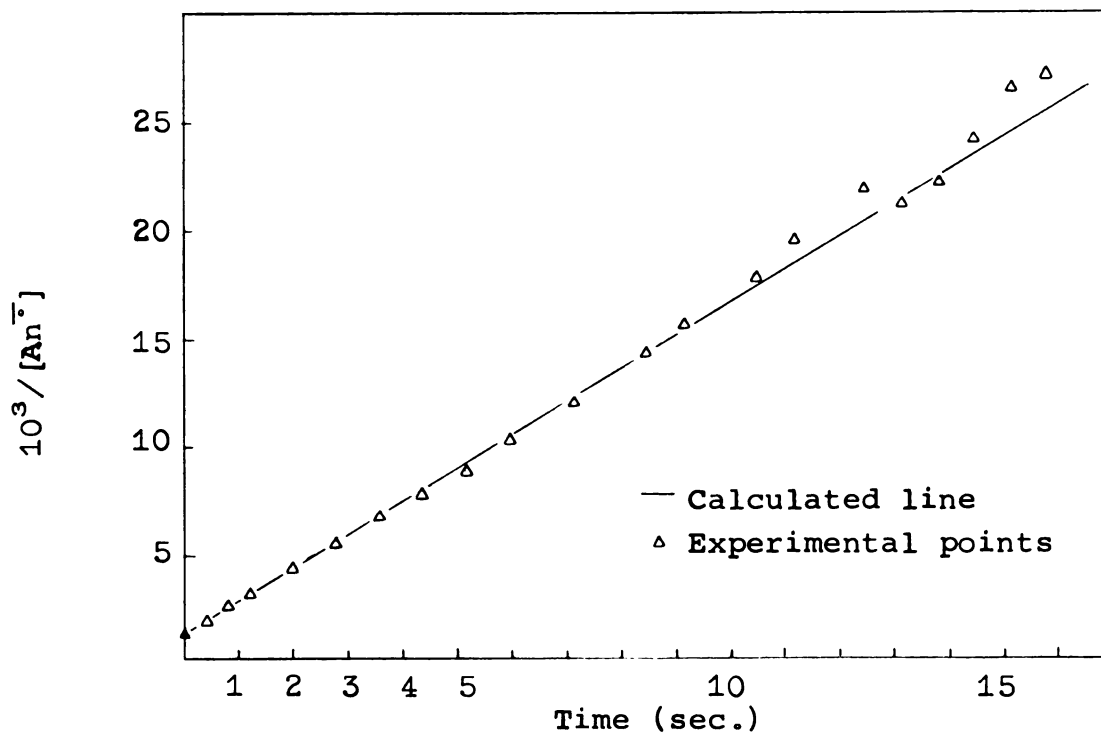


Figure 18b. Pseudo-second-order plot of the reaction of potassium anthracenide with $.00263\text{ M ethanol}$ in DME.

TABLE 5

Pseudo-second-order Rate Constants for the Reactions
of Potassium Anthracenide with (a) Ethanol and
(b) Water in DME

5a			
Run	$[\text{EtOH}] \times 10^3 \text{M}$	$[\text{An}^-] \times 10^4 \text{M}$	$\bar{k} (\text{M}^{-1} \text{sec}^{-1}) \times 10^{-3}$
KR13,6*	0.68	5.5	$0.96 \pm .02$
KR13,7*	1.33	6.2	$0.79 \pm .02$
KR13,8	2.63	7.2	$1.46 \pm .02$
5b			
Run	$[\text{H}_2\text{O}] \times 10^2 \text{M}$	$[\text{An}^-] \times 10^4 \text{M}$	$\bar{k} (\text{M}^{-1} \text{sec}^{-1}) \times 10^{-3}$
KR13,2	0.36	1.4	$4.83 \pm .09$
KR13,4	3.57	4.4	$4.54 \pm .09$
KR13,5	1.18	5.9	$5.31 \pm .07$

* This concentration is so low that pseudo-second-order kinetics certainly are not applicable.

low concentrations of ethanol which were used, the pseudo-order method could not be used to determine the order with respect to $[\text{ROH}]$. The results shown in Table 5 indicate that it is greater than zero, however.

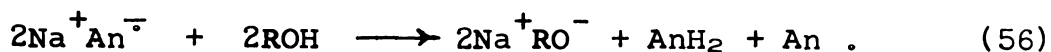
Thus, it appears that stronger solvation does not enhance the rate of the reaction. Rather, the results in DME suggest that the mechanism which applies in THF also applies in DME and that this mechanism utilizes an intermediate step, prior to the protonation step, which is hindered by stronger solvation. The zero-order dependence on water indicates that, in this case, the intermediate step is slower than the protonation process.

This inhibition of the reaction by a change in the solvent was even more striking when potassium anthracenide was mixed with water in ethylenediamine. In this instance, no reaction was observed, even over a period of 5 to 10 minutes. Such a result might mean that the reaction with water requires an intermediate ion-paired form of the anion which was unavailable in the solvent of higher solvating ability. An alternative explanation might be that the water was tied up with the solvent through hydrogen bonding and therefore did not react.

6. Dependence on the Cation

In a further attempt to elucidate the importance of ion-pairing, the reactions of water and of ethanol with the sodium salts of the anthracene radical anion were studied. This cation was chosen on the basis of conductance data which indicated the sodium salts to be less strongly ion-paired than the potassium salts (22). Although the lithium salt would have been a better choice from the standpoint of minimization of ion-pairing, metal purification would present greater experimental difficulties for lithium than for sodium. One would expect, however, that either cation would reduce the rate of reaction to something slower than that observed for potassium anthracenide if the reaction were to proceed preferentially via a contact ion-pair.

The general reaction which was studied was, of course,



Two proton sources, ethanol and water, and two solvents, THF and DME, were employed. Unfortunately, mechanical difficulties caused about half of the work in THF to be discarded. The reader is referred to section IV-A for a discussion of these difficulties. In the following sections, the data which remained are discussed.

a. The reactions of Na^+An^- in THF: The reaction of sodium anthracenide with ethanol in THF could be described by the rate law

$$\frac{-d[\text{An}^-]}{dt} = k_{ps} [\text{An}^-]^2 \quad (57)$$

A representative fit of this rate law to the data is shown in Figure 19. Rate constants calculated from Equation 57 are given in Table 6.

TABLE 6

Pseudo-second-order Rate Constants for the Reaction
 $\text{Na}^+\text{An}^- + \text{EtOH}$ in THF

Run	$[\text{EtOH}] \times 10^3 \text{M}$	$[\text{An}^-] \times 10^3 \text{M}$	$\bar{k}_{ps} \times 10^{-4} \text{M}^{-1} \text{sec}^{-1}$
KR11,7	0.845	0.40	0.86 *
KR11,8	1.69	0.36	1.71
KR11,9	2.82	0.26	1.87

*Pseudo-second-order treatment not valid.

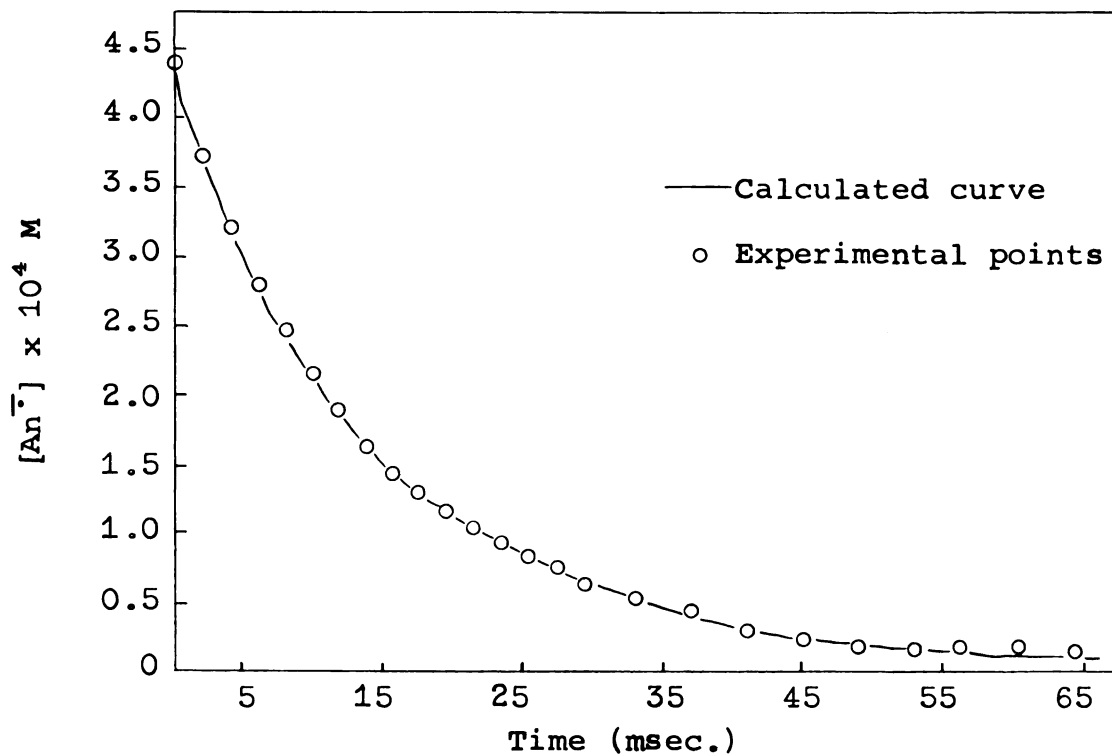


Figure 20. Parallel first- and second-order equation applied to the reaction: $\text{Na}^+\text{An}^- + 0.00236\text{M H}_2\text{O}$ in THF.

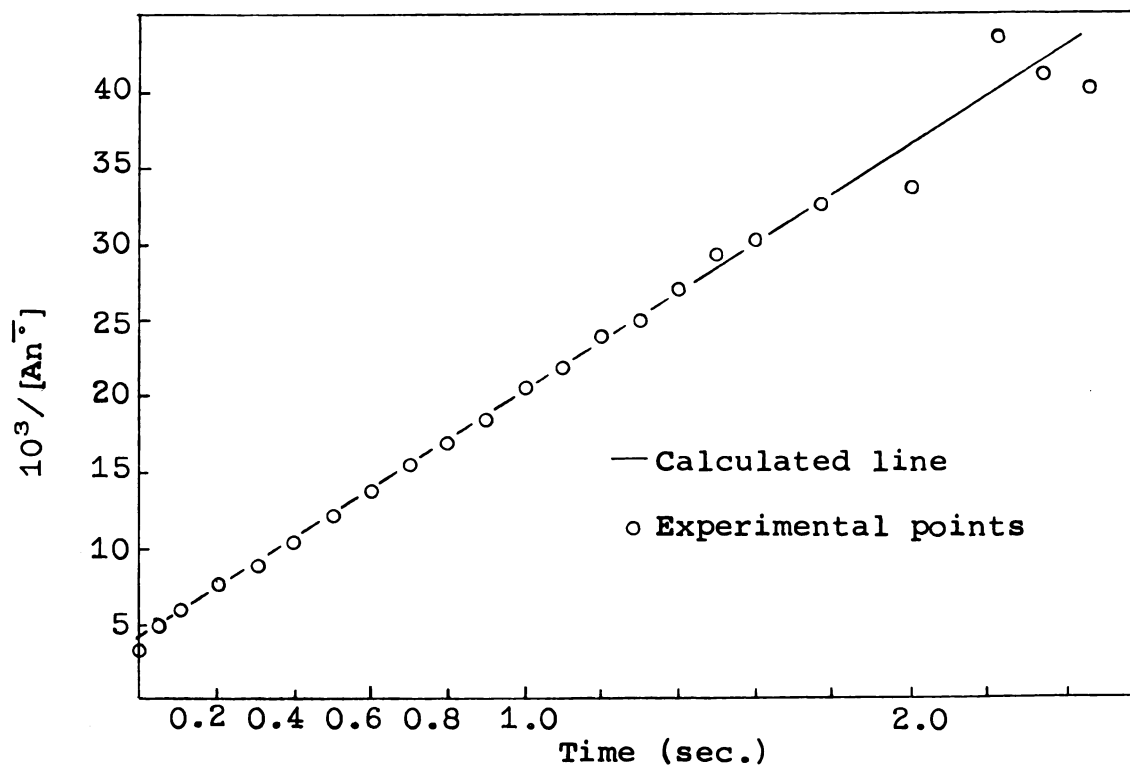


Figure 19. Pseudo-second-order kinetics applied to the reaction: $\text{Na}^+\text{An}^- + 0.00282\text{M EtOH}$ in THF.

Surprisingly, a pseudo-order treatment gave a good fit to the data, even for the lowest concentration studied. This probably indicates a low order for the dependence on the ethanol concentrations. Thus, the results seem to indicate no striking differences between the reactions of K^+An^- and of Na^+An^- with ethanol in THF.

This statement can not be made with regard to the reaction between Na^+An^- and water in THF, however. In this case, the decay of the anion could not be described by either a first- or a second-order dependence on the anion. Rather, a fractional order between one and two seemed necessary. Moreover, the two sets of experiments with this system produced different results. While some of the decay curves were obviously unusable because of the mechanical problems discussed earlier, many decay curves did not appear to be seriously affected, yet did not give consistent results.

We were unable to discover a reason for the inconsistencies. Nevertheless, as we will show later, there was reason to suspect that a combination of first- and second-order decays,

$$\frac{-d[An^-]}{dt} = k_f [An^-] + k_s [An^-]^2 \quad , \quad (58)$$

might fit the data. A representative decay curve and the tabulated results of the application of Equation 58 are given in Figure 20 and Table 7, respectively. The rate constants for experiments KR9 indicate a reaction in which both the

TABLE 7

Rate Constants Which Result From Application of a
Parallel First- and Second-order Rate Law
(Equation 58) to the Reaction of Na^+An^-
with Water in THF

Run	$[\text{H}_2\text{O}]_0 (\text{M})$	$k_s (\text{M}^{-1}\text{sec}^{-1}) \times 10^{-5}$	$k_f (\text{sec}^{-1})$	% First Order
KR11, 10.4	0.0163	0.82 ± 0.04	-1.29 ± 0.19	7
KR11, 10.8	0.0163	1.59 ± 0.05	-6.71 ± 0.43	17
KR11, 11.3	0.0325	2.34 ± 0.06	-4.93 ± 0.52	7
KR11, 11.4	0.0325	2.43 ± 0.06	-5.11 ± 0.53	7
KR11, 12.4	0.0399	2.89 ± 0.04	-9.03 ± 0.41	10
KR9, 8.3	0.00114	0.77 ± 0.04	39.2 ± 0.7	57
KR9, 8.5	0.00114	0.95 ± 0.07	40.0 ± 1.3	52
KR9, 7.4	0.00236	0.69 ± 0.05	52.7 ± 1.0	60
KR9, 2.3	0.00467	1.12 ± 0.16	15.5 ± 1.9	35
KR9, 2.6	0.00467	1.12 ± 0.14	18.7 ± 2.3	35

* The "per cent first-order" is the per cent of the initial rate which is due to the first-order term.

first- and second-order components contribute equally to the initial rate of decay. Experiments KR11, however, resulted in data which can best be described by a nearly second-order decay with a systematic negative contribution from a first-order term. This term contributes little to the initial rate of decay, which makes its sign less alarming than if it were a major contributor.

Two conclusions might be drawn from the data given in Table 7. First, changing the concentration of water did not cause large variations in the rate of the reaction. This is in agreement with our observations for the reactions of K^+An^- . Second, however, the rate constants for the second-order decay are consistently three to four times those calculated for the reactions of K^+An^- with comparable concentrations of water. Since the order of the decay was neither reproducible nor consistent with the results of other reactions of Na^+An^- , we attributed these results to some unknown and therefore uncontrolled chemical cause and did not include them in our considerations of a general mechanism.

b. The reactions of Na^+An^- in DME: Two major points can be made with regard to the reaction of Na^+An^- with ethanol in DME. First, the reaction is very slow when compared with the same reaction in THF. Since solvation of the cation is greater in DME, that solvent should also diminish the degree of contact-ion-pair formation. Thus, one would expect the rate of reaction to be lower. Second, the data could be fit

by the bimolecular second-order mechanism

$$\frac{-d[\text{An}^-]}{dt} = k_b [\text{An}^-] [\text{EtOH}] \quad (59)$$

Figure 21 contains a representative data set and the comparison with the calculated curve. The rate constants obtained from the least-squares analyses of the data are given in Table 8. The one value of k_b which seems out of line comes from the one experiment of the three which was most likely to be in error, since it was done after a series of reactions of potassium anthracenide. Contamination by potassium ions would be expected to increase the rate and cause a deviation from Equation 59. It is possible, therefore, that Equation 59 does, in fact, describe this experiment. However, the small number of data points involved does not permit evaluation of a valid rate constant. The first-order nature of the decay with respect to $[\text{An}^-]$ is, however, evident in all cases.

For the reaction of $\text{Na}^+ \text{An}^-$ with water in DME, a pseudo-first-order rate law was able to describe the decay of anthracenide. Figure 22 shows an example of this behavior. Once again, the reaction in DME was found to be slow compared to its counterpart in THF. The rate constants are listed in Table 9. Surprisingly, the dependence on the water concentration is low. A possible explanation for this phenomenon will be given later.

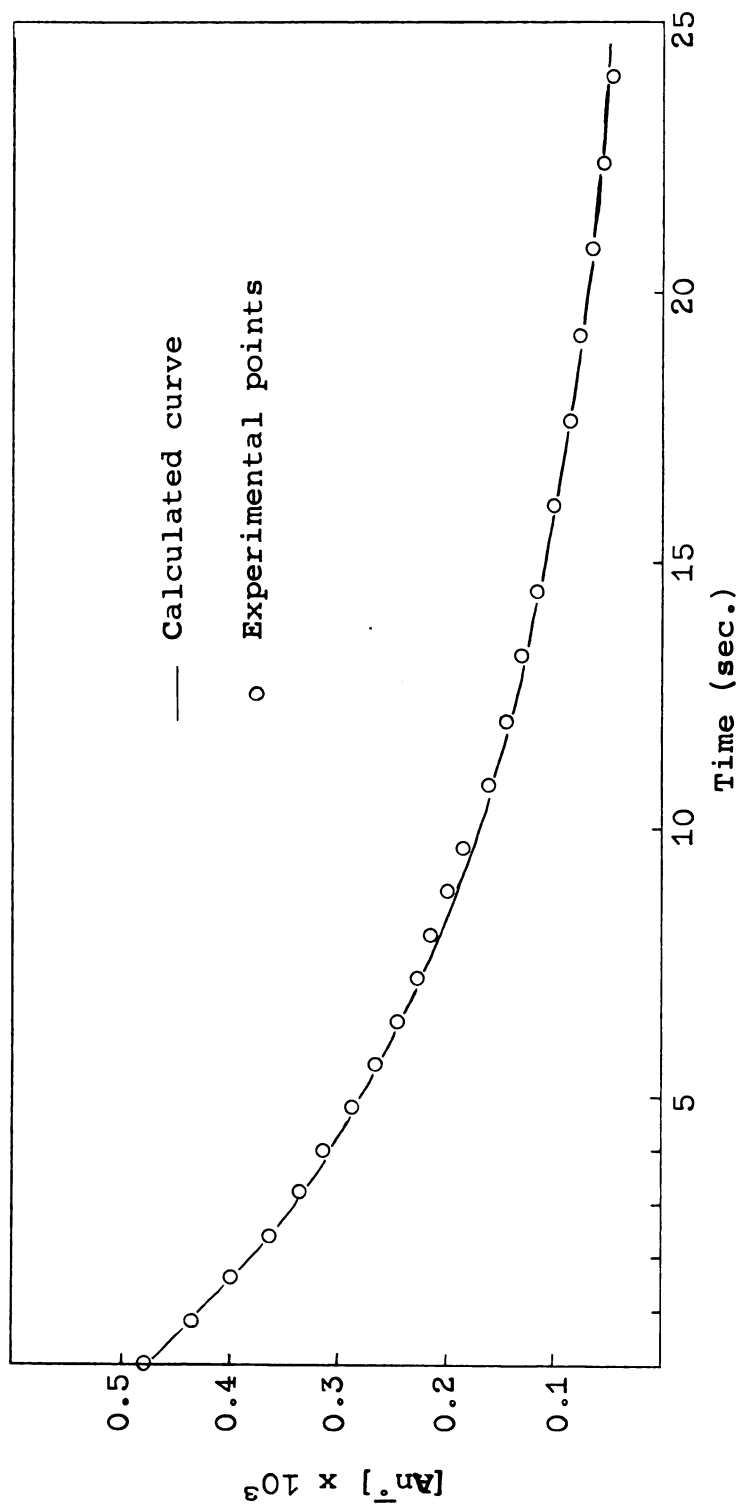


Figure 21. Reaction of $Na^+An^- + EtOH$ in DME, $[EtOH] = 1.34 \times 10^{-3}M$.
Bimolecular second-order fit of the decay.

TABLE 8

Bimolecular Second-order Rate Constants for the Reaction of
Sodium Anthracenide with Ethanol in DME

Run	$[\text{EtOH}] \times 10^3 \text{M}$	$[\text{An}^-] \times 10^4 \text{M}$	$\bar{k} (\text{M}^{-1} \text{sec}^{-1}) \times 10^{-2}$
KR13,9	2.63	6.7	$2.14 \pm .07$
KR13,10	1.34	4.4	$0.94 \pm .004$
KR13,11	0.91	4.8	$0.95 \pm .01$

TABLE 9

Pseudo-first-order Rate Constants for the Reaction
of Sodium Anthracenide with Water in DME

Run	$[\text{H}_2\text{O}] \times 10^2 \text{M}$	$[\text{An}^-] \times 10^4 \text{M}$	$\bar{k} (\text{sec}^{-1})$
KR13,12	0.85	5.0	$0.418 \pm .004$
KR13,13	1.24	6.3	$0.231 \pm .003$
KR13,14	1.80	5.5	$0.223 \pm .004$
KR13,15	3.57	6.5	$0.330 \pm .006$

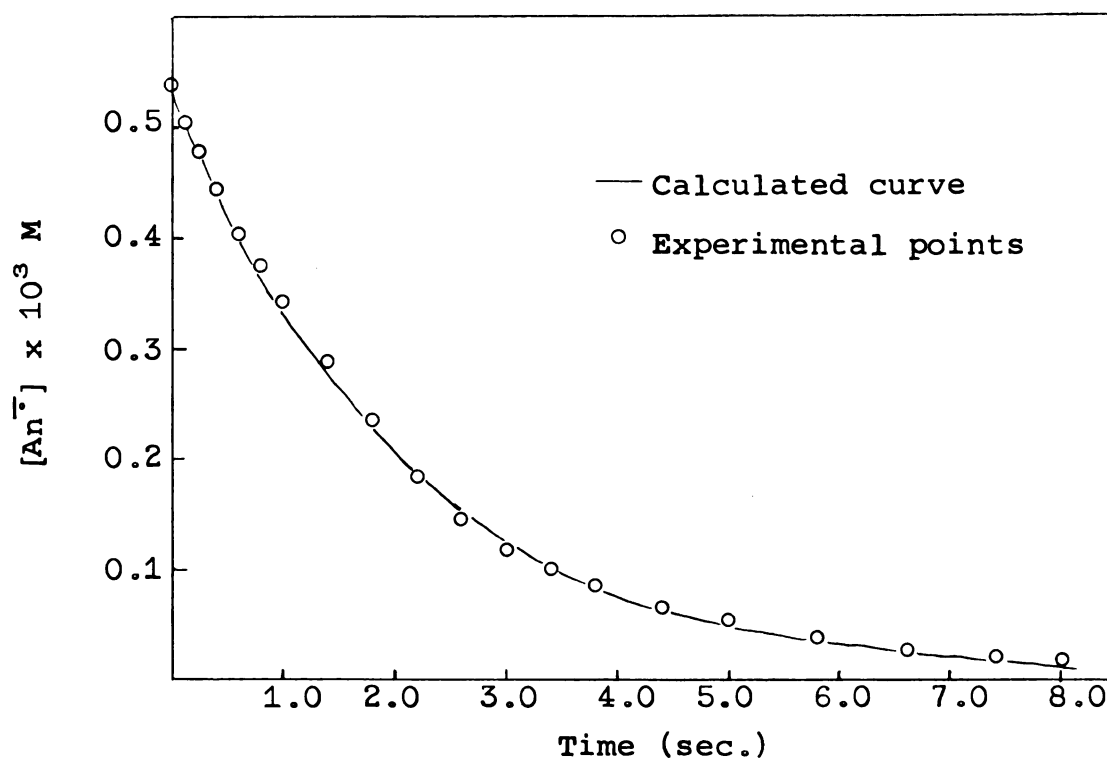


Figure 22. Reaction of $\text{Na}^+ \text{An}^- + 0.0085\text{M H}_2\text{O}$ in DME. A pseudo-first-order fit of the decay.

c. Conclusions: While the results of the experiments with sodium anthracenide contain more uncertainty than we would like, some conclusions seem valid. The solvent dimethoxyethane certainly inhibits the rate of the reactions. Furthermore, in DME the reactions proceed more slowly when sodium, rather than potassium, is the cation. In order to show this, let us apply the pseudo-second-order rate law (Equation 12) to the data for the reactions of both Na^+An^- and K^+An^- with water in DME. Of course, the fit is not good for the sodium salt, but it should be good enough to permit an estimate of relative rates. The calculated rates are of the order of 4×10^2 and $4 \times 10^3 \text{ M}^{-1} \text{ sec}^{-1}$ for the sodium and potassium salts, respectively. Lastly, there does appear to be a change in the rate law which describes the disappearance of the anthracenide anion. There is a progression from a strictly second-order decay with K^+An^- in THF to one which is first order for Na^+An^- in DME. These results are consistent with a mechanism in which ion-pairing leads to a fast, second-order reaction. Under some circumstances, this mode of reaction predominates over a slower, first-order reaction which does not require such pairing. Under circumstances unfavorable to ion-pairing, the first-order reaction becomes apparent.

7. Dependence on the Anion

Another factor which can affect the extent of ion-pairing is the nature of the anion. In order to study this effect

and, at the same time, to test the generality of the results obtained for the anthracenide system, the reactions of potassium terphenylide with water and with ethanol in THF were studied.

The reaction of K^+Ter^- with ethanol in THF appears to be another example of a reaction which proceeds via the first-order mechanism. Figure 23 is an example of the results obtained by fitting Equation 60

$$\frac{-d[Ter^-]}{dt} = k [Ter^-] [EtOH] \quad (60)$$

to the data. Table 10 contains a list of the rate constants which were obtained at various concentrations of ethanol. The concentration independence of the rate constant is further evidence that Equation 60 does apply.

When a solution of potassium terphenylide was mixed with water in THF, no decay of the anion was observed. While this K^+Ter^- solution was one in which decomposition to the red solution had occurred, e.s.r. and optical evidence indicate that significant quantities of terphenylide were still present in such solutions. Thus, the terphenylide anion does not appear to react with water in THF.

The results obtained with ethanol indicate that p-terphenylide is an example of an anion which has access to a fast first-order reaction with ROH. Conductance and optical studies of solutions of Na^+Ter^- in THF indicate that approximately equimolar concentrations of free ions, solvent-separated

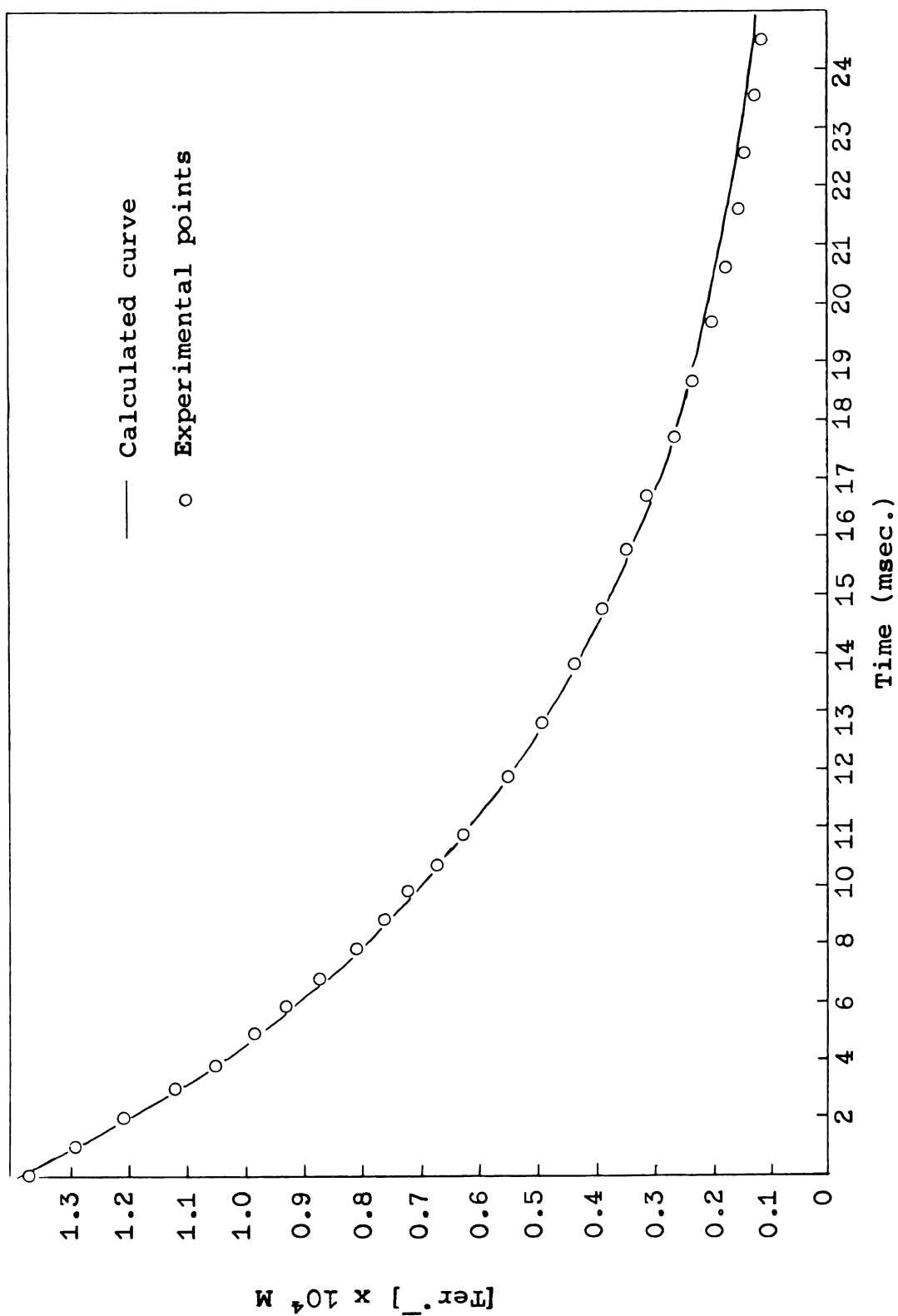


Figure 23. Bimolecular second-order kinetics applied to the reaction:
 $\text{K Ter}^\cdot + 5.75 \times 10^{-4} \text{ M ethanol in THF.}$

TABLE 10

Bimolecular Second-order Rate Constants for the Reaction of Potassium Terphenylide with Ethanol in THF

Run	$[\text{EtOH}] \times 10^3 \text{M}$	$[\text{Ter}^-] \times 10^4 \text{M}$	$\bar{k} (\text{M}^{-1} \text{sec}^{-1}) \times 10^5$
KR14,2	2.57	0.50	$0.57 \pm .01$
KR14,3	0.975	0.70	$1.38 \pm .05$
KR14,4	0.575	1.40	$1.22 \pm .01$
KR14,5	0.418	1.70	$1.24 \pm .01$

ion-pairs, and contact ion-pairs are present in solutions of low (approximately $1 \times 10^{-4} \text{ M}$) total anion concentration at room temperature (50). The e.s.r. spectra of both the lithium and the sodium salts in THF show no structure due to the cation (45). These results suggest that potassium terphenylide solutions in THF contain appreciable quantities of both contact and solvent-separated ion-pairs. If this is true, then the first-order process in the reaction with ethanol must be fast enough to compete favorably with the second-order process, if, indeed, such a process exists for terphenylide.

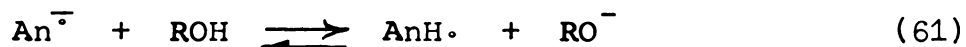
C. A Discussion of Mechanisms

1. Inapplicable Mechanisms

Before considering a final mechanism, let us digress for a moment to review some preliminary ideas which proved not to be in accord with the results. This evolutionary

approach will outline the basic problems which arose and the steps which led to development of a consistent mechanism.

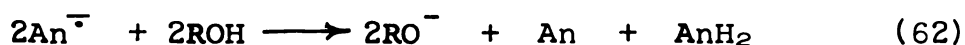
We have seen that no previously postulated mechanism predicts a second-order disappearance of the anion. The existence of an equilibrium such as



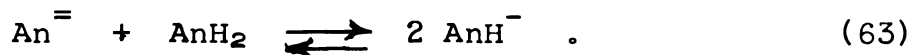
could explain the low order in ROH. However, the absence of an alkoxide effect ruled out such an equilibrium. Thus, the previously postulated mechanisms were inconsistent with two of our most basic observations.

Using the stoichiometry of the reaction as a basis, Weissman had suggested a mechanism which contained consecutive proton and electron transfers (p. 19). Another possible sequence might be one in which an electron transfer precedes the proton attachment, thereby creating a species with an enhanced proton affinity. This species might then react with a proton much faster than could the anthracenide anion itself.

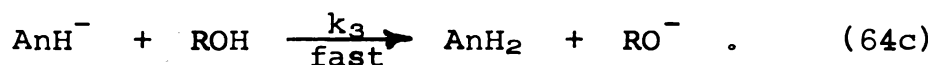
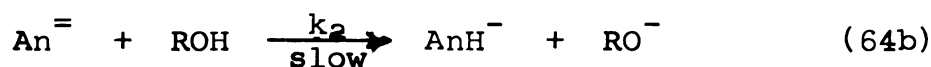
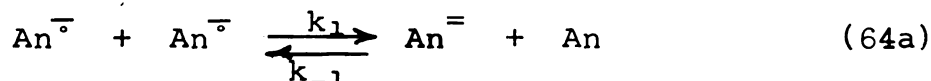
Several studies have indicated the existence of an equilibrium between mono- and di-negative anions (51-53). Other studies suggest that, in the case of anthracene anions, the di-anion has a higher proton affinity than does the mono-anion. This conclusion is based on the observations that the reaction



appears to be irreversible, yet a proton can be abstracted from the dihydroproduct in the reaction



These ideas suggested the following mechanism for the reaction under investigation:



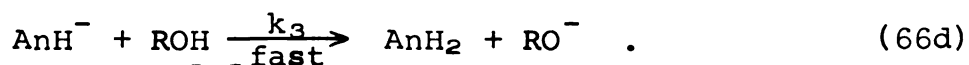
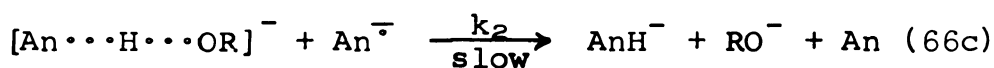
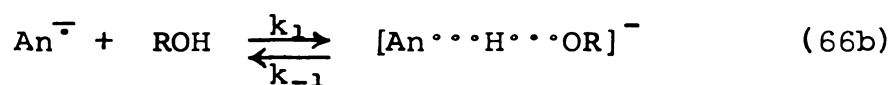
Since no observable concentrations of the dianion were present in our experiments, application of the steady-state assumption for $[\text{An}^=]$ seemed justified. This led to the rate law:

$$\frac{-d[\text{An}^{\circ-}]}{dt} = 2 k_1 [\text{An}^{\circ-}]^2 \left\{ \frac{1}{1 + \frac{k_{-1}[\text{An}]}{k_2[\text{ROH}]}} \right\} \quad (65)$$

Although such a form seemed capable of explaining both the second-order decay of $\text{An}^{\circ-}$ and the low dependence on the concentration of ROH, it was unable to fit the data. The values of both $[\text{An}]$ and $[\text{ROH}]$ were known and had been varied from run to run, so that an adequate test of this mechanism was available. Therefore, it was necessary to discard the mechanism.

There is evidence for the effect of clusters in ROH in the kinetics of proton exchange reactions in aqueous solutions

of imidazolium ions [54]. In this instance, hydrogen bonding within the clusters appears to compete with the protonation process. It seemed reasonable to expect that such clusters could also exist in media of low dielectric constant. If hydrogen bonding were competitive with proton transfer, the effective concentration of available protons and, consequently, the order of the ROH dependence would be lowered. A mechanism which describes this situation is given below:



The intermediate in Equation 66b was suggested by the absence of an alkoxide effect. If we make the steady-state assumption for the concentration of this intermediate, the rate law given by Equation 67 can be derived:

$$\frac{-d[\text{An}^-]}{dt} = \frac{k_1 k_2}{2K} \cdot \frac{[\text{An}^-]^2}{k_2 [\text{An}^-] + k_{-1}} \left\{ (8K[\text{ROH}]_t + 1)^{\frac{1}{2}} - 1 \right\}. \quad (67)$$

The term, $[\text{ROH}]_t$, refers to the total concentration of alcohol,

$$[\text{ROH}]_t = [\text{ROH}] + [(\text{ROH})_2] \quad (68)$$

This mechanism contained two very attractive aspects. First of all, depending on the relative magnitudes of k_{-1} and k_2 , the order of the dependence on $[An^-]$ could be first, second, or something in between these. One would expect this competition between k_{-1} and k_2 to be dependent on the particular anion used. An effect due to the cation would be allowed, but its cause would not be obvious. The order with respect to the anion would also be expected to be dependent upon the acidity of the alcohol, however. That particular dependence was not observed. Since the magnitude of that effect is not known, its apparent absence should not destroy the credibility of the mechanism.

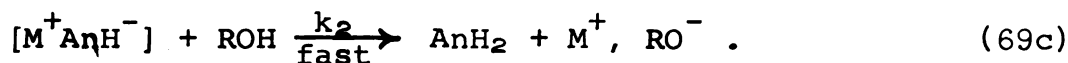
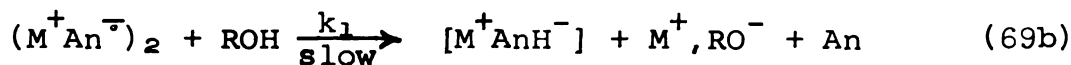
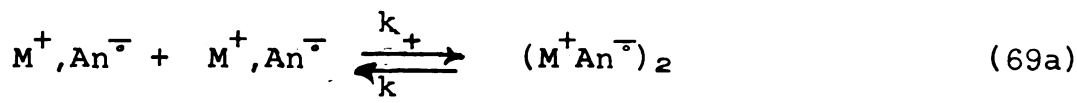
The second facet of the mechanism which interested us was its prediction that the order with respect to the alcohol concentration should depend upon the particular alcohol. However, since the hydrogen bonding should be greatest for the smaller alcohols, these are the ones which should exhibit the lowest order. The reverse of this is observed.

Another failure of this mechanism resided in our inability to fit it to the data. At least three explanations are possible. We have found that, as the number of parameters and the non-linear dependence on them increase, the curve-fitting program demands better initial estimates of the parameters. We may have failed to produce sufficient estimates. Secondly, a correct mechanism might require formation of higher aggregates of alcohol molecules.

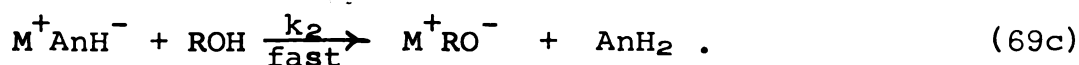
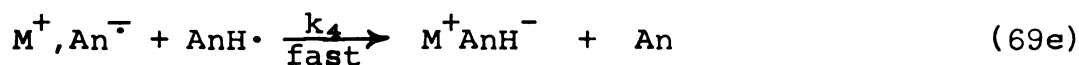
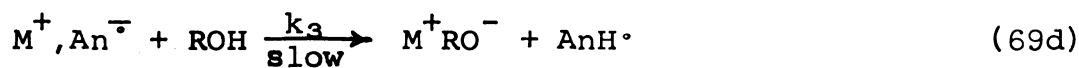
However, this would lead to more parameters with no obvious increase in the correctness. In fact, the reactions in DME exhibited the lowest ROH dependence of all. Thus, this explanation would require that larger clusters exist in DME than in THF, which is the reverse of what would be expected on the basis of solvating ability. Lastly, the mechanism might simply be incorrect. In view of a later mechanism which seemed both quantitatively and qualitatively superior to this one, we favor the third explanation.

2. A Suggested Mechanism

a. Formulation: While the two previously discussed mechanisms were deemed to be incorrect, they contained ideas which led to yet another scheme for the reaction process. It seemed that, if neutral molecules could form clusters, so also might neutral ion-pairs. As far as this author knows, no direct evidence for ion-quadruples exists for aromatic radical anion systems, but evidence for such species is available for other systems (55,56). Current theories suggest the existence of several kinds of ion-pairs in solutions of anions. Consequently, the presence of paired ion-pairs in solvents of low dielectric constant seems possible. The reaction with a proton donor might proceed preferentially through such a species since the necessary electron transfer would already be at least partially completed. Our proposed mechanism is:



Since there seemed to be no a priori reason to assume that the contact ion-pair, M^+, An^- , could not also react with the alcohol, a first-order reaction was included in the general mechanism. We expected this to contribute very little to the overall rate of reaction and added it only for completeness. Specifically, this part of the mechanism consisted of the sequence:



If a steady state concentration is assumed for the species, $(M^+ An^-)_2$, the general rate law for steps 69a-e becomes

$$\frac{-d[M^+, An^-]}{dt} = 2 k_+ [M^+, An^-]^2 \left\{ 1 - \frac{k_-}{k_- + k_1 [ROH]} \right\} + k_3 [M^+, An^-] [ROH] . \quad (70)$$

The form which was actually used by the curve-fitting program was derived from this one by minor algebraic manipulations:

$$\frac{-d[M^+, An^-]}{dt} = 2k_+[M^+, An^-]^2 \left\{ \frac{1}{1 + \frac{k_-}{k_1 [ROH]}} \right\} + k_3 [M^+, An^-] [ROH] \quad (71)$$

Three parameters were defined for the computer. They were $u(1) = 2 k_+$, $u(2) = k_-/k_1$, and $u(3) = k_3$, where $u(I)$ designates the I^{th} parameter. We could find no way to determine more than the ratio of k_1 and k_- .

b. Experimental basis: In order to obtain the most statistically rigorous treatment of the data, three or more data sets were fit simultaneously by the program. Each data set consisted of a concentration versus time curve for the reaction of anthracenide with one concentration of a particular alcohol. If, for example, three data sets were used, each set represented a different initial concentration of ROH. Therefore, when the program minimized the sum of the squares of the residuals of all three data sets, it was required to handle both the anthracenide and the alcohol dependence simultaneously. Some representative results of this procedure are shown in Figure 24. Table 11 contains the resultant rate constants.

Although the good agreement between the shapes of the predicted and experimental decay curves speaks strongly for the mechanism, other criteria must also be met. The rate constants k_+ and k_- should be constant for the reactions of potassium anthracenide in THF. The value of k_- is hidden in a ratio, but the value of k_+ is, within one standard

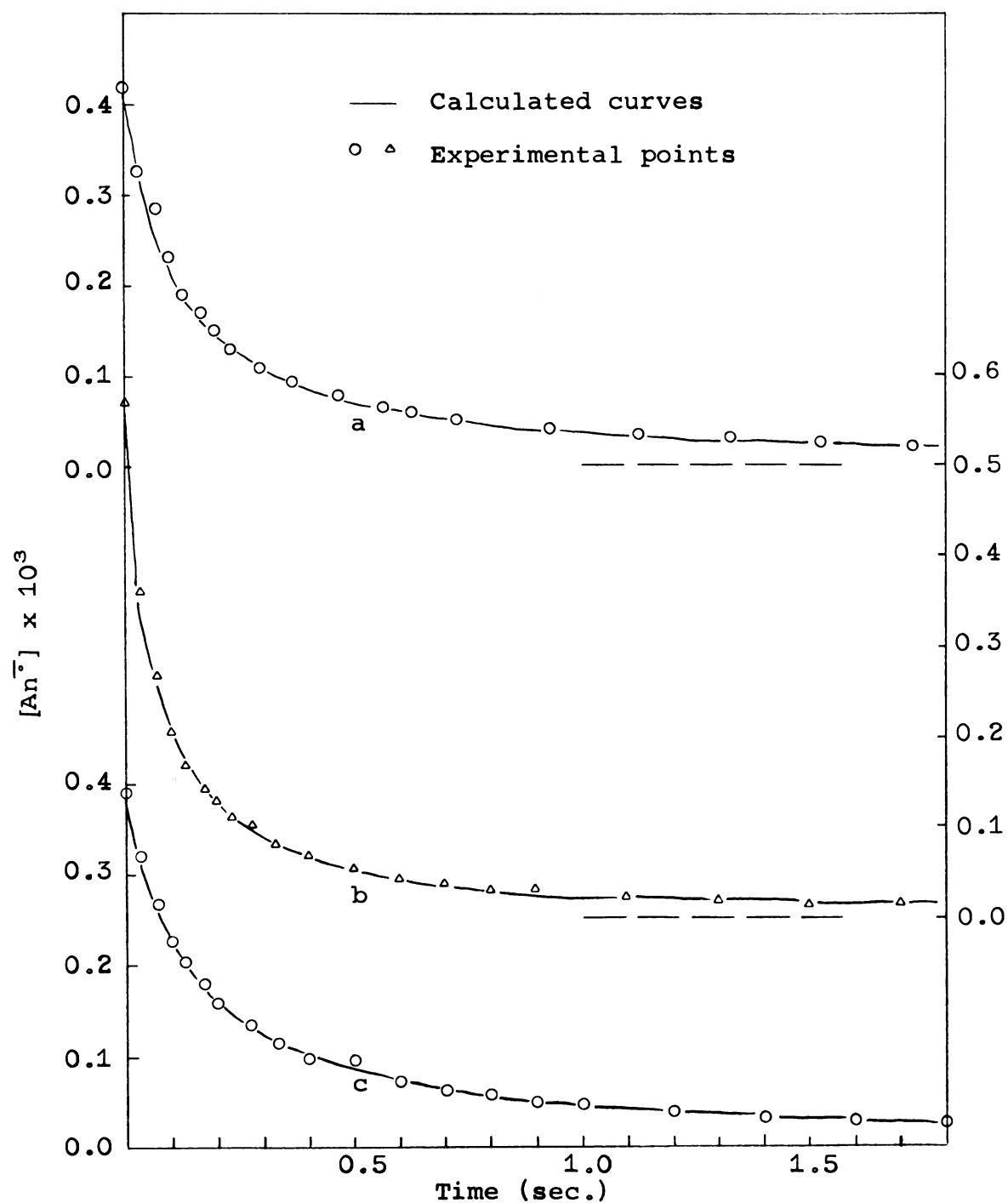


Figure 24. Simultaneous fitting of Equation 71 to three data sets. The reactions of K^+An^- with (a) 0.008 M, (b) 0.02 M, and (c) 0.0054 M $t\text{-BuOH}$ in THF are treated.

TABLE 11A

Rate Constants Which Result From Application of Equation 71 to the Protonations of K^+An^- and Na^+An^- in THF and in DME

Reaction	k_+ ($M^{-1}sec^{-1}$)	k_-/k_+ (M)	k_2 ($M^{-1}sec^{-1}$)
$K^+An^- + MeOH$ in THF	$(2.35 \pm 0.10) \times 10^4$	$(5.24 \pm 0.25) \times 10^{-3}$	-2.01 ± 10.4
$K^+An^- + EtOH$ in THF	$(2.50 \pm 0.07) \times 10^4$	$(4.09 \pm 0.15) \times 10^{-3}$	5.63 ± 6.04
$K^+An^- + iso-PROH$ in THF	$(2.08 \pm 0.05) \times 10^4$	$(8.66 \pm 0.48) \times 10^{-3}$	16.0 ± 1.3
$K^+An^- + t-BuOH$ in THF	$(1.84 \pm 0.04) \times 10^4$	$(6.44 \pm 0.26) \times 10^{-3}$	23.9 ± 2.6
$K^+An^- + H_2O$ in THF	$(1.77 \pm 0.08) \times 10^4$	$(1.55 \pm 0.13) \times 10^{-2}$	11.2 ± 1.6
$Na^+An^- + EtOH$ in THF	$(1.99 \pm 0.09) \times 10^4$	$(1.97 \pm 0.12) \times 10^{-3}$	-114.0 ± 17.0
$K^+An^- + EtOH$ in DME	$(4.55 \pm 0.25) \times 10^2$	$(0.77 \pm 0.38) \times 10^{-4}$	40.3 ± 8.7
$K^+An^- + H_2O$ in DME	$(1.33 \pm 0.05) \times 10^3$	$(-3.34 \pm 0.26) \times 10^{-3}$	7.5 ± 0.7

TABLE 11B

Estimates of Uncertainty for the Rate Constants in Table 11A*

Reaction	$\sigma(k_+)$	$\sigma(k_-/k_1)$	$\sigma(k_2)$	Groups
$K^+An^- + MeOH$ in THF	0.00×10^4	$\pm 1.03 \times 10^{-3}$	2
$K^+An^- + EtOH$ in THF	$\pm 0.20 \times 10^4$	$\pm 0.37 \times 10^{-3}$	± 6.04	2
$K^+An^- + iso-PrOH$ in THF	0.00×10^4	$\pm 3.30 \times 10^{-3}$	± 0.30	2
$K^+An^- + t-BuOH$ in THF	$\pm 0.18 \times 10^4$	$\pm 2.15 \times 10^{-3}$	± 1.90	3
$K^+An^- + H_2O$ in THF	$\pm 0.47 \times 10^4$	$\pm 0.89 \times 10^{-2}$	± 2.45	5
$Na^+An^- + EtOH$ in THF	1
$K^+An^- + EtOH$ in DME	$\pm 0.14 \times 10^2$	$\pm 1.48 \times 10^{-4}$	± 17.7	2
$K^+An^- + H_2O$ in DME	$\pm 0.91 \times 10^3$	$\pm 3.78 \times 10^{-3}$	± 6.57	2

*The uncertainty limits in Table 11A are averaged estimates of the standard deviation within a group, where a group consists of two to five data sets fit simultaneously. In Table 11B, standard deviations of the results obtained from different groups are given. Thus, Table 11A indicates the "goodness of fit", while Table 11B indicates the consistency of the results.

deviation $(2.11 \pm 0.32) \times 10^4 \text{ M}^{-1} \text{ sec}^{-1}$.

If the value of k_- is considered to be constant, the variation in the ratio, k_-/k_1 , should be due to a variation in k_1 . The rate constant k_1 is, of course, directly related to the acidity of the alcohol. Since k_1 should decrease, k_-/k_1 should increase as the acidity of the alcohol becomes smaller. While the acidity of the proton donor has a surprisingly small effect in our systems, the expected trend is present for the alcohols. However, the reaction with water is slower than would be expected on the basis of acidity alone.

There appears to be no order in the variation of k_3 . The effect of the first-order component is small. If that part of the mechanism does apply, its effect is too small to allow the curve-fitting procedure to assign more than a rough estimate of the rate constant.

The mechanism predicts that the rate should be dependent upon the degree of ion-pairing in the solution. Table 11 indicates that Na^+An^- in THF is still strongly paired and is not greatly different from the potassium salt in this respect. The size and sign of the first-order rate constant emphasize our difficulties with the sodium data for the THF solvent system. Table 11 also shows that changing to a more strongly solvating medium (DME) reduces the rate of ion-quadruple formation and, consequently, the rate of the reaction. The first-order component remains relatively constant, but its

contribution to the overall rate of reaction now becomes appreciable. The ratio k_-/k_1 is so small for the DME solvent system that it has virtually no effect on the shapes of the decay curves. Therefore its values are ill-defined and should be given little weight. This low value of k_-/k_1 is simply a restatement of the earlier observation that the reactions of potassium anthracenide in DME are of very low order in [ROH]. In these cases, the rate-limiting step becomes the formation of the ion-quadruple.

c. Implications: For a particular reaction, the ratio k_-/k_1 should remain constant. A very interesting possibility arises from this fact. Equation 71 states that the ROH dependence of the reaction is determined by the term $1 + k_-/(k_1 \cdot [\text{ROH}])$. If $1 \gg k_-/(k_1 [\text{ROH}])$, the reaction should be virtually independent of the concentration of ROH. Such a situation would be most likely to occur at high concentrations of the alcohol. Conversely, low concentrations of alcohol would be expected to cause the order with respect to [ROH] to increase until a limiting order of unity were reached. A value of k_-/k_1 of 10^{-2} ought to allow one to observe a change in order from one to zero by changing the alcohol concentration over a range of 10^{-3} to 1 M.

Although, in our experiments, the alcohol concentration was not varied over such a wide range, we have indications that the phenomenon may apply. In our studies of the reaction $\text{K}^+\text{An}^- + \text{ROH}$ in THF, the initial concentrations of ethanol

were of the order of 10^{-3} M, whereas those of isopropanol were 10^{-1} to 10^{-2} M. The order in ethanol was 0.5 or possibly higher, whereas for isopropanol the order was only 0.3.

The second major implication is that the order of the dependence on the concentration of the anion should decrease as the extent of ion-pairing diminishes. This effect should be dependent on the solvation properties of the medium, the nature of either the cation or the anion, and the temperature.

The kinetic studies which were discussed in the historical section are probably instances in which both the cation and solvent effects reduced ion-pairing. Another such instance would be our study of the reactions of sodium anthracenide in DME, in which the decay was first-order in $[\text{Na}^+\text{An}^-]$. The first-order dependence on terphenylide in its reaction with ethanol in THF represents an example in which the nature of the anion is apparently the deciding factor.

Several other combinations of variables should be good tests of the effect of ion-pairing. The extension of studies of potassium anthracenide to more polar solvents, the use of lithium, rather than potassium, anthracenide in THF, and a study of the reactions of K^+An^- in THF at lower temperatures are instances which should result in a first-order dependence on anthracenide. On the other hand, a study of the reactions of K^+Ter^- in methyltetrahydrofuran or some

other weakly-solvating medium might result in a second-order dependence on $[\text{Ter}^-]$. This would be a good test of the generality of the anthracenide results.

D. Conclusions

The reactions of potassium anthracenide with various proton donors in THF proceed via a mechanism which is second-order in anthracenide. The importance of this second-order process appears to be diminished by conditions which decrease ion-pairing. While the reaction of Na^+An^- with ethanol in THF is probably similar to that of K^+An^- , the rate of the reactions of K^+An^- with ethanol and water in a more strongly solvating medium (DME) is greatly reduced. When the same reactions of Na^+An^- are studied in DME, the rates are even slower and the dependence on $[\text{An}^-]$ is first order. This observation indicates that a first-order path for the protonation of anthracenide does exist, but that it is much slower than the second-order process and only predominates when contact ion-pairs are absent.

The rate of this first-order process may well be dependent upon the nature of the anion. A fast, first-order decay of the anion was observed in the reaction of potassium terphenylide with ethanol in THF. In this case, the first-order process may be fast enough to compete favorably with the second-order path, even in the presence of an appreciable quantity of contact ion-pairs.

While the rates of the reactions of K^+An^- with various alcohols in THF appear to increase with the acidity of the alcohol, the effect of acidity is a small one. This is thought to be caused by the dependence of the total rate on both the rate of formation of a reactive, ion-paired species and the rate of its subsequent protonation.

The reactions with water are somewhat anomalous. While the kinetics observed for the reactions with water are the same as those for the alcohols, the rates with water are slower than might be expected on the basis of relative acidities. Indeed, in ethylenediamine, water does not react with potassium anthracenide. This may indicate that water interacts with the solvent more strongly than do the alcohols. An interesting test of this would be a study of the reaction (or lack of a reaction) of ethanol with K^+An^- in ethylenediamine.

Several tests of these ideas have been suggested in a previous section. An extension of our studies to a wider range of alcohol concentrations would examine the validity of Equation 71. A more basic study would be one which further examines the effects of ion-pairing upon the reactions. Also, the studies should be extended to other aromatic anions to determine the generality of our observations.

REFERENCES

REFERENCES

1. W. Schlenk, J. Appenrodt, A. Michael, and A. Thal, Ber., 47, 479 (1914).
2. N. D. Scott, J. F. Walker, and V. L. Hansley, J. Am. Chem. Soc., 58, 2442 (1936).
3. A. Maccoll, Nature, 163, 178 (1949).
4. H. A. Laitinen and S. Wawzonek, J. Am. Chem. Soc., 64, 1765 (1942).
5. G. J. Hoijsink and J. van Schooten, Rec. Trav. Chim., 71, 1089 (1952).
6. G. J. Hoijsink, E. DeBoer, P. H. Van Der Meij, and W. P. Weijland, Rec. Trav. Chim., 75, 487 (1956).
7. G. J. Hoijsink, J. van Schooten, E. DeBoer, and W. Ij. Aalbersberg, Rec. Trav. Chim., 73, 355 (1954).
8. D. E. Paul, D. Lipkin, and S. I. Weissman, J. Am. Chem. Soc., 78, 116 (1956).
9. P. Balk, G. J. Hoijsink, and J. W. H. Schreurs, Rec. Trav. Chim., 76, 813 (1957).
10. E. DeBoer and S. I. Weissman, Rec. Trav. Chim., 76, 824 (1957).
11. G. J. Hoijsink and P. J. Zandstra, Mol. Phys., 3, 371 (1960).
12. K. H. J. Buschow, J. Dieleman, and G. J. Hoijsink, Mol. Phys., 7, 1 (1963-64).
13. T. L. Chu and S. C. Yu, J. Am. Chem. Soc., 76, 3367 (1954).
14. T. R. Tuttle, Jr., R. L. Ward, and S. I. Weissman, J. Chem. Phys., 25, 189 (1956).

15. E. DeBoer, J. Chem. Phys., 25, 190 (1956).
16. E. DeBoer and S. I. Weissman, J. Am. Chem. Soc., 80, 4549 (1958).
17. R. L. Ward and S. I. Weissman, J. Am. Chem. Soc., 79, 2086 (1957).
18. M. Szwarc, Accounts Chem. Res., 2, 87 (1969).
19. N. M. Atherton and S. I. Weissman, J. Am. Chem. Soc., 83, 1330 (1961).
20. A. Crowley, N. Hirota, and R. Kreilick, J. Chem. Phys., 46, 4815 (1967).
21. C. L. Dodson and A. H. Reddoch, J. Chem. Phys., 48, 3226 (1968).
22. K. H. J. Buschow, J. Dieleman, and G. J. Hoijsink, J. Chem. Phys., 42, 1993 (1965).
23. R. V. Slates and M. Szwarc, J. Phys. Chem., 69, 4124 (1965).
24. T. E. Hogen-Esch and J. Smid, J. Am. Chem. Soc., 88, 307 (1966).
25. P. Biloen, T. Fransen, A. Tulp, and G. J. Hoijsink, J. Phys. Chem., 73, 1581 (1969).
26. N. Hirota, R. Carraway, and W. Schook, J. Am. Chem. Soc., 90, 3611 (1968).
27. T. E. Hogen-Esch and J. Smid, J. Am. Chem. Soc., 88, 318 (1966).
28. N. Hirota, J. Am. Chem. Soc., 90, 3603 (1968).
29. P. Chang, R. V. Slates and M. Szwarc, J. Phys. Chem., 70, 3180 (1966).
30. W. E. Bachmann, J. Org. Chem., 1, 347 (1936).
31. J. F. Walker and N. D. Scott, J. Am. Chem. Soc., 60, 951 (1938).
32. A. P. Krapcho and A. A. Bothner-By, J. Am. Chem. Soc., 81, 3658 (1959).
33. A. P. Krapcho and A. A. Bothner-By, J. Am. Chem. Soc., 82, 751 (1960).

34. O. J. Jacobus and J. F. Eastham, J. Am. Chem. Soc., 87, 5799 (1965).
35. J. P. Keene, E. J. Land, and A. J. Swallow, J. Am. Chem. Soc., 87, 5284 (1965).
36. S. Arai and L. M. Dorfman, J. Chem. Phys., 41, 2190 (1964).
37. S. Arai and L. M. Dorfman, J. Phys. Chem., 69, 2239 (1965).
38. L. M. Dorfman, N. E. Shank, and S. Arai, Advances in Chemistry Series, 82, "Radiation Chemistry-2", R. F. Gould, Ed., American Chemical Society, Washington, D. C., 1968, p. 58.
39. S. Arai, E. L. Tremba, J. R. Brandon, and L. M. Dorfman, Can. J. Chem., 45, 1119 (1967).
40. L. M. Dorfman, personal communication.
41. N. H. Velthorst and G. J. Hoijtink, J. Am. Chem. Soc., 87, 4529 (1965).
42. N. H. Velthorst and G. J. Hoijtink, J. Am. Chem. Soc., 89, 209 (1967).
43. K. Umemoto, Bull. Chem. Soc. Japan, 40, 1058 (1967).
44. G. W. Watt and D. M. Sowards, J. Am. Chem. Soc., 76, 4742 (1954).
45. K. H. Hausser, L. Mongini, and R. van Steenwinkel, Z. Naturforsch., 19a, 777 (1964).
46. L. H. Feldman, Ph. D. Thesis, Michigan State University, 1966.
47. E. M. Hansen, Ph. D. Thesis, Michigan State University, 1970.
48. V. A. Nicely, Ph. D. Thesis, Michigan State University, 1969.
49. W. E. Wentworth, J. Chem. Educ., 42, 96 (1965).
50. J. D. Olson, personal communication.
51. K. H. J. Buschow and G. J. Hoijtink, J. Chem. Phys., 40, 2501 (1964).

52. G. Henrici-Olivé and S. Olivé, Z. physik.Chem. Neue Folge, 43, 327 (1964).
53. K. K. Brandes and R. J. Gerdes, J. Phys. Chem., 71, 508 (1967).
54. E. K. Ralph, III and E. Grunwald, J. Am. Chem. Soc., 90, 517 (1968).
55. S. Bruckenstein and Saito, J. Am. Chem. Soc., 87, 698 (1965).
56. S. Bruckenstein and D. F. Untereker, J. Am. Chem. Soc., 91, 5741 (1969).

APPENDIX

REPRESENTATIVE SETS OF KINETIC DATA

REACTION OF K+AN- + MEQH IN THF

MEQH=.000448M		MEQH=.00120M		MEQH=.00376M	
AR- CONC.	TIME(SEC.)	AR- CONC.	TIME(SEC.)	AR- CONC.	TIME(SEC.)
.585E-03	0.	.490E-03	0.	.384E-03	0.
.442E-03	.667E-01	.374E-03	.667E-01	.229E-03	.667E-01
.367E-03	.133E+00	.302E-03	.133E+00	.166E-03	.133E+00
.318E-03	.200E+00	.267E-03	.200E+00	.132E-03	.200E+00
.280E-03	.267E+00	.235E-03	.267E+00	.111E-03	.267E+00
.254E-03	.333E+00	.210E-03	.333E+00	.964E-04	.333E+00
.233E-03	.400E+00	.193E-03	.400E+00	.828E-04	.400E+00
.212E-03	.467E+00	.178E-03	.467E+00	.751E-04	.467E+00
.194E-03	.533E+00	.162E-03	.533E+00	.670E-04	.533E+00
.180E-03	.600E+00	.152E-03	.600E+00	.604E-04	.600E+00
.170E-03	.667E+00	.138E-03	.700E+00	.549E-04	.667E+00
.159E-03	.733E+00	.123E-03	.833E+00	.505E-04	.733E+00
.149E-03	.800E+00	.112E-03	.967E+00	.471E-04	.800E+00
.141E-03	.867E+00	.101E-03	.110E+01	.471E-04	.867E+00
.132E-03	.933E+00	.926E-04	.123E+01	.430E-04	.933E+00
.126E-03	.100E+01	.882E-04	.137E+01	.372E-04	.100E+01
.120E-03	.107E+01	.810E-04	.150E+01	.369E-04	.107E+01
.114E-03	.113E+01	.765E-04	.163E+01	.349E-04	.113E+01
.110E-03	.120E+01	.722E-04	.177E+01	.343E-04	.120E+01
.104E-03	.127E+01	.683E-04	.190E+01	.301E-04	.127E+01
.100E-03	.133E+01	.613E-04	.210E+01	.295E-04	.133E+01
.955E-04	.140E+01	.539E-04	.237E+01	.287E-04	.140E+01
.935E-04	.147E+01	.512E-04	.263E+01	.266E-04	.147E+01
.881E-04	.153E+01	.481E-04	.290E+01	.260E-04	.153E+01
.874E-04	.160E+01	.441E-04	.317E+01	.239E-04	.160E+01
.826E-04	.167E+01	.415E-04	.343E+01	.242E-04	.167E+01
.817E-04	.173E+01	.383E-04	.370E+01	.226E-04	.173E+01
.765E-04	.180E+01	.357E-04	.397E+01	.199E-04	.180E+01
.745E-04	.187E+01	0.	0.	.220E-04	.187E+01
.711E-04	.193E+01	0.	0.	.190E-04	.193E+01
.702E-04	.200E+01	0.	0.	.185E-04	.200E+01

REACTION OF K+AN- + ETOH IN THF

ETOH=.00175M		ETOH=.00308M		ETOH=.00645M	
AR- CONC.	TIME(SEC.)	AR- CONC.	TIME(SEC.)	AR- CONC.	TIME(SEC.)
.510E-03	0.	.380E-03	0.	.420E-03	0.
.341E-03	.667E-01	.256E-03	.667E-01	.295E-03	.333E-01
.261E-03	.133E+00	.195E-03	.133E+00	.224E-03	.667E-01
.217E-03	.200E+00	.160E-03	.200E+00	.183E-03	.100E+00
.186E-03	.267E+00	.132E-03	.267E+00	.153E-03	.133E+00
.166E-03	.333E+00	.114E-03	.333E+00	.129E-03	.167E+00
.149E-03	.400E+00	.102E-03	.400E+00	.120E-03	.200E+00

AR- CONC.	TIME (SEC.)	AR- CONC.	TIME (SEC.)	AR- CONC.	TIME (SEC.)
.137E-03	.467E+00	.916E-04	.467E+00	.105E-03	.233E+00
.122E-03	.533E+00	.805E-04	.533E+00	.976E-04	.267E+00
.115E-03	.600E+00	.728E-04	.600E+00	.866E-04	.300E+00
.105E-03	.667E+00	.673E-04	.700E+00	.812E-04	.350E+00
.973E-04	.733E+00	.545E-04	.833E+00	.709E-04	.417E+00
.930E-04	.800E+00	.500E-04	.967E+00	.602E-04	.483E+00
.874E-04	.867E+00	.458E-04	.110E+01	.539E-04	.550E+00
.829E-04	.933E+00	.406E-04	.123E+01	.516E-04	.617E+00
.776E-04	.100E+01	.398E-04	.137E+01	.380E-04	.683E+00
.738E-04	.107E+01	.341E-04	.150E+01	.389E-04	.750E+00
.694E-04	.113E+01	.310E-04	.163E+01	.371E-04	.817E+00
.656E-04	.120E+01	.263E-04	.177E+01	.322E-04	.883E+00
.637E-04	.127E+01	.264E-04	.190E+01	.356E-04	.950E+00
.613E-04	.133E+01	.245E-04	.210E+01	.307E-04	.105E+01
.567E-04	.140E+01	.217E-04	.237E+01	.254E-04	.118E+01
.538E-04	.147E+01	.198E-04	.263E+01	.226E-04	.132E+01
.527E-04	.153E+01	.169E-04	.290E+01	.221E-04	.145E+01
.514E-04	.160E+01	.161E-04	.317E+01	.201E-04	.158E+01
.500E-04	.167E+01	.145E-04	.343E+01	.174E-04	.172E+01
.482E-04	.173E+01	.129E-04	.370E+01	.197E-04	.185E+01
.471E-04	.180E+01	.114E-04	.397E+01	0.	0.
.452E-04	.187E+01	0.	0.	0.	0.
.454E-04	.193E+01	0.	0.	0.	0.

REACTION OF K+AN- + ISO-PROH IN THF

PROH=.114M

PROH=.0555M

PROH=.01165M

.564E-03	0.	.535E-03	0.	.500E-03	0.
.320E-03	.333E-01	.323E-03	.333E-01	.258E-03	.667E-01
.172E-03	.667E-01	.235E-03	.667E-01	.178E-03	.133E+00
.132E-03	.100E+00	.173E-03	.100E+00	.134E-03	.200E+00
.106E-03	.133E+00	.140E-03	.133E+00	.106E-03	.267E+00
.921E-04	.167E+00	.119E-03	.167E+00	.885E-04	.333E+00
.771E-04	.200E+00	.997E-04	.200E+00	.745E-04	.400E+00
.584E-04	.233E+00	.848E-04	.233E+00	.654E-04	.467E+00
.608E-04	.267E+00	.787E-04	.267E+00	.551E-04	.533E+00
.503E-04	.300E+00	.690E-04	.300E+00	.504E-04	.600E+00
.400E-04	.333E+00	.636E-04	.333E+00	.451E-04	.667E+00
.460E-04	.367E+00	.618E-04	.367E+00	.400E-04	.733E+00
.380E-04	.400E+00	.524E-04	.400E+00	.383E-04	.800E+00
.375E-04	.450E+00	.449E-04	.433E+00	.337E-04	.867E+00
.240E-04	.517E+00	.440E-04	.467E+00	.339E-04	.933E+00
.290E-04	.583E+00	.436E-04	.500E+00	.307E-04	.100E+01
.203E-04	.650E+00	.354E-04	.533E+00	.299E-04	.107E+01
.207E-04	.717E+00	.320E-04	.567E+00	.259E-04	.113E+01
.172E-04	.783E+00	.337E-04	.600E+00	.254E-04	.120E+01
.186E-04	.850E+00	.327E-04	.633E+00	.236E-04	.127E+01
.182E-04	.917E+00	.292E-04	.667E+00	.196E-04	.133E+01
.568E-05	.983E+00	.273E-04	.700E+00	.222E-04	.140E+01
0.	0.	.249E-04	.733E+00	.214E-04	.147E+01

AR- CONC.	TIME (SEC.)	AR- CONC.	TIME (SEC.)	AR- CONC.	TIME (SEC.)
0.	0.	.331E-04	.767E+00	.203E-04	.153E+01
0.	0.	.245E-04	.800E+00	.187E-04	.160E+01
0.	0.	.264E-04	.833E+00	.160E-04	.167E+01
0.	0.	.200E-04	.867E+00	.175E-04	.173E+01
0.	0.	.192E-04	.900E+00	.167E-04	.180E+01
0.	0.	.265E-04	.933E+00	.128E-04	.187E+01
0.	0.	0.	0.	.157E-04	.193E+01
0.	0.	0.	0.	.137E-04	.200E+01
0.	0.	0.	0.	.114E-04	.207E+01

REACTION OF K+AN- + BUOH IN THE

BUOH=.0054M		BUOH=.008M		BUOH=.0204M	
.390E-03	0.	.430E-03	0.	.570E-03	0.
.268E-03	.667E-01	.273E-03	.667E-01	.268E-03	.667E-01
.202E-03	.133E+00	.198E-03	.133E+00	.169E-03	.133E+00
.156E-03	.200E+00	.154E-03	.200E+00	.130E-03	.200E+00
.133E-03	.267E+00	.127E-03	.267E+00	.104E-03	.267E+00
.112E-03	.333E+00	.108E-03	.333E+00	.832E-04	.333E+00
.970E-04	.400E+00	.940E-04	.400E+00	.711E-04	.400E+00
.904E-04	.467E+00	.817E-04	.467E+00	.576E-04	.467E+00
.716E-04	.600E+00	.711E-04	.533E+00	.507E-04	.533E+00
.573E-04	.800E+00	.650E-04	.600E+00	.444E-04	.600E+00
.458E-04	.100E+01	.592E-04	.667E+00	.413E-04	.667E+00
.376E-04	.120E+01	.537E-04	.733E+00	.373E-04	.733E+00
.308E-04	.140E+01	.433E-04	.933E+00	.325E-04	.800E+00
.279E-04	.160E+01	.350E-04	.113E+01	.324E-04	.867E+00
.260E-04	.180E+01	.285E-04	.133E+01	.264E-04	.100E+01
.207E-04	.200E+01	.231E-04	.153E+01	.246E-04	.120E+01
0.	0.	.231E-04	.173E+01	.175E-04	.140E+01
0.	0.	.185E-04	.193E+01	.160E-04	.160E+01

REACTION OF K+AN- + H2O IN THE

H2O=.185M		H2O=.00414M		H2O=.0471M	
.170E-03	0.	.548E-03	0.	.587E-03	0.
.130E-03	.333E-01	.420E-03	.333E-01	.354E-03	.333E-01
.921E-04	.667E-01	.361E-03	.667E-01	.257E-03	.667E-01
.897E-04	.100E+00	.305E-03	.100E+00	.187E-03	.100E+00
.764E-04	.133E+00	.262E-03	.133E+00	.151E-03	.133E+00
.655E-04	.167E+00	.245E-03	.167E+00	.129E-03	.167E+00
.602E-04	.200E+00	.221E-03	.200E+00	.101E-03	.200E+00
.464E-04	.233E+00	.198E-03	.233E+00	.910E-04	.233E+00
.406E-04	.267E+00	.182E-03	.267E+00	.796E-04	.267E+00
.435E-04	.300E+00	.175E-03	.300E+00	.797E-04	.300E+00
.363E-04	.333E+00	.164E-03	.333E+00	.627E-04	.333E+00
.339E-04	.367E+00	.144E-03	.367E+00	.525E-04	.367E+00
.333E-04	.400E+00	.147E-03	.400E+00	.524E-04	.400E+00

AR- CONC.	TIME (SEC.)	AR- CONC.	TIME (SEC.)	AR- CONC.	TIME (SEC.)
.249E-04	.433E+00	.127E-03	.433E+00	.389E-04	.500E+00
.306E-04	.467E+00	.125E-03	.467E+00	.432E-04	.600E+00
.260E-04	.500E+00	.113E-03	.533E+00	.364E-04	.700E+00
.219E-04	.533E+00	.108E-03	.633E+00	.236E-04	.800E+00
.236E-04	.567E+00	.797E-04	.733E+00	.233E-04	.900E+00
.244E-04	.600E+00	.750E-04	.833E+00	.213E-04	.100E+01
.136E-04	.633E+00	.695E-04	.933E+00	.185E-04	.110E+01
.211E-04	.667E+00	.694E-04	.103E+01	.158E-04	.133E+01
.196E-04	.700E+00	.496E-04	.113E+01	.949E-05	.157E+01
.152E-04	.733E+00	.590E-04	.123E+01	.143E-04	.180E+01
.181E-04	.767E+00	.519E-04	.133E+01	0.	0.
.188E-04	.800E+00	.470E-04	.143E+01	0.	0.
.129E-04	.833E+00	.425E-04	.153E+01	0.	0.
.147E-04	.867E+00	.388E-04	.163E+01	0.	0.
.164E-04	.900E+00	.329E-04	.173E+01	0.	0.
0.	0.	.284E-04	.183E+01	0.	0.
0.	0.	.245E-04	.193E+01	0.	0.

REACTION OF K+AN- + ETOH IN DME

ETOH=.00068M

ETOH=.00133M

ETOH=.00263M

.590E-03	0.	.590E-03	0.	.690E-03	0.
.502E-03	.267E+00	.507E-03	.267E+00	.528E-03	.267E+00
.443E-03	.533E+00	.443E-03	.533E+00	.434E-03	.533E+00
.396E-03	.800E+00	.401E-03	.800E+00	.376E-03	.800E+00
.362E-03	.107E+01	.369E-03	.107E+01	.330E-03	.107E+01
.329E-03	.133E+01	.342E-03	.133E+01	.295E-03	.133E+01
.306E-03	.160E+01	.318E-03	.160E+01	.266E-03	.173E+01
.288E-03	.187E+01	.300E-03	.187E+01	.229E-03	.227E+01
.272E-03	.213E+01	.285E-03	.213E+01	.192E-03	.280E+01
.258E-03	.240E+01	.266E-03	.240E+01	.171E-03	.333E+01
.244E-03	.267E+01	.252E-03	.267E+01	.151E-03	.387E+01
.231E-03	.293E+01	.244E-03	.293E+01	.135E-03	.440E+01
.219E-03	.320E+01	.234E-03	.320E+01	.119E-03	.493E+01
.195E-03	.400E+01	.223E-03	.347E+01	.113E-03	.547E+01
.175E-03	.480E+01	.211E-03	.373E+01	.101E-03	.600E+01
.160E-03	.560E+01	.194E-03	.427E+01	.954E-04	.653E+01
.147E-03	.640E+01	.176E-03	.507E+01	.762E-04	.773E+01
.136E-03	.720E+01	.162E-03	.587E+01	.565E-04	.960E+01
.124E-03	.800E+01	.148E-03	.667E+01	.430E-04	.115E+02
.118E-03	.830E+01	.139E-03	.747E+01	.360E-04	.133E+02
.110E-03	.960E+01	.127E-03	.827E+01	.255E-04	.152E+02
.104E-03	.104E+02	.116E-03	.907E+01	0.	0.
.971E-04	.112E+02	.102E-03	.104E+02	0.	0.
.907E-04	.120E+02	.909E-04	.123E+02	0.	0.
.871E-04	.128E+02	.776E-04	.141E+02	0.	0.
.849E-04	.136E+02	.696E-04	.160E+02	0.	0.
.806E-04	.144E+02	0.	0.	0.	0.
.773E-04	.152E+02	0.	0.	0.	0.
.705E-04	.160E+02	0.	0.	0.	0.

REACTION OF K+AN- + H2O IN DME

H2O=.00360M		H2O=.0357M		H2O=.0118M	
AR- CONC.	TIME(SEC.)	AR- CONC.	TIME(SEC.)	AR- CONC.	TIME(SEC.)
.130E-03	0.	.515E-03	0.	.630E-03	0.
.119E-03	.200E+00	.403E-03	.133E+00	.540E-03	.667E-01
.110E-03	.400E+00	.332E-03	.267E+00	.484E-03	.133E+00
.993E-04	.600E+00	.284E-03	.400E+00	.429E-03	.200E+00
.909E-04	.800E+00	.243E-03	.533E+00	.389E-03	.267E+00
.825E-04	.110E+01	.218E-03	.667E+00	.352E-03	.333E+00
.724E-04	.150E+01	.195E-03	.800E+00	.317E-03	.400E+00
.626E-04	.190E+01	.171E-03	.933E+00	.295E-03	.467E+00
.559E-04	.230E+01	.147E-03	.120E+01	.276E-03	.533E+00
.511E-04	.270E+01	.125E-03	.147E+01	.258E-03	.600E+00
.457E-04	.310E+01	.111E-03	.173E+01	.229E-03	.733E+00
.421E-04	.350E+01	.963E-04	.200E+01	.193E-03	.933E+00
.380E-04	.390E+01	.877E-04	.227E+01	.170E-03	.113E+01
.356E-04	.430E+01	.788E-04	.253E+01	.149E-03	.133E+01
.331E-04	.470E+01	.703E-04	.280E+01	.133E-03	.153E+01
.305E-04	.510E+01	.655E-04	.307E+01	.122E-03	.173E+01
.283E-04	.550E+01	.569E-04	.347E+01	.110E-03	.193E+01
.266E-04	.590E+01	.486E-04	.400E+01	.990E-04	.213E+01
.252E-04	.630E+01	.416E-04	.453E+01	.949E-04	.233E+01
.241E-04	.670E+01	.387E-04	.507E+01	.893E-04	.253E+01
.227E-04	.710E+01	.364E-04	.560E+01	.808E-04	.283E+01
.223E-04	.750E+01	.321E-04	.613E+01	.718E-04	.323E+01
.202E-04	.790E+01	.294E-04	.667E+01	.583E-04	.363E+01
.187E-04	.830E+01	.269E-04	.720E+01	0.	0.
.174E-04	.870E+01	0.	0.	0.	0.
.170E-04	.910E+01	0.	0.	0.	0.
.162E-04	.950E+01	0.	0.	0.	0.
.154E-04	.990E+01	0.	0.	0.	0.
.141E-04	.103E+02	0.	0.	0.	0.
.138E-04	.107E+02	0.	0.	0.	0.
.133E-04	.111E+02	0.	0.	0.	0.
.132E-04	.115E+02	0.	0.	0.	0.

REACTION OF NA+AN- + ETOH IN THF

ETOH=.000845M		ETOH=.00169M		ETOH=.00282M	
AR- CONC.	TIME(SEC.)	AR- CONC.	TIME(SEC.)	AR- CONC.	TIME(SEC.)
.390E-03	0.	.370E-03	0.	.297E-03	0.
.301E-03	.667E-01	.299E-03	.333E-01	.216E-03	.333E-01
.252E-03	.133E+00	.257E-03	.667E-01	.186E-03	.667E-01
.213E-03	.200E+00	.225E-03	.100E+00	.167E-03	.100E+00
.193E-03	.267E+00	.198E-03	.133E+00	.155E-03	.133E+00
.175E-03	.333E+00	.178E-03	.167E+00	.144E-03	.167E+00
.157E-03	.400E+00	.167E-03	.200E+00	.132E-03	.200E+00
.147E-03	.467E+00	.147E-03	.233E+00	.125E-03	.233E+00
.134E-03	.533E+00	.135E-03	.267E+00	.119E-03	.267E+00
.123E-03	.600E+00	.126E-03	.300E+00	.112E-03	.300E+00

AR- CONC.	TIME (SEC.)	AR- CONC.	TIME (SEC.)	AR- CONC.	TIME (SEC.)
.116E-03	.667E+00	.120E-03	.333E+00	.106E-03	.333E+00
.112E-03	.733E+00	.111E-03	.367E+00	.100E-03	.367E+00
.103E-03	.800E+00	.107E-03	.400E+00	.952E-04	.400E+00
.963E-04	.933E+00	.861E-04	.500E+00	.938E-04	.433E+00
.871E-04	.107E+01	.802E-04	.600E+00	.859E-04	.467E+00
.802E-04	.120E+01	.730E-04	.700E+00	.818E-04	.500E+00
.739E-04	.133E+01	.631E-04	.800E+00	.772E-04	.533E+00
.701E-04	.147E+01	.590E-04	.900E+00	.771E-04	.567E+00
.651E-04	.160E+01	.498E-04	.100E+01	.729E-04	.600E+00
.601E-04	.173E+01	.434E-04	.110E+01	.711E-04	.633E+00
.545E-04	.187E+01	.440E-04	.120E+01	.647E-04	.700E+00
.505E-04	.200E+01	.395E-04	.130E+01	.594E-04	.800E+00
.497E-04	.213E+01	.379E-04	.140E+01	.542E-04	.900E+00
.459E-04	.227E+01	.356E-04	.150E+01	.487E-04	.100E+01
.422E-04	.240E+01	.320E-04	.160E+01	.457E-04	.110E+01
.387E-04	.263E+01	.307E-04	.170E+01	.419E-04	.120E+01
.368E-04	.297E+01	.282E-04	.130E+01	.401E-04	.130E+01
.340E-04	.330E+01	0.	0.	.373E-04	.140E+01
.306E-04	.363E+01	0.	0.	.341E-04	.150E+01
.276E-04	.397E+01	0.	0.	.332E-04	.160E+01
0.	0.	0.	0.	.307E-04	.177E+01
0.	0.	0.	0.	.259E-04	.200E+01
0.	0.	0.	0.	.229E-04	.223E+01
0.	0.	0.	0.	.249E-04	.247E+01
0.	0.	0.	0.	.173E-04	.270E+01

REACTION OF NA+AN- + H2O IN THF

H2O=.0163M

H2O=.0325M

H2O=.0399M

.220E-03	0.	.360E-03	0.	.314E-03	0.
.123E-03	.333E-01	.275E-03	.489E-02	.242E-03	.391E-02
.101E-03	.667E-01	.200E-03	.978E-02	.193E-03	.781E-02
.849E-04	.100E+00	.160E-03	.147E-01	.164E-03	.117E-01
.758E-04	.133E+00	.136E-03	.196E-01	.140E-03	.156E-01
.701E-04	.167E+00	.118E-03	.244E-01	.125E-03	.195E-01
.622E-04	.200E+00	.107E-03	.293E-01	.114E-03	.234E-01
.551E-04	.267E+00	.982E-04	.342E-01	.105E-03	.273E-01
.469E-04	.367E+00	.737E-04	.538E-01	.993E-04	.313E-01
.379E-04	.467E+00	.617E-04	.734E-01	.815E-04	.430E-01
.343E-04	.567E+00	.592E-04	.929E-01	.695E-04	.625E-01
.316E-04	.667E+00	.478E-04	.112E+00	.559E-04	.820E-01
.284E-04	.767E+00	.473E-04	.132E+00	.506E-04	.102E+00
.247E-04	.867E+00	.443E-04	.152E+00	.487E-04	.121E+00
.227E-04	.967E+00	.374E-04	.171E+00	.401E-04	.141E+00

AR- CONC.	TIME (SEC.)	AR- CONC.	TIME (SEC.)	AR- CONC.	TIME (SEC.)
.194E-04	.107E+01	.374E-04	.191E+00	.419E-04	.160E+00
.212E-04	.117E+01	.356E-04	.210E+00	.365E-04	.180E+00
.198E-04	.127E+01	.299E-04	.259E+00	.310E-04	.199E+00
.155E-04	.137E+01	.270E-04	.308E+00	.332E-04	.219E+00
.148E-04	.147E+01	.243E-04	.357E+00	0.	0.
.156E-04	.157E+01	.234E-04	.406E+00	0.	0.
.132E-04	.167E+01	.194E-04	.455E+00	0.	0.
.123E-04	.177E+01	.190E-04	.503E+00	0.	0.
.111E-04	.187E+01	.172E-04	.553E+00	0.	0.
.131E-04	.197E+01	.146E-04	.601E+00	0.	0.

REACTION OF NA+AN- + ETOH IN DME

ETOH=.00263M

ETOH=.00091M

ETOH=.00134M

.670E-03	0.	.570E-03	0.	.400E-03	.333E+00
.585E-03	.200E+00	.526E-03	.120E+01	.353E-03	.133E+01
.509E-03	.400E+00	.483E-03	.240E+01	.311E-03	.233E+01
.440E-03	.600E+00	.447E-03	.360E+01	.275E-03	.333E+01
.383E-03	.800E+00	.392E-03	.599E+01	.245E-03	.433E+01
.334E-03	.100E+01	.346E-03	.839E+01	.218E-03	.533E+01
.294E-03	.120E+01	.306E-03	.108E+02	.197E-03	.633E+01
.264E-03	.140E+01	.272E-03	.132E+02	.177E-03	.733E+01
.238E-03	.160E+01	.241E-03	.156E+02	.158E-03	.833E+01
.216E-03	.180E+01	.215E-03	.180E+02	.144E-03	.933E+01
.199E-03	.200E+01	.185E-03	.220E+02	.131E-03	.103E+02
.183E-03	.220E+01	.155E-03	.260E+02	.117E-03	.113E+02
.171E-03	.240E+01	.131E-03	.300E+02	.108E-03	.123E+02
.159E-03	.260E+01	.110E-03	.340E+02	.955E-04	.133E+02
.153E-03	.280E+01	.900E-04	.380E+02	.869E-04	.143E+02
.144E-03	.300E+01	.790E-04	.418E+02	.778E-04	.153E+02
.134E-03	.320E+01	.660E-04	.458E+02	.692E-04	.163E+02
.125E-03	.340E+01	0.	0.	.636E-04	.173E+02
.118E-03	.380E+01	0.	0.	.564E-04	.183E+02
.104E-03	.420E+01	0.	0.	.522E-04	.193E+02
.976E-04	.460E+01	0.	0.	.504E-04	.203E+02
.906E-04	.500E+01	0.	0.	0.	0.
.843E-04	.540E+01	0.	0.	0.	0.
.788E-04	.580E+01	0.	0.	0.	0.
.727E-04	.620E+01	0.	0.	0.	0.
.664E-04	.660E+01	0.	0.	0.	0.
.626E-04	.700E+01	0.	0.	0.	0.
.570E-04	.800E+01	0.	0.	0.	0.
.498E-04	.900E+01	0.	0.	0.	0.
.432E-04	.100E+02	0.	0.	0.	0.
.387E-04	.110E+02	0.	0.	0.	0.
.342E-04	.120E+02	0.	0.	0.	0.

REACTION OF NA+AN- + H2O IN DMF

H2O=.0124M		H2O=.0180M		H2O=.0357M	
AR- CONC.	TIME (SEC.)	AR- CONC.	TIME (SEC.)	AR- CONC.	TIME (SEC.)
.660E-03	0.	.526E-03	0.	.630E-03	0.
.627E-03	.200E+00	.482E-03	.267E+00	.559E-03	.333E+00
.594E-03	.400E+00	.449E-03	.533E+00	.496E-03	.667E+00
.565E-03	.600E+00	.415E-03	.800E+00	.436E-03	.100E+01
.538E-03	.800E+00	.391E-03	.107E+01	.385E-03	.133E+01
.512E-03	.100E+01	.361E-03	.133E+01	.340E-03	.167E+01
.485E-03	.120E+01	.333E-03	.160E+01	.300E-03	.200E+01
.464E-03	.140E+01	.293E-03	.213E+01	.266E-03	.233E+01
.443E-03	.160E+01	.260E-03	.267E+01	.235E-03	.267E+01
.424E-03	.180E+01	.224E-03	.320E+01	.209E-03	.300E+01
.386E-03	.220E+01	.197E-03	.373E+01	.190E-03	.333E+01
.333E-03	.280E+01	.143E-03	.427E+01	.171E-03	.367E+01
.284E-03	.340E+01	.159E-03	.480E+01	.154E-03	.400E+01
.239E-03	.400E+01	.137E-03	.547E+01	.139E-03	.433E+01
.204E-03	.460E+01	.115E-03	.627E+01	.125E-03	.467E+01
.178E-03	.520E+01	.970E-04	.707E+01	.116E-03	.500E+01
.153E-03	.580E+01	.780E-04	.800E+01	.107E-03	.533E+01
.133E-03	.640E+01	.650E-04	.920E+01	.102E-03	.567E+01
.114E-03	.700E+01	.470E-04	.107E+02	.941E-04	.600E+01
.963E-04	.760E+01	.390E-04	.120E+02	.901E-04	.633E+01
.802E-04	.820E+01	.290E-04	.140E+02	.827E-04	.667E+01
.671E-04	.880E+01	0.	0.	.752E-04	.700E+01
.553E-04	.940E+01	0.	0.	.695E-04	.733E+01
.469E-04	.100E+02	0.	0.	.642E-04	.767E+01
.414E-04	.106E+02	0.	0.	.589E-04	.800E+01
.363E-04	.112E+02	0.	0.	.530E-04	.833E+01
0.	0.	0.	0.	.536E-04	.867E+01
0.	0.	0.	0.	.491E-04	.900E+01
0.	0.	0.	0.	.444E-04	.933E+01
0.	0.	0.	0.	.395E-04	.967E+01

REACTION OF K+IER- + ETOH IN THE

ETOH=.000975M		ETOH=.000575M		ETOH=.000418M	
AR- CONC.	TIME (SEC.)	AR- CONC.	TIME (SEC.)	AR- CONC.	TIME (SEC.)
.639E-04	0.	.144E-03	0.	.167E-03	0.
.570E-04	.976E-03	.124E-03	.195E-02	.150E-03	.195E-02
.515E-04	.195E-02	.108E-03	.390E-02	.135E-03	.390E-02
.462E-04	.293E-02	.959E-04	.585E-02	.123E-03	.585E-02
.407E-04	.390E-02	.843E-04	.781E-02	.112E-03	.781E-02
.360E-04	.489E-02	.760E-04	.976E-02	.101E-03	.976E-02
.319E-04	.585E-02	.679E-04	.117E-01	.925E-04	.117E-01
.291E-04	.683E-02	.609E-04	.137E-01	.845E-04	.137E-01
.250E-04	.781E-02	.558E-04	.156E-01	.783E-04	.156E-01
.224E-04	.878E-02	.506E-04	.176E-01	.726E-04	.176E-01
.193E-04	.976E-02	.448E-04	.195E-01	.683E-04	.195E-01
.180E-04	.107E-01	.407E-04	.215E-01	.636E-04	.215E-01

AR- CONC.	TIME (SEC.)	AR- CONC.	TIME (SEC.)	AR- CONC.	TIME (SEC.)
.162E-04	.117E-01	.368E-04	.234E-01	.583E-04	.234E-01
.143E-04	.127E-01	.334E-04	.254E-01	.542E-04	.254E-01
.130E-04	.137E-01	.296E-04	.273E-01	.502E-04	.273E-01
.117E-04	.146E-01	.265E-04	.293E-01	.462E-04	.293E-01
.982E-05	.156E-01	.230E-04	.312E-01	.432E-04	.312E-01
.970E-05	.166E-01	.210E-04	.332E-01	.406E-04	.332E-01
.899E-05	.176E-01	.195E-04	.351E-01	.374E-04	.351E-01
.826E-05	.185E-01	.168E-04	.371E-01	.349E-04	.371E-01
.784E-05	.195E-01	.140E-04	.390E-01	.324E-04	.390E-01
.767E-05	.205E-01	.116E-04	.410E-01	.294E-04	.410E-01
0.	0.	0.	0.	.266E-04	.429E-01
0.	0.	0.	0.	.251E-04	.449E-01
0.	0.	0.	0.	.231E-04	.468E-01
0.	0.	0.	0.	.213E-04	.488E-01
0.	0.	0.	0.	.202E-04	.507E-01
0.	0.	0.	0.	.190E-04	.527E-01
0.	0.	0.	0.	.187E-04	.546E-01
0.	0.	0.	0.	.179E-04	.566E-01